

**University of Alberta**

**Mediators of Hyperoxic-Inhibited Alveolarization in the Newborn Rat Pup**

by

**Gayle Elizabeth Hosford**



A thesis submitted to the Faculty of Graduate Studies and Research in partial fulfillment  
of the

requirements for the degree of **Doctor of Philosophy**

Department of Physiology

Edmonton, Alberta

Spring 2003

National Library  
of Canada

Acquisitions and  
Bibliographic Services

395 Wellington Street  
Ottawa ON K1A 0N4  
Canada

Bibliothèque nationale  
du Canada

Acquisitons et  
services bibliographiques

395, rue Wellington  
Ottawa ON K1A 0N4  
Canada

*Your file* *Votre référence*

*ISBN: 0-612-82117-X*

*Our file* *Notre référence*

*ISBN: 0-612-82117-X*

The author has granted a non-exclusive licence allowing the National Library of Canada to reproduce, loan, distribute or sell copies of this thesis in microform, paper or electronic formats.

The author retains ownership of the copyright in this thesis. Neither the thesis nor substantial extracts from it may be printed or otherwise reproduced without the author's permission.

L'auteur a accordé une licence non exclusive permettant à la Bibliothèque nationale du Canada de reproduire, prêter, distribuer ou vendre des copies de cette thèse sous la forme de microfiche/film, de reproduction sur papier ou sur format électronique.

L'auteur conserve la propriété du droit d'auteur qui protège cette thèse. Ni la thèse ni des extraits substantiels de celle-ci ne doivent être imprimés ou autrement reproduits sans son autorisation.

# Canada

**University of Alberta**

**Library Release Form**

Name of Author: **Gayle Elizabeth Hosford**

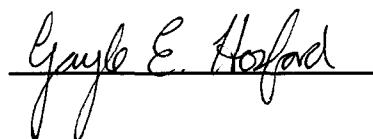
Title of Thesis: **Mediators of Hyperoxic-Inhibited Alveolarization in the Newborn Rat Pup**

Degree: **Doctor of Philosophy**

Year this Degree Granted: **2003**

Permission is hereby granted to the University of Alberta Library to reproduce single copies of this thesis and to lend or sell such copies for private, scholarly or scientific research purposes only.

The author reserves all other publication and other rights in association with the copyright in the thesis, and except as herein before provided, neither the thesis nor any substantial portion thereof may be printed or otherwise reproduced in any material form whatever without the author's prior written permission.

A handwritten signature in cursive script, reading "Gayle E. Hosford", is written over a horizontal line.

16 St. Helen's Road

Boosterstown

Co. Dublin

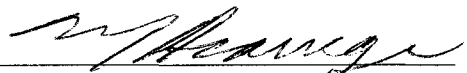
Ireland

Date submitted to the Faculty of Graduate Studies and Research:

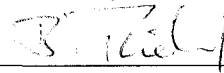
University of Alberta

Faculty of Graduate Studies and Research

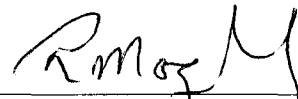
The undersigned certify that they have read, and recommend to the Faculty of Graduate Studies and Research for acceptance, a thesis entitled **Mediators of Hyperoxic-Inhibited Alveolarization in the Newborn Rat Pup** submitted by **Gayle Elizabeth Hosford** in partial fulfillment of the requirements for the degree of Doctor of Philosophy.



Dr. M. J. Acarregui (External Examiner)



Dr. B. Thebaud



Dr. R. Moqbel



Dr. J. Greer



Dr. D. M. Olson

Date: October 30, 2002

## ABSTRACT

---

Alveolarization, the final stage of lung development; occurs through a process of septation, where immature saccules are divided into smaller airspaces. When newborn rats are exposed to hyperoxia during the period of alveolar development (postnatal day (d) 4 to 14), septation is inhibited.

As the development of blood vessels has been shown to be necessary for alveolarization, the angiogenic factor, Vascular Endothelial Growth Factor (VEGF), and a transcription factor for VEGF sensitive to O<sub>2</sub> tension, hypoxia-inducible factor-2 $\alpha$  (HIF-2 $\alpha$ ), were studied during exposure of rat pups to hyperoxia. Lung tissue mRNA levels of HIF-2 $\alpha$  and VEGF increased from d4-14 in normoxic animals, but hyperoxia suppressed these increases. VEGF<sub>164</sub> protein levels increased with hyperoxia to d9, but continuing hyperoxia decreased levels by d12. VEGFR(receptor)1 and R2 mRNA and protein were also decreased during hyperoxia.

Our original hypothesis anticipated that matrix metalloproteinases (MMPs) -2 and -9, enzymes often associated with O<sub>2</sub>-induced inflammation, would increase in a hyperoxic-environment. Contrary to our hypothesis, hyperoxia significantly decreased levels of MMP-9 mRNA, proMMP-9 protein, and MMP-2 and -9 enzyme activity. Doxycycline, a pan-MMP activity inhibitor, also inhibited lung alveolarization. Further, the mRNA expression of an endogenous inhibitor of MMP activity, tissue inhibitor of metalloproteinase-1 (TIMP), increased on day 14 in lungs of oxygen-exposed pups.

The cysteinyl-leukotrienes (cysteinyl-LTs) have been previously shown to be mediators of hyperoxic-inhibited alveolarization. Protein mass of the enzyme responsible for LT synthesis, 5-lipoxygenase (5-LO) and its activating protein (FLAP), increased in normoxic animals from d4 to d14 ( $p < 0.05$ ). Hyperoxia exposure increased the mass of both proteins ( $p < 0.05$ ) and immunohistochemistry localized 5-LO and FLAP mainly to alveolar macrophages on d14. Exposure of rat pups to  $>95\%$   $O_2$  from d1 to d7 also stimulated an increase in  $LTB_4$  output.

These results extend our knowledge about factors that may be involved in normal alveolar development in the rat pup, and how they are affected when alveolarization is inhibited due to hyperoxia. These experiments provide a new basis for therapeutic strategies in the treatment of premature infants suffering from bronchopulmonary dysplasia, as elevated  $O_2$  concentrations are likely associated with inhibited lung development seen in the pathogenesis of this disease.

## ACKNOWLEDGMENTS

---

I would like to thank my supervisor, Dave Olson, and my committee members, Redwan Moqbel and John Greer, for their help and support over the last five years.

A special thanks to Dean Zaragoza who was a great friend as well as an excellent help in the lab.

All the friends who have loved and supported me throughout this ordeal, you know who you are and how much you mean to me.

And finally Dad and Mum, who have supported me from the very beginning, through the good times as well as the hard – I love you both.

## TABLE OF CONTENTS

---

---

<b>CHAPTER 1. LITERATURE REVIEW</b>	<b>1</b>
<b>1.1 DEVELOPMENT OF THE LUNG</b>	<b>1</b>
1.1.1 <i>Comparative lung development</i>	3
1.1.2 <i>Cell proliferation</i>	4
1.1.3 <i>Vascular development</i>	4
<b>1.2 ALVEOLAR DEVELOPMENT</b>	<b>6</b>
1.2.1 <i>Microvascular maturation</i>	7
1.2.2 <i>Apoptosis</i>	7
1.2.3 <i>Intussusceptive growth</i>	8
<b>1.3 BRONCHOPULMONARY DYSPLASIA</b>	<b>9</b>
<b>1.4 FACTORS AFFECTING ALVEOLAR DEVELOPMENT</b>	<b>10</b>
1.4.1 <i>Dexamethasone</i>	11
1.4.2 <i>Retinoic Acid</i>	12
1.4.3 <i>Hypoxia</i>	13
<b>1.5 HYPEROXIA</b>	<b>14</b>
1.5.1 <i>Hyperoxia and Lung Development</i>	16
1.5.2 <i>Hyperoxia and models of BPD</i>	19
<b>1.6 VASCULAR ENDOTHELIAL GROWTH FACTOR AND ANGIOGENESIS</b>	<b>22</b>
1.6.1 <i>Angiogenesis</i>	22
1.6.2 <i>Vascular Endothelial Growth Factor</i>	23
1.6.3 <i>VEGF and lung development</i>	27
1.6.4 <i>VEGF and neonatal hyperoxic lung injury</i>	29
1.6.5 <i>Hypoxia inducible factors</i>	30
1.6.6 <i>VEGF and epithelial cells</i>	31
<b>1.7 EXTRACELLULAR MATRIX AND MATRIX METALLOPROTEINASES</b>	<b>32</b>
1.7.1 <i>Matrix metalloproteinases</i>	33
1.7.2 <i>MMPs and alveolar development</i>	35
1.7.3 <i>MMPs and hyperoxia</i>	35
1.7.4 <i>TIMPS and alveolar development</i>	36
<b>1.8 LEUKOTRIENES</b>	<b>36</b>
1.8.1 <i>Leukotrienes and hyperoxia</i>	38
<b>1.9 REFERENCES</b>	<b>46</b>
<b>CHAPTER 2. RATIONALE</b>	<b>61</b>
<b>CHAPTER 3. METHODS</b>	<b>63</b>
<b>3.1 ANIMALS</b>	<b>63</b>
3.1.1 <i>O<sub>2</sub> Exposure</i>	63
3.1.2 <i>Preparation of lung samples</i>	64



<b>3.2</b>	<b>REVERSE TRANSCRIPTION (RT) AND REAL-TIME QUANTITATIVE POLYMERASE CHAIN REACTION (PCR).....</b>	<b>64</b>
3.2.1	<i>Reverse Transcription (RT) .....</i>	66
3.2.2	<i>Real-time PCR .....</i>	66
3.2.3	<i>Analysis of real time PCR results .....</i>	67
<b>3.3</b>	<b>PROTEIN ANALYSIS.....</b>	<b>68</b>
3.3.1	<i>Protein extraction .....</i>	68
3.3.2	<i>Western Immunoblotting.....</i>	69
<b>3.4</b>	<b>STATISTICAL ANALYSES .....</b>	<b>70</b>
<b>3.5</b>	<b>REFERENCES .....</b>	<b>71</b>
<b><u>CHAPTER 4. EFFECTS OF HYPEROXIA ON VEGF, ITS RECEPTORS AND HIF-2<math>\alpha</math> IN THE NEWBORN RAT LUNG _____</u></b>		<b>79</b>
<b>4.1</b>	<b>INTRODUCTION .....</b>	<b>79</b>
<b>4.2</b>	<b>METHODS.....</b>	<b>82</b>
4.2.1	<i>VEGF Immunoassay .....</i>	82
<b>4.3</b>	<b>RESULTS.....</b>	<b>83</b>
4.3.1	<i>VEGF .....</i>	83
4.3.2	<i>VEGFR1 .....</i>	84
4.3.3	<i>VEGFR2.....</i>	84
4.3.4	<i>HIF-2<math>\alpha</math>.....</i>	85
<b>4.4</b>	<b>DISCUSSION.....</b>	<b>86</b>
<b>4.5</b>	<b>REFERENCES.....</b>	<b>95</b>
<b><u>CHAPTER 5. THE EFFECTS OF HYPEROXIA ON MATRIX METALLOPROTEINASES -2 AND -9 IN THE NEWBORN RAT LUNG _</u></b>		<b>98</b>
<b>5.1</b>	<b>INTRODUCTION.....</b>	<b>98</b>
<b>5.2</b>	<b>MATERIALS AND METHODS .....</b>	<b>100</b>
5.2.1	<i>Gelatinase Zymography.....</i>	101
5.2.2	<i>MMP inhibition.....</i>	101
<b>5.3</b>	<b>RESULTS.....</b>	<b>104</b>
5.3.1	<i>MMP mRNA levels.....</i>	104
5.3.2	<i>MMP protein and activity levels .....</i>	104
5.3.3	<i>ProMMP 2 .....</i>	105
5.3.4	<i>Active MMP-2 .....</i>	105
5.3.5	<i>Pro-MMP-9.....</i>	106
5.3.6	<i>MMP inhibition.....</i>	106
5.3.7	<i>TIMP mRNA levels.....</i>	108
<b>5.4</b>	<b>DISCUSSION.....</b>	<b>108</b>
<b>5.5</b>	<b>REFERENCES.....</b>	<b>123</b>
<b><u>CHAPTER 6. HYPEROXIA AFFECTS PROTEIN MASS OF 5-LIPOXYGENASE AND ITS ACTIVATING PROTEIN, FLAP, AND LTB<sub>4</sub> OUTPUT IN NEWBORN RAT LUNGS _____</u></b>		<b>127</b>
<b>6.1</b>	<b>INTRODUCTION.....</b>	<b>127</b>
<b>6.2</b>	<b>METHODS.....</b>	<b>129</b>

6.2.1	<i>Animals</i> .....	129
6.2.2	<i>Explant technique</i> .....	130
6.2.3	<i>Radioimmunoassay</i> .....	133
6.2.4	<i>Immunohistochemistry</i> .....	133
<b>6.3</b>	<b>RESULTS</b> .....	<b>136</b>
6.3.1	<i>LTB<sub>4</sub> release</i> .....	136
6.3.2	<i>5-LO and FLAP protein levels</i> .....	137
<b>6.4</b>	<b>DISCUSSION</b> .....	<b>138</b>
<b>6.5</b>	<b>REFERENCES</b> .....	<b>147</b>
<b><u>CHAPTER 7. GENERAL DISCUSSION</u></b> .....		<b>149</b>
<b>7.1</b>	<b>DISCUSSION</b> .....	<b>149</b>
7.1.1	<i>Angiogenesis and alveolarization</i> .....	149
7.1.2	<i>Angiogenesis: stimulation or inhibition?</i> .....	150
7.1.3	<i>Windows of opportunity</i> .....	153
<b>7.2</b>	<b>SPECULATIONS</b> .....	<b>153</b>
7.2.1	<i>No stimulation of angiogenesis</i> .....	153
7.2.2	<i>VEGF effects MMPs</i> .....	154
7.2.3	<i>VEGF and epithelial cells</i> .....	155
7.2.4	<i>Basement membrane discontinuities</i> .....	155
7.2.5	<i>MMPs and elastin</i> .....	156
<b>7.3</b>	<b>LIMITATIONS</b> .....	<b>156</b>
<b>7.4</b>	<b>CONCLUSIONS</b> .....	<b>157</b>
<b>7.5</b>	<b>FUTURE DIRECTIONS</b> .....	<b>157</b>
<b>7.6</b>	<b>REFERENCES</b> .....	<b>160</b>
<b><u>APPENDICES</u></b> .....		<b>163</b>
<b>APPENDIX TO CHAPTER 4</b> .....		<b>163</b>
<b>A.1</b>	<b>DIFFERENTIAL EXPRESSION OF VEGF SPLICE VARIANTS</b> .....	<b>163</b>
A.1.1	<i>Preparation of cRNA Probe</i> .....	163
A.1.2	<i>Ribonuclease Protection Assay</i> .....	167
<b>A.1.3</b>	<b>RESULTS</b> .....	<b>170</b>

## LIST OF FIGURES

---

Figure 1.1	Stages of Branching Morphogenesis.....	41
Figure 1.2	Timing of the stages of development of human and rat lung ..	42
Figure 1.3	Septation of saccules..	43
Figure 1.4	MT1-MMP activation of MMP-2.....	44
Figure 1.5	Leukotriene synthesis pathway.....	45
Figure 3.1	Scheme showing the hyperoxic-exposure protocol.....	74
Figure 3.2	Representative photomicrographs of the effect of A) air and B) O <sub>2</sub> on the morphometry of rat lungs at d 14... ..	75
Figure 3.3	The chemistry of real time PCR .....	76
Figure 3.4	PCR products for each gene of interest. ....	77
Figure 3.5	Example of the results obtained from a real-time PCR reaction... ..	78
Figure 4.1	Time course and effects of >95% O <sub>2</sub> from day 4 to 14 on (A) VEGF mRNA expression and (B) VEGF protein levels.....	91
Figure 4.2	Time course and effects of >95% O <sub>2</sub> from day 6 to 14 on (A) VEGFR1 mRNA expression and (B) VEGFR1 protein levels.....	92
Figure 4.3	Time course and effects of >95% O <sub>2</sub> from day 4 to 14 on (A) VEGFR2 mRNA expression and (B) VEGFR2 protein levels.....	93
Figure 4.4	Time course and effects of >95% O <sub>2</sub> from day 6 to 14 on (A) HIF-2 $\alpha$ mRNA expression and (B) correlation between VEGF and HIF-2 $\alpha$ mRNA expression. ....	94
Figure 5.1	Time course and effects of > 95 % O <sub>2</sub> from d 4 to d 14 on (A) MMP-2 and (B) MMP-9 mRNA expression..	116
Figure 5.2	Time course and effects of > 95 % O <sub>2</sub> from d 4 to d 14 on MMP-2 and MMP-9 protein and activity.....	117
Figure 5.3	Time course and effects of > 95 % O <sub>2</sub> from d 4 to d 14 on (A) pro-MMP-2 protein levels and (B) pro-MMP-2 activity levels. ....	118
Figure 5.4	Time course and effects of > 95 % O <sub>2</sub> from d 4 to d 14 on (A) active MMP-2 protein levels and (B) active MMP-2 activity levels.....	119

Figure 5.5	Time course and effects of > 95 % O <sub>2</sub> from d 4 to d 14 on (A) pro-MMP-9 protein levels and (B) pro-MMP-9 activity levels..	120
Figure 5.6	Representative photomicrographs of lung parenchyma of 14-day-old rats treated with saline vehicle (A) or doxycycline (B) from d 4 to d 14...	121
Figure 5.7	Time course and effects of > 95 % O <sub>2</sub> from d 4 to d 14 on (A) TIMP-1 and (B) TIMP-2 mRNA expression.....	122
Figure 6.1	LTB <sub>4</sub> release from <i>in vitro</i> lung explants of rat pups. ...	142
Figure 6.2	LTB <sub>4</sub> release from <i>in vitro</i> lung explants of rat pups stimulated with Ca <sup>2+</sup> ionophore.....	143
Figure 6.3	Time course and effects of > 95 % O <sub>2</sub> from d 4 to d 14 on 5-LO protein levels in newborn rat lung... ..	144
Figure 6.4	Time course and effects of > 95 % O <sub>2</sub> from d 4 to d 14 on FLAP protein levels in newborn rat lung. ....	145
Figure 6.5	Representative immunohistochemistry demonstrating localization of 5-LO and FLAP in d 14 rat lung. ....	146
Figure 7.1	Activity of MMP-2 and MMP-9 at d 28 after exposure of rat pups to air or > 95 % O <sub>2</sub> from d 4 to d 14... ..	158

## LIST OF TABLES

---

Table 3.1	Primers and Fluorescent Beacons used for real-time PCR.....	72
Table 3.2	Antibodies used for Western Immunoblotting Experiments. ....	73
Table 5.1	Lung morphometry of 14-day-old rat pups treated with 0.9 % saline or doxycycline (20 mg/kg twice daily). ....	115

## ABBREVIATIONS AND UNITS

---

The following abbreviations, definitions and units have been used throughout this thesis, in addition to those abbreviations commonly accepted.

°C.....	degrees Celsius
-/-.....	knockout
[ <sup>32</sup> P].....	<sup>32</sup> Phosphorus
5-HPETE.....	5(S)-hydroperoxy-6- <i>trans</i> -8,11,14- <i>cis</i> -eicosatetraenoic acid
5-LO.....	5-lipoxygenase
A.....	absorbance
AA.....	arachidonic acid
<i>ad libitum</i> .....	(Latin, 'without preparation')
ADP.....	adenosine diphosphate
ANOVA.....	analysis of variance
ATP.....	adenosine triphosphate
B.....	percentage bound
BAL.....	bronchoalveolar lavage
BLT.....	LTB <sub>4</sub> receptor
B <sub>0</sub> .....	maximum binding
bp.....	base pair

BPD ..... bronchopulmonary dysplasia

Ca<sup>2+</sup> ..... calcium ion

CaCl<sub>2</sub> ..... calcium chloride

cDNA ..... complementary deoxyribonucleic acid

Ci ..... Curie(s)

CINC-1 ..... cytokine induced neutrophil chemoattractant

CO<sub>2</sub> ..... carbon dioxide

cPLA<sub>2</sub> ..... cytosolic phospholipase A<sub>2</sub>

cpm ..... counts per minute

CREB ..... cyclic AMP response element binding protein

C<sub>T</sub> ..... threshold cycle

CysLT ..... cysteinyl LT receptor

d ..... postnatal day

Da ..... alveolar diameter

DMSO ..... dimethyl sulphoxide

DNA ..... deoxyribonucleic acid

dNTP ..... deoxy nucleic acid triphosphate

dpm ..... disintegrations per minute

E of reaction .. ..... efficiency of reaction

E ..... embryonic day

ECM ..... extracellular matrix

EDTA..... ethylenediaminetetraacetic acid di-sodium salt

EGF ..... epidermal growth factor

*et al*..... *et alii* (Latin, 'and others')

EtBr ..... ethidium bromide

EtOH..... ethanol

F value ..... contribution of the independent variables in predicting the dependant variable

FA..... field area

FGF..... fibroblast growth factor

FiO<sub>2</sub> ..... fraction of inspired oxygen

FLAP ..... 5-LO activating protein

Flk-1 ..... fetal liver kinase

Flt-1 ..... *fms*-like tyrosine kinase

*g*..... acceleration due to Earth's gravity (9.8 m·s<sup>-2</sup>)

*g*..... gram(s)

*h*..... hour(s)

H<sub>2</sub>O..... water

H<sub>2</sub>O<sub>2</sub> ..... hydrogen peroxide

HBSS ..... Hank's Balanced Salt Solution

Hg ..... mercury

HIF ..... hypoxia-inducible factor

*i.e.* ..... *id est* (Latin, 'that is')



IHC ..... immunohistochemistry

IL ..... interleukin

kb ..... kilobase(s)

l ..... litre(s)

LB media ..... Luria-Bertani media

LB<sub>AMP</sub> ..... LB with ampicillin

LDH ..... lactose dehydrogenase

LIC ..... lipid containing interstitial cell

LT ..... leukotriene

m ..... meter(s)

M ..... moles·l<sup>-1</sup>

min ..... minute(s)

MIP-2 ..... macrophage inflammatory protein-2

MMP ..... matrix metalloproteinase

mRNA ..... messenger ribonucleic acid

MT-MMP ..... membrane-type MMP

n ..... number of animals

NaAc ..... sodium acetate

NaCl ..... sodium chloride

NADH ..... coenzyme nicotinamide adenine dinucleotide

NaN<sub>3</sub> ..... sodium azide

NSB ..... non-specific binding

*N*-terminal..... amino-terminal

O<sub>2</sub>..... molecular oxygen

O<sub>2</sub>..... (also used for hyperoxia)

O<sub>2</sub><sup>-</sup> ..... superoxide anion

OD ..... optical density

OH<sup>·</sup> ..... hydroxyl radical

*p* value ..... probability of incorrectly rejecting the null hypothesis

P/A..... perimeter to airspace ratio

PA..... plasminogen activator

p<sub>a</sub>CO<sub>2</sub>..... partial pressure of carbon dioxide in arterial blood

p<sub>a</sub>O<sub>2</sub> ..... partial pressure of oxygen in arterial blood

PAS..... Periodic acid-Schiff

PCR ..... polymerase chain reaction

PDGF..... platelet derived growth factor

PECAM..... platelet-Endothelial Cell Adhesion Molecule

*pg.* ..... page

pO<sub>2</sub>..... partial pressure of oxygen

RDS ..... respiratory distress syndrome

RIA ..... radioimmunoassay

RNA ..... ribonucleic acid

ROS ..... reactive oxygen species

RT..... reverse transcription

s ..... second(s)

SD..... standard deviation of the mean

SDS..... sodium dodecylsulphate

SEM..... standard error of the mean

SISA ..... specific internal surface area

SP ..... surfactant protein

T ..... total binding

TBS..... tris-buffered saline

TGF ..... transforming growth factor

$T_{\text{sept}}$ ..... septal thickness

TIMP ..... tissue inhibitor of metalloproteinase

TNF ..... tumor necrosis factor

Tris-Cl ..... tris[hydroxymethyl]-amino methane hydrochloride

tRNA ..... transfer ribonucleic acid

TUNEL..... terminal deoxynucleotidyl transferase UTP nick end labeling

uPA..... urokinase plasminogen activator

V ..... volts

Vasp..... volume of airspace

VEGF ..... vascular endothelial growth factor

VEGFR..... VEGF receptor

Vp..... volume of parenchyma

WT..... wild-type

Mathematical prefixes

k..... kilo ( $10^3$ )

c..... centi ( $10^{-1}$ )

m..... milli ( $10^{-3}$ )

$\mu$ ..... micro ( $10^{-6}$ )

n..... nano ( $10^{-9}$ )

p..... pico ( $10^{-12}$ )

***1.1 DEVELOPMENT OF THE LUNG***

The development of a viable gas-exchange area culminates an intricate sequence of events in which the epithelial cells of the prospective lung invade the surrounding mesenchyme, while increasing in size and complexity by branching continuously outwards. Post-embryonic lung development, occurring mostly during fetal life, is divided into four overlapping phases, based on morphometrical observations that distinguish one phase from the next; the pseudoglandular, canalicular, saccular and alveolar stages. These stages of lung development are shown schematically in Figure 1. I will first review aspects of the early stages of lung development before concentrating on the development of the alveoli, which is the focus of this thesis.

The lung bud first appears as a ventral outpouching from the primitive foregut at gestational day (E) 26 in the human fetus. The laryngotracheal grooves appear laterally on both sides and, as they deepen, begin to separate the lung bud from the prospective oesophagus in a caudocranial direction. This early embryonic period continues as the lung bud elongates and divides dichotomously, forming the two major bronchi (2). By about 4.5 weeks the lung has two small saccules on the left-hand side and three on the right. These form the prospective lobar bronchi and lung lobes. By the 7th week, successive dichotomous divisions have formed the future airway tree, as far down as the subsegmental branches.

The pseudoglandular phase, is so named because the lung resembles a small gland, with the lung epithelial branches surrounded by mesenchyme. The entire set of airway divisions are complete by the end of the pseudoglandular period, at about 16 weeks of age (27). During this phase the pseudostratified epithelial cells decrease in height, with successive branching, and form columnar cells. At this stage the epithelial tubes contain no lumen.

When the prospective gas-exchanging tissue becomes visible in the light microscope the next phase of lung development, the canalicular stage, is considered to have begun. This transition from pseudoglandular to canalicular stage has been described as the 'birth of the acinus' (30). Terminal and respiratory bronchioles are seen by the end of this phase. A lumen is present in many tubules, epithelial cells become more cuboidal than columnar and their glycogen content increases. Differentiation of cells throughout lung development occurs in a centrifugal manner so that the first ciliated cells, and also the goblet and basal cells, appear first in the central airways and spread to the more peripheral tubules. The mesenchyme thins out and is invaded by capillaries, which form a loose network and eventually rearrange to lie close to the epithelial layer of the tubules. Towards the end of the canalicular stage epithelial cells begin to differentiate into type I and type II cells, with the type II cells maturing to contain lamellar bodies which store the components of surfactant (123).

At around 24 weeks of gestation, the terminal airways form clusters of widened air spaces termed saccules, hence this is called the saccular stage of lung development (27). During this phase the airspaces distal to the bronchioles lengthen and widen, and the last

generations of airspaces are added on, so that the parenchyma of the prospective gas-exchange region increases dramatically. Numerous developing air sacs open up at this stage, although the dividing walls remain thick and cellular. The cuboidal epithelial cells show a rapid decrease in glycogen content and an increase in lamellar bodies is observed within cells that can now be classed as type II pneumocytes. Several studies have demonstrated that the type I cell is a derivative of the type II cell (3, 4). Many type II cells, especially those in close contact with capillaries lose their ability to produce surfactant and thin to become the squamous type I epithelial cells (3).

The final stage of lung development involves maturation of the saccules into functional alveoli, through a process of subdivision known as septation. In the human, the alveolar stage begins around 36 weeks of gestation, and is thought to continue to some extent up to 3 years of postnatal life (27). The process of septation will be discussed in more detail in subsequent sections.

### ***1.1.1 Comparative lung development***

The process of lung development described above follows a similar pattern in most species, with the main difference being the timing of the processes, which depends on the animal's maturity and mobility at birth. A precocial animal is 'capable of moving around on its own soon after birth' and includes animals such as sheep and guinea pigs; these species septate mainly *in utero* (8, 46). Rats and mice, however, septate after birth; they are born hairless, with their eyes closed and have little locomotive ability, and are therefore classed as altricial animals (10, 31). As mentioned above, humans begin

septation *in utero* and are therefore a precocial species. Figure 1.2 shows the timing of the stages of lung development in the human and rat.

### ***1.1.2 Cell proliferation***

Studies of fetal rats have shown that total protein and DNA levels in the lung begin to increase rapidly at the beginning of the pseudoglandular phase (E 17). Using the tritiated thymidine incorporation method, Adamson and King (5) demonstrated that maximal cell proliferation occurred at E 17 and that cell division declined from then on. The proportion of cells that are epithelial rise up to E 20, with the number of dividing cells that are interstitial (mostly fibroblasts) falls correspondingly. At E 21 this pattern has switched, with low levels of epithelial cell division and increased fibroblast proliferation. Endothelial cells show a small but steady increase in division throughout gestation in the rat.

### ***1.1.3 Vascular development***

There is some disagreement about the development of the vasculature of the lung. As the lung buds form and begin to branch they are immersed in a mesenchymal bed containing a loose vascular network, derived from the vascular network of the foregut. Arteries differentiate from stretches of this network that lie alongside the airways and eventually connect to pulmonary arteries that have grown towards to lung anlage from the sixth branchial arch (172). Other experiments indicate that the pulmonary artery is the most cranial vessel of a system of ventral splanchnic vessels connecting the pulmonary plexus with the dorsal aorta, and the only vessel to persist, the others being transient (79).



It is generally accepted that the pulmonary arteries then branch in association with the airways.

It is known that vascular growth in the embryo occurs by two main processes 1) vasculogenesis; the development of blood vessels from isolated vascular lakes within solid mesenchyme and 2) angiogenesis; the branching of new vessels from pre-existing ones. De Mello *et al.* (53) identified both these processes in the lung and elucidated a probable sequence of events in the development of a mature pulmonary vasculature in the mouse from E 9 to term. They showed that central branching occurs from the large blood vessels up to seven generations along an axial artery to one lung. At the same time, intercellular spaces develop within the lung's mesenchyme, this space increases and cells reform to provided a flattened endothelium surrounding the space. These isolated lakes increase in size and number and adjacent lakes coalesce to form sinusoidal spaces. Eventually the central and peripheral vessel systems fuse and join together; the majority of the increasing complexity of the vascular system is due to angiogenesis from the peripheral sinusoidal system (53). A similar developmental pattern has recently been demonstrated in the human fetal lung (108).

However, Hall *et al.* recently proposed a different mechanism of pulmonary artery formation (75). Their studies on 10 human fetuses suggest that from at least 34 days of gestation onwards, the intrapulmonary branching system develops by continuous expansion of the mesenchymal capillary plexus, whereby the intrapulmonary arteries are formed by sustained addition of newly formed endothelial tubes at the lung periphery. This mechanism is supported by the evidence that the arteries increase in size with age

and become invested with smooth muscle cells that also mature with age judged by their cytoskeletal protein expression. Thus the more proximal arteries have a more mature cytoskeleton during development than the peripheral arteries (75).

Therefore two distinct potential mechanisms exist for the development of intrapulmonary artery formation. However, both hypotheses agree that the development of the pulmonary arteries in humans is closely related to the branching of the airways.

### **1.2 ALVEOLAR DEVELOPMENT**

As mentioned previously, development of the alveoli is the final stage in lung development (though recently it has been suggested that the stage of vascular maturation is a new phase occurring after the alveolar period (173)). After the saccular phase, alveolarization starts with the appearance of low ridges along both sides of the preexisting saccular walls, these ridges then elongate and incompletely subdivide the saccules into smaller units, the alveoli (29). This also happens within the transitory channels, which then become alveolar ducts. The new interalveolar walls are referred to as secondary septa because they arise from the intersaccular walls which are the primary septa present at birth . These secondary septa are relatively thick and contain a double capillary network flanking a central sheet of connective tissue (Figure 1.3). Fibers of elastin are often found at the tips of the secondary septum (or just below a capillary loop if the capillaries from either edge of the septum are joined together); it is now well accepted that interalveolar walls will appear along the primary septum where elastin has been deposited (29) (Figure 1.3). Due to this unique arrangement of capillaries and elastin, Burri *et al.* have described a likely mechanism of secondary septal formation,

namely that new alveoli are formed by the alternate upfolding of one of the two capillary layers on either side of the primary septa (28). Consequently of this implies that if the double capillary network does not exist, no further septation is possible (34).

### ***1.2.1 Microvascular maturation***

The transformation from an immature septa (containing a double capillary network) to a thin, mature septa (with a single capillary network) is the last step in the development of a functional alveoli, and has been termed the stage of microvascular maturation. At this time the absolute amount of interstitial tissue decreases by 30 %, despite a 55 % increase in lung volume (164). Due to the reduction of the interstitial layer within the septa, the capillaries from either side of the septum come into direct close contact in places, and will then merge together into one (31, 34). Microvascular maturation overlaps with the end of alveolarization, occurring in the 2nd – 3rd postnatal week in rats and at about 6 months of life in the human.

### ***1.2.2 Apoptosis***

Apoptosis (programmed cell death) occurs unaccompanied by an inflammatory reaction and leads to immediate phagocytosis of individual cells by their healthy neighbors. Apoptosis has recently been shown to be a necessary event in the restructuring of the initial alveolar structures. In the late alveolar stage and during the phase of microvascular maturation the short, thick secondary septa are turned into tall, thin interalveolar walls, the double capillary layers are transformed into a single capillary layer with a high meshwork density, and the central layer of connective tissue is reduced to a fibrous meshwork interwoven with the capillary network (29, 31). While the volume of the lung

increases by about 25 % during this stage (93), the number of fibroblasts decreases by 10-20 % and the number of total epithelial cells decreases by 10 % (27, 93). In addition to this, the number of type II cells actually decreases by more than 20 %, due to differentiation into type I cells.

It has been shown that DNA fragmentation as assessed by terminal deoxynucleotidyl transferase UTP nick end labeling (TUNEL) staining (a classic apoptosis marker) increased 8-fold toward the end of the 3rd week of postnatal rat lung development, when compared to the days before and after this time point (147). The apoptotic cells were identified as fibroblasts and type II epithelial cells. Two subsets of fibroblasts are identified in the postnatal rat lung, lipid-containing interstitial cells (LICs) and non-LICs. Awonusonu *et al.* (14) demonstrated that the apoptosis occurred primarily, if not exclusively, in LICs. The authors suggest that this may indicate a specific role for LICs during alveolarization, and suggest that this may be due to their role in storing retinyl esters, which are converted to retinoic acid before septation.

### ***1.2.3 Intussusceptive growth***

In addition to vasculogenesis and angiogenesis, a novel method of blood vessel formation, designated intussusceptive angiogenesis, was reported by Burri *et al.* in 1990 (32). This group reported that the rat lung increased its capillary surface area more than 20 times and the capillary volume more than 35 times in the first 8 postnatal weeks (32). Instead of observing a great number of capillary sprouts to achieve this massive growth, they found tiny holes in the vascular casts. These holes were found to correspond to slender transcapillary tissue pillars. They are thought to occur by a zone of contact

forming between endothelial cells of the opposite walls and leading to the formation of the pillar, which is then invaded by interstitium. These slender pillars then have the ability, with no further structural alteration, to form a full size capillary mesh.

### **1.3 BRONCHOPULMONARY DYSPLASIA**

Bronchopulmonary dysplasia (BPD) was first described by Northway *et al.* in 1967. He described the clinical, pathological and radiologic changes evident in premature infants with severe respiratory distress syndrome (RDS) who had been treated with elevated oxygen concentrations (80 – 100 %) and mechanical ventilation (40). The pathology of the progression of BPD was divided into four stages. Stage I included hyaline membrane disease and atelectasis, consistent with RDS. Histological examination of infants during stage II showed necrosis and repair of alveolar epithelium with emphysematous coalescence of alveoli; increased patchy bronchiolar necrosis with patchy squamous metaplasia; and focal thickening of the capillary basement membranes. Stage III, the transition to chronic disease, consisted of widespread bronchial and bronchiolar mucosal metaplasia and hyperplasia, marked secretion of mucous and alveolar coalescence progressing to spherically circumscribed groups of emphysematous alveoli with atelectasis of surrounding alveoli. By stage IV there was marked hypertrophy of peribronchiolar smooth muscle, with focally circumscribed groups of emphysematous alveoli and atelectatic alveolar areas. There was focal thickening of basement membranes with separation of capillaries from alveolar epithelium. Vascular lesions as well as marked heterotopia of alveolar epithelial cells types and widespread metaplasia of bronchiolar mucosa were also seen. These progressive pathological changes of the

immature lung affected both the parenchyma and airways and appeared to alter normal lung growth, hence the name bronchopulmonary dysplasia (16).

In 1989 the diagnostic criteria for development of BPD was defined as requirement for supplemental oxygen longer than 28 days of age to maintain a PaO<sub>2</sub> higher than 50 mmHg, combined with chest radiograph findings characteristic of BPD (131). Since the initial description of the disease, the etiology of BPD has changed for a number of reasons. Antenatal glucocorticoid therapy, gentler ventilation strategies and surfactant treatments mean that fewer infants develop severe lung injury. At the same time, however, these same interventions lead to survival of more very low birth weight infants. BPD is now infrequent in infants of more than 1,200 g birth weight or with gestational age greater than 30 weeks (115). However, BPD is now the most common complication of care of infants born weighing < 1 kg (154). The more recent findings in lungs of infants dying from BPD is that there is less fibrosis, but there are also fewer and larger alveoli (indicative of inhibited septation), and decreased pulmonary microvascular development (18, 84). These pathologies characterize the 'new BPD', and appear to result from an interference with normal alveolar and vascular development (89, 90).

#### ***1.4 FACTORS AFFECTING ALVEOLAR DEVELOPMENT***

Some of the factors that are discussed below, such as dexamethasone and hyperoxia may be causative in the development of the 'new' BPD. Others such as retinoic acid, may actually lead to an improvement in the outcome of these premature infants.

### ***1.4.1 Dexamethasone***

In 1985 Massaro *et al.* showed for the first time that administration of dexamethasone (a glucocorticoid) to rat pups from postnatal day (d) 3 to d 14 markedly impaired saccule septation and diminished the extent of increase of alveolar surface normally observed during this time (118). This inhibition of septation was maintained up to at least d 60, leading to the hypothesis that there is a critical period during which septation can occur. This group further discovered that after 2 days of treatment dexamethasone-treated rat pups had a 20 % thinner gas exchange wall, a 35 % lower volume density and absolute volume of interstitial fibroblasts and a 45 % greater volume density of type II cells. They concluded that dexamethasone accelerates alveolar wall thinning and suggested that dexamethasone diminishes replication of fibroblasts (and type II cells to a lesser extent), impairs conversion of type II to type I cells, but does not decrease replication of endothelial cells. In 1995, Tschanz *et al.* demonstrated that the effects of glucocorticoids were mainly due to their induction of precocious microvascular maturation. Rat pups treated with Decadron® (a glucocorticoid) from d 2 to d 15 had significantly reduced interstitial mass, decreased outgrowth of new septa and alveolar walls that were slender and contained larger areas with a single-capillary network (164). As described in the section on alveolar development, after maturation of the pulmonary vasculature no further alveolarization is possible, except in regions containing remnants of the immature capillary structure. One week after withdrawal of Decadron® the alveolar walls appeared thicker (likely due to fibroblasts proliferating once the inhibitory effect of glucocorticoids was stopped) and the septa again contained sections with a double capillary network, however despite this 'second round' of septation, the full complement of alveoli was

unable to be formed and the d 60 lung was emphysematous in nature (large and few airspaces) (164). Finally, studies investigating the effects of glucocorticoids on later lung development showed that dexamethasone administered to rat pups during the 3rd and 4th postnatal week had no inhibitory effect on alveolar formation, further supporting the concept that there is a critical period for septation to occur (20).

#### ***1.4.2 Retinoic Acid***

More recently Massaro and Massaro demonstrated that treatment with retinoic acid prevented the low number of alveoli and the low body mass-specific gas-exchange surface area produced by treatment with dexamethasone (119), these results were later confirmed (167). However, a recent paper showed no difference between treatment with dexamethasone and treatment with dexamethasone plus retinoic acid (both from d 3 to d 14) in rat lungs at 1 month (152). Research in our laboratory has been unable to reproduce the initial work on rescuing the inhibited alveolarization from dexamethasone with retinoic acid (106), shedding doubt on the real benefits of retinoic acid on alveolar development. Further, retinoic acid, when administered alone (in rat pups from d 3 to d 14), was also shown to increase the number of alveoli by 50 %, however this was achieved without an increase in body-mass specific surface area (119). The authors attributed this to an unknown regulatory mechanism to prevent unneeded surface area, and suggest that it may be related to the 22 % larger volume of gas-exchange tissue in the retinoic acid treated pups (119), however this still appears to be a curious result.

In newborn rats exposed to > 90 % O<sub>2</sub> from d 3 to d 14 (which inhibits alveolar development) and concurrently treated with retinoic acid from d 3 – d 13, retinoic acid



did not improve septal formation or decrease airspace size in animals (167). However, a worrying result of this study was the high mortality (50 %) of the newborn rats exposed to hyperoxia, as well as a 13 % mortality of the untreated rats, which is unusual and may have confounded the results.

### **1.4.3 Hypoxia**

Lung function in humans native to high altitude (highlanders), who are born into a low  $pO_2$  environment, have altered lung function when compared to individuals native to sea level (lowlanders). As well as possessing a larger residual volume, highlanders have larger and more numerous alveoli (23). As the conducting airways are formed before birth whilst protected from the full impact of low  $pO_2$  *in utero* by maternal adaptive responses, they develop similarly to those of lowlanders. However the majority of the alveoli are formed after birth and under the stimulatory effect of low inspired  $pO_2$  at high altitude. This has led to a hypothesis of dysnaptic growth (23), where the gas-exchange region is too large to be adequately supplied by the cross-sectional area of the conducting airways. This would explain the low maximum flow rate per lung volume and low upstream conductance in highlanders compared to lowlanders (23).

Interestingly, when rats were placed in a 10 %  $O_2$  environment from birth to d 7 or d 12, they had larger air spaces than pups breathing room air (125). This result was confirmed by Massaro and colleagues who concluded that a hypoxic environment actually inhibited normal postnatal septation (121). Later studies by the same group used a slightly higher  $pO_2$  (13 %  $O_2$ ), acclimated the dams to hypoxia for 3 weeks prior to mating, and maintained dams in 13 %  $O_2$  throughout gestation (120). Results conclusively

demonstrated that pups born into a hypoxic environment and maintained in 13 % O<sub>2</sub> until d 40 do not undergo septation. Further, pups removed from the hypoxic-environment at d 15 and kept in room air until d 40 also did not septate, leading the authors to again conclude that a 'critical period' for septation exists (120).

### **1.5 HYPEROXIA**

The primary physiological role of the lung is to provide O<sub>2</sub> and remove CO<sub>2</sub>. Molecular oxygen (O<sub>2</sub>) is essential for the survival of all aerobic organisms. The major pathway for O<sub>2</sub> utilization is through mitochondrial cytochrome oxidase for the reduction of oxygen to H<sub>2</sub>O with the formation of ATP. The hydrolysis of ATP to ADP is then the immediate energy source for practically all energy-requiring processes in the cell (95).

Partially reduced and highly reactive metabolites of O<sub>2</sub> may be formed during the electron transfer reactions, these are referred to as reactive oxygen species (ROS) due to their higher reactivities relative to molecular O<sub>2</sub>. These O<sub>2</sub> metabolites include superoxide ion (O<sub>2</sub><sup>-</sup>) and hydrogen peroxide (H<sub>2</sub>O<sub>2</sub>), formed by one- and two-electron reductions, respectively. In the presence of transition metal ions, the even more reactive hydroxyl radical (OH<sup>•</sup>) can be formed (160). In rats, an average of about 10 trillion O<sub>2</sub> molecules are processed by each cell daily under basal conditions, and the leakage of partially reduced O<sub>2</sub> molecules is about 2 % (9).

ROS regulate critical steps in the signal transduction cascades and many important cellular events including protein phosphorylation, gene expression, transcription factor activation, DNA synthesis, cellular proliferation and apoptosis (70, 148). However the

realization that low concentrations of ROS operate as signaling mechanisms is relatively recent. ROS have been traditionally regarded as toxic by-products of metabolism with the potential to cause damage to lipids, proteins and DNA (76). One of the most damaging aspects of ROS is the reaction with polyunsaturated fatty acid side chains of membrane lipids initiating lipid peroxidation. The resulting lipid hydroperoxide products are potent inhibitors of cellular enzymes and can directly damage proteins or membranes (76).

Cells possess several antioxidant enzymes to protect against the potentially damaging effects of ROS, these include superoxide dismutase (which reduces  $O_2^{\cdot-}$  to  $H_2O_2$ ) and catalase (which reduces  $H_2O_2$  to  $H_2O$ ). Oxidative stress, therefore, can be defined as an imbalance between oxidant production and antioxidant capacity of the cell to prevent oxidative injury (160). Because the premature lung is deficient in its antioxidant capacity (12) exposure to oxygen is likely to lead to oxygen radical formation (68).

Safe sequestration of iron, which participates in the formation of  $OH^{\cdot}$ , is crucial in the lung's defense. Shah *et al.* initially described experiments demonstrating that supplementation of iron-free transferrin (the major iron transport protein) to hyperoxic-exposed preterm rabbits, increased the iron-binding capacity of plasma; but no improvement in histology was seen (149). Yang and colleagues, however, used a mouse line defective in transferrin to show that tolerance to hyperoxic lung injury was greater in hypotransferrinemic mice than in wild-type mice, as documented by histopathology and biochemical indexes of lung damage (177). This protection was associated with elevated levels of ferritin and lactoferrin, especially in alveolar macrophages, suggesting that these

molecules protect against oxidative stress, most likely via their capacity to sequester iron (177).

### ***1.5.1 Hyperoxia and Lung Development***

It has been demonstrated that exposing newborn animals to a hyperoxic environment can severely damage the lung and prevent septation of the saccules. Bucher and Roberts exposed newborn rats to greater than 0.95 FiO<sub>2</sub> for up to 12 days. The rat pups showed microscopic evidence of lung injury and retarded alveolar development, with secondary septal development delayed by as much as 88 %. There was also lower whole lung DNA content (50% of control), decreased lung-to-body-weight ratios (by as much as 18%), and significantly less compliance in the lungs (25). Subsequent studies demonstrated that growth of rat pups from birth until d 7 in > 97 % hyperoxia had no effect on the number of ventilatory units but, compared to controls, total lung volume and ventilatory unit volume were reduced 32% and 16%, respectively (138). Exposure of rat pups to hyperoxia for 7 days stopped alveolarization; the surface area to volume ratio (Sa/V) of the ventilatory unit was lower, alveolar number was the same as at birth, and the alveoli present were large (139).

In our own laboratory, exposure of neonatal rat pups to > 95 % O<sub>2</sub> causes marked interstitial and intra-alveolar edema and proteinosis. O<sub>2</sub>-exposed animals also had fewer and enlarged alveoli and alveolar ducts compared with air-exposed animals, with lung architecture similar to that of d 3 animals (22). These impressions were confirmed by morphometric measurements, which showed an increase in mean linear chord length, and

volume of airspace units, and a decrease in specific internal surface area and parenchymal/airspace volume (a measure of the complexity of the lung.) (22).

#### *1.5.1.1 Hyperoxic Exposure and Inflammation*

As mentioned above, prolonged exposure to oxygen in newborn rats results in lung damage characterized by interstitial and alveolar edema, followed by infiltration of protein, entry of cells and finally hemorrhage into alveolar space (39). This inflammatory sequence is accompanied by rapid neutrophil infiltration into the lung. Activated neutrophils are known to produce large quantities of ROS and nitrogen intermediates, as well as elastase and arachidonic acid metabolites that can damage the pulmonary parenchyma. In a study of chronic lung disease in premature baboons, Coalson and colleagues found that increased tracheal aspirate IL-8 and neutrophils preceded morphometric changes consistent with human chronic lung disease of prematurity (44).

In a neonatal rat model of hyperoxic damage, the potent neutrophil chemokines, cytokine-induced neutrophil chemoattractant-1 (CINC-1) and macrophage inflammatory protein-2 (MIP-2), were increased after exposure to > 95 % O<sub>2</sub> from birth to postnatal d 8 (54). Anti-CINC-1 and anti-MIP-2 treatment reduced the number of neutrophils in BAL, and, further, anti-chemokine treatment on d 3 or 4 inhibited alveolar septal thickening on d 6 (54). Neutrophil chemokines IL-8 and MIP-2 have previously been found to be induced in newborn mice and rabbits (51, 52). Further studies demonstrated that treatment with anti-CINC-1 prevented airway neutrophil influx and preserved lung compliance, alveolar development and lung proliferation in a rat model of BPD, where newborn rats are exposed to 95 % O<sub>2</sub> for 8 days (13).

Many different cells in the lung can express inflammatory mediators (94), but the alveolar macrophage is the most likely initial source of cytokines after exposure to hyperoxia (17). Rozycki *et al.* demonstrated that macrophages isolated from preterm rabbits showed a significant increase in cytokines (IL-1 $\beta$  and IL-8) after overnight incubation in 95 % O<sub>2</sub>; this response was not seen in term cells (145). Further, only the preterm and not the term macrophages had a significant increase in intracellular oxygen radical content after incubation in 95 % O<sub>2</sub> (145), suggesting that premature macrophages exhibit an enhanced inflammatory response to oxygen. The authors suggest that this may be one mechanism involved in early development of CLD in premature infants.

#### 1.5.1.2 *Hyperoxia and DNA Synthesis*

Exposure of newborn rats to 95 % O<sub>2</sub> for 1 wk also profoundly inhibits lung DNA synthesis (77). Recovery of synthesis in the same experiment did not occur during a second week in 60% O<sub>2</sub> (77). Indeed earlier work had previously shown that as little as 2 h exposure to 100 % O<sub>2</sub> caused a significant reduction in DNA synthesis in neonatal rat (174).

#### 1.5.1.3 *Hyperoxia and Apoptosis*

Exposure to high O<sub>2</sub> concentrations in the neonatal mouse lung has also been shown to increase apoptosis in the peripheral lung (122). The number of cells undergoing apoptosis increased the longer the exposure to O<sub>2</sub>, and the number of apoptotic cells correlated with lung injury (122).

### ***1.5.2 Hyperoxia and models of BPD***

As described above, 95 % O<sub>2</sub> during the period of alveolar development in the rat lung causes an almost complete inhibition of septation. In our laboratory we take the interpretation that this is a model of inhibited alveolar development as opposed to a model of BPD. However, one of the arguments against this model was, historically, that the dysplastic lesions observed in chronic human neonatal lung injury did not develop. On the other hand, the inhibited septation observed in the > 95 % O<sub>2</sub>-exposed rat pup is similar to that seen in cases of BPD in very premature infants, the so called 'new BPD' as described earlier, which describes the pathologic features seen in most intensive care units today (90).

#### ***1.5.2.1 Rat Model***

It is clear that the rat pup is not a perfect model, however most models are not. As the rat lung is in an immature state of structural development, it is obvious that these pups are well able to survive outside the womb. This is due to ventilation occurring through the bronchioles, as they are still in close contact with the vasculature at this stage (as in premature infants) and the immature saccules. Further the biochemical markers of lung development such as antioxidants and surfactant are already well developed in the neonatal rat (158). This is one of the reasons that such high O<sub>2</sub> concentrations are used in our experiments; to appreciably increase the oxidant : antioxidant ratio.

The rat is widely used to study lung development and inhibited lung development (116-118), as rat pups are relatively inexpensive, available in large numbers and easily manipulated (for instance a whole litter may be placed in hyperoxic chambers at the same

time). They also develop rapidly, thus alveolarization occurs in a discrete period from d 4 to d 14; even studying animals into relative maturity can be completed in about 4 months. As mentioned earlier, the progression of the stages of lung development are similar in the rat and the human, and it is very likely that the processes driving this development are also very similar. Yet the fact that the rat pup undergoes alveolarization postnatally abolishes the need for a model involving premature birth.

#### *1.5.2.2 60 % O<sub>2</sub> Newborn Rat Model*

Another model involving exposure of neonatal rats to 60 % O<sub>2</sub> for 2 weeks results in an overall, but inhomogeneous, reduction in lung cell DNA synthesis. Analysis of affected cell types suggested that inhibition of DNA synthesis affected endothelial cells more than interstitial cells, whereas DNA synthesis increased in type II pneumocytes (77). Areas of reduced DNA synthesis were interspersed with patchy areas of parenchymal thickening and active DNA synthesis, consistent with a direct effect of O<sub>2</sub> causing dysplastic lung cell growth, as was previously seen in premature infants and actually led to the term bronchopulmonary dysplasia (77).

#### *1.5.2.3 Premature Baboon Model of BPD*

Perhaps the most analogous model of BPD existing today is that of the prematurely delivered baboon, delivered at E 140 of a 185 day gestation (41). Coalson *et al.* found that alveolar formation was impaired in premature baboons that were treated with positive pressure ventilation and ventilated with 100 % O<sub>2</sub> for at least 1 week followed by approximately 80 % O<sub>2</sub> for 2 more weeks, compared with other premature baboons that were initially ventilated with 100 % O<sub>2</sub> and subsequently maintained with sufficient



inspired O<sub>2</sub> to keep normal arterial oxygen tension (60 – 80 mm Hg) (43). They also found non-uniform inflation, accumulation of ECM components, fibrosis, metaplasia and dysplasia of airway epithelial cells, and inflammation and edema. Further, morphometric analysis of long term survivors of this model of BPD showed a significant decrease in alveolar number, suggesting that the early injuries had a long term adverse effect on postnatal lung development (42). These studies highlight the importance of sustained hyperoxia in the development of the altered lung growth seen in BPD.

Further studies tested two ventilation strategies, either slow, deep ventilation or rapid, shallow ventilation on a model of BPD in lambs that are delivered prematurely and ventilated for 3 – 4 weeks after birth (7). Slow, deep ventilation was associated with less atelectasis and more alveolarization compared with rapid, shallow ventilation. They concluded that prolonged mechanical ventilation of preterm lambs disrupts lung development and produces pulmonary histopathologic changes that are similar to those seen in lungs of infants dying from BPD.

As various derivations of the hyperoxic model of inhibited alveolarization have been used for many years, a wealth of knowledge is available on numerous factors which change during or after the exposure period. However, only two growth factors have been shown to be unequivocally necessary for normal alveolar development. One is vascular endothelial growth factor (VEGF), which will be discussed in detail in the next section; the other is platelet derived growth factor-AA (PDGF-AA) (105).

## **1.6 VASCULAR ENDOTHELIAL GROWTH FACTOR AND ANGIOGENESIS**

### ***1.6.1 Angiogenesis***

As mentioned previously, two mechanisms of blood vessel development exist in the lung, and indeed throughout the body. The first is vasculogenesis which occurs when vessels are formed from undifferentiated mesodermal cells. Once the mesodermal cells differentiate into endothelial cells, they proliferate and organize into clusters or islands. These islands then send out endothelial cells to connect them to adjacent islands. Cells present between islands develop tight cell-cell interactions and organize around a central lumen forming a vessel. The second method is angiogenesis in which vascular structures are derived from existing vessels. The vessels send out sprouts of endothelial cells that connect to each other via cell-cell adhesion molecules and organize around a lumen extending the length of the vessel (142).

Proliferation of blood vessels is a process necessary for the normal growth and development of the lung. In the adults angiogenesis occurs infrequently, exceptions being during the female reproductive cycle (159) and during the body's normal repair process (107). However uncontrolled angiogenesis can often be pathological, for example during the vascularization of solid tumors or diabetic retinopathy vascularization of the retina (151).

Many factors that stimulate angiogenesis have been described. These include both basic (b) and acidic (a) fibroblast growth factors (FGF) which are mitogenic and chemotactic for endothelial cells, stimulate endothelial cell production of collagenase and plasminogen activator proteins capable of degrading the basement membrane (important

in angiogenesis) and induces cultured endothelial cells to form capillary-like tubes (99). Other angiogenic factors include PDGF, epidermal growth factor (EGF) and transforming growth factor-alpha (TGF- $\alpha$ ) all of which directly stimulate endothelial cell migration and proliferation. Factors such as angiotropin stimulate endothelial cell migration but not proliferation, and angiogenin stimulates angiogenesis but has no effect on endothelial cell proliferation or migration. Finally TGF- $\beta$  and tumor necrosis factor- $\alpha$  are inhibitors of endothelial cell proliferation but can induce three-dimensional tube formation and angiogenesis (99). There are also factors which can act to inhibit angiogenesis (angiostatic steroids, platlet factor IV, TGF- $\beta$ , thrombospondin, TNF- $\alpha$  and  $\gamma$ -interferon (99). Therefore, it is apparent that the regulation of angiogenesis is a complex process which requires precise control.

### ***1.6.2 Vascular Endothelial Growth Factor***

One of the most fundamental angiogenic factors is vascular endothelial growth factor (VEGF); it is a highly specific mitogen for vascular endothelial cells and causes angiogenesis and endothelial cell proliferation. VEGF was originally isolated from tumor cell lines in culture in the late 1970s where it was shown to increase microvascular permeability to plasma protein and was therefore originally named vascular permeability factor (58). Currently six species of VEGF exist, resulting from alternate splicing of VEGF mRNA. The major splice variants include; 121, 165, 189 and 206 amino acids (aa), each one comprising a specific exon addition. More recently other splice variants of 145 (137) and 183 (88) aa have also been described. Most cell types produce several VEGF variants simultaneously. VEGF<sub>121</sub> and VEGF<sub>165</sub> are the predominant isoforms, but

VEGF<sub>189</sub> can also be expressed in most VEGF-producing cell types (15). The 165, 189 and 206 aa variants contain heparin-binding domains, which help anchor them in the extracellular matrix and are involved in binding to heparin sulphate and presentation to VEGF receptors. These heparin-binding forms have more mitogenic activity than the soluble VEGF<sub>121</sub>; VEGF<sub>165</sub> is also secreted though a significant proportion remains bound to the cell surface and the ECM (83). The mouse and rat exhibit similar VEGF splice variants to the human, with one amino acid less in each variant; hence, VEGF<sub>188</sub>, VEGF<sub>164</sub> and VEGF<sub>120</sub> (63).

VEGF shares significant homology with PDGF, conserving all eight cysteines found in the PDGF-B chain (163). VEGF is also 53% identical to placenta growth factor (109). In 1996 Olofsson *et al.* (132) further described a novel endothelial cell-specific growth factor structurally related to VEGF, designated VEGF-B. In the same year the discovery of VEGF-C further expanded the VEGF family (91). The following discussion will focus exclusively on VEGF (also referred to as VEGF-A) and its actions.

The VEGF receptor family consists of three high-affinity transmembrane tyrosine kinase receptors containing multiple IgG-like extracellular domains. VEGF-A binds to VEGF receptor 1 (VEGFR1, also known as flt-1 or fms-like tyrosine kinase-1) and VEGFR2 (also known as KDR/flk-1 or fetal liver kinase 1). VEGFR3 (flt-4) is only activated by VEGF-C and VEGF-D (87). Endothelial cells also express two other VEGF receptors which bind VEGF-A, neuropilin-1 and neuropilin-2 (129). Neuropilin-1 binds VEGF<sub>165</sub>, and when co-expressed in cells with VEGFR2 enhances binding to VEGFR2

and VEGF<sub>165</sub>-mediated chemotaxis, suggesting that neuropilin-1 may present VEGF<sub>165</sub> to VEGFR2 and thereby enhance the effectiveness of VEGFR2 signaling (74).

VEGFR1 and VEGFR2 act through different signal transduction pathways. Waltenberger *et al.* initially described that VEGFR2 transduced signals for mitogenicity, chemotaxis, actin reorganization, and changes in gross morphology of the cell, whereas VEGFR1 did not transduce any of these effects although it bound VEGF with a higher affinity than VEGFR2 (169). Supporting these experiments it was later found that although targeted disruption of either VEGFR1 or VEGFR2 in mice prevents normal vascularization and embryonic development, the two knockouts have distinctly different phenotypes.

VEGFR1 knockout mice possess mature, differentiated endothelial cells but have large, disorganized vessels (64). This defect seems to result from an overproduction of endothelial progenitor cells rather than vascular disorganization, and is consistent with a negative regulatory role for VEGFR1 (65). Hiratsuka *et al.* demonstrated that mice expressing only the extracellular domain of VEGFR1 (i.e. lacking the tyrosine kinase signaling domain but maintaining the ability to bind VEGF) develop normally, without any defect in embryonic development or angiogenesis (81). Further, overexpression of the naturally occurring soluble VEGFR1 inhibits VEGF-induced migration and proliferation of human umbilical vein endothelial cells by forming an inactive complex with VEGF and the full-length VEGFR2 (96, 143), again corroborating the concept that the VEGFR1 receptor acts to negatively regulate binding to the VEGFR2 receptor.

VEGFR2-deficient mice however, possess no hematopoietic precursors and do not produce either differentiated endothelial cells or organized blood vessels (142, 150). Porcine aortic endothelial cells possessing no VEGF receptors display chemotaxis and mitogenesis in response to VEGF when transfected with a plasmid coding for VEGFR2 but not VEGFR1 (169). The main functional responses to VEGF signaling, therefore, have been shown to be through activation of VEGFR2.

The most widely reported function of VEGF is to act as a regulator of both physiological and pathological angiogenesis through stimulation of migration and mitogenesis of endothelial cells. VEGF also upregulates interstitial collagenase expression in human umbilical vein endothelial cells (166) and matrix metalloproteinase expression in vascular smooth muscle cells (170). Expression of serine proteases urokinase-type and tissue-type plasminogen activators (PAs), as well as plasminogen activator inhibitor-1, is also induced by VEGF in cultured bovine microvascular endothelial cells (136). As will be discussed later, the production of these enzymes are likely to aid the degradation of the surrounding ECM to allow for outgrowth of new vessels.

Another important action of VEGF is to maintain and protect the vasculature. Evidence for this protective effect initially came from experiments showing that perivascular gene transfer of VEGF inhibits neo-intima formation in rabbit carotid arteries (100). Zachary *et al.* described this protective effect as a VEGF-induced enhancement of endothelial functions that mediate the inhibition of vascular smooth muscle proliferation, enhanced vascular endothelial cell survival, suppression of thrombosis, and anti-inflammatory

effects (178). Many of the vascular protective effects can be attributed to the ability of VEGF to stimulate production of nitric oxide and prostacyclin.

### ***1.6.3 VEGF and lung development***

An absolute requirement for VEGF during embryonic development has been demonstrated by the fact that VEGF-null mice embryos die at around E 9.5 (35, 62). VEGF has been shown to be uniformly present in the airway epithelium and subepithelial matrix of E 11.5 mouse lungs (80). At later time points VEGF was restricted to the branching tips of airways in the distal lung and VEGF<sub>164</sub> was the predominant isoform present (80). Another study demonstrated again that VEGF<sub>164</sub> was the predominant isoform in fetal mouse lungs at E13, but that VEGF<sub>164</sub> then decreased with a concurrent increase in VEGF<sub>188</sub>, so that prior to birth VEGF<sub>188</sub> was the predominant isoform (130). VEGF<sub>188</sub> remained the predominant VEGF isoform throughout the neonatal period, although levels dipped (along with total VEGF) on d 10.

It has been demonstrated that grafting VEGF<sub>164</sub> beads onto lung explants locally stimulates a marked neovascular response (80). Further, targeted exon deletion of VEGF<sub>188</sub> and VEGF<sub>164</sub> led to mice with significantly reduced airspace formation (retarded septation) and capillary growth (130), demonstrating the fact that different VEGF isoforms have distinct functions in vascular development. In the midtrimester human fetal lung, immunostaining for VEGF protein was also seen primarily in airway epithelial cells, however after 4 d of incubation of an explant in 20 % O<sub>2</sub>, VEGF protein was localized primarily in the basement membrane subjacent to airway epithelial cells, suggesting that translocation of VEGF protein occurs after its synthesis in the epithelium

(1). The authors suggest that localization of VEGF to the basement membrane of airway epithelial cells may be important for directing capillary development in the human lung.

Interestingly, when VEGF is overexpressed, embryonic development is also disrupted. A two- to threefold overexpression of VEGF results in severe abnormalities in heart development and embryonic lethality at E 12.5 – E 14 (124). VEGF was also overexpressed in the developing pulmonary epithelium under the control of promoter from the human SP-C gene (the SP-C-VEGF DNA construct was microinjected into oocytes), so that abnormalities were confined to the lung (179). On E 15 and E 17 lungs consisted of large, abnormally dilated tubules, the number of acinar buds and saccules was markedly reduced, and the amount of mesenchyme was decreased. Vasculogenesis was markedly advanced in VEGF overexpressing embryos; at E15 vessels demonstrated increased luminal diameter and were found in close contact with the respiratory epithelium, a situation that does not normally occur until E 17 (179). Further, maturation of Type II cells and cytodifferentiation into Type I cells was inhibited in this model, suggesting that VEGF affects more than endothelial cells.

Some of the first evidence that angiogenesis was necessary for normal development of the alveoli came from studies of the Fawn-Hooded rat, which demonstrates reduced alveolarization in the newborn and adult and reduced pulmonary arterial density in the adult (101). Subsequent studies showed that inhibiting angiogenesis with thalidomide, fumagillin or SU-5416 (a VEGFR2 blocker) all also resulted in decreased alveolarization as well as arterial density (86). Other evidence that the development of the lung alveoli is dependant on angiogenesis comes from an experiment where tracheal occlusion, which



stretches the lung by retaining lung fluid, led to tightly coordinated capillary and alveolar proliferation suggesting some joint coordination of their growth (57). Cyclical stretch of a mixed primary pulmonary cell culture upregulated VEGF, suggesting that VEGF may cause the increased angiogenesis and alveolarization seen during tracheal occlusion (126).

#### ***1.6.4 VEGF and neonatal hyperoxic lung injury***

Maniscalco and colleagues have previously examined the effects of hyperoxia on VEGF in the adult and neonatal rabbit lung. Normal adult lungs and isolated type II cells have relatively little VEGF mRNA, however after recovery from acute O<sub>2</sub> injury, alveolar epithelial cells showed increased VEGF expression (112). Newborn rabbits exposed to 100 % O<sub>2</sub> for 9 d showed an 80 % reduction in lung VEGF mRNA expression, decreased alveolar epithelial cell VEGF expression, and decreased VEGF immunostaining (111). Further work showed that the relative proportion of VEGF<sub>189</sub> mRNA declined significantly during hyperoxic injury of the newborn. Total VEGF lavage protein however increased early during hyperoxic exposure before decreasing to below normoxic levels on d 9 (171).

In the adult lung inhibition of VEGFR2 causes lung alveolar septal cell apoptosis as well as a pruning of the arterial tree (92). Interestingly, transgenic mice that overexpress IL-13 show increased VEGF when exposed to 100 % O<sub>2</sub> and have enhanced survival compared to wild-type mice, which is in part, mediated by VEGF (48).

### 1.6.5 Hypoxia inducible factors

HIF(hypoxia inducible factor)-2 $\alpha$  was first described in 1997 as a transcription factor that is closely related to HIF-1 $\alpha$  and regulates VEGF expression (59, 162). HIF-1 $\alpha$  mediates transcriptional activation of VEGF by binding to a *cis*-acting hypoxia-response element located 1 kb 5' to the transcriptional start site of the human VEGF gene (67). The molecular mechanisms of sensing and signal transduction by which changes in O<sub>2</sub> concentration result in changes in HIF-1 $\alpha$  activity are poorly understood, but recent evidence suggests that the O<sub>2</sub> signal is converted to a redox signal (36, 72). Under hypoxic conditions, HIF-1 $\alpha$  mRNA and protein levels increase dramatically and the fraction of protein that is ubiquitinated decreases (155).

HIF-2  $\alpha$  exhibits very similar characteristics to HIF-1 $\alpha$  in properties of dimerization, DNA-binding and transcriptional activation, however their modes of expression are very different from each other (59). HIF-2 $\alpha$  mRNA is abundantly expressed in a variety of organs in the normoxic state, whereas HIF-1 $\alpha$  is ubiquitous at much lower O<sub>2</sub> levels. HIF-2 $\alpha$  was found to be expressed in the vascular endothelial cells around the middle of gestation and mRNA expression was markedly enhanced around partuition, while the low levels of HIF-1 $\alpha$  remained unchanged. These expression patterns were found to closely parallel the mRNA expression of VEGF, which was found to increase dramatically between d 5 and d 14 in the postnatal rat lung (59). HIF-2 $\alpha$  increases both basal and hypoxia-induced VEGF promoter activity in human MG63 osteoblast-like cells (6). Although HIF-2 $\alpha$  has been shown to colocalize with the VEGFR transcripts in the endothelial cells of blood vessels, more capillaries produced VEGFR1 and VEGFR2 than

HIF-2 $\alpha$ , suggesting that other transcription factors may be involved in regulating the expression of VEGF receptors in some capillaries (60). Initial data reported that HIF-2 $\alpha$ <sup>-/-</sup> mice die at mid-gestation with pronounced bradycardia (161). However, a recent publication showed that although half the embryos die of cardiac failure at E 13.5, the rest of the HIF-2 $\alpha$ <sup>-/-</sup> mice died within 2 – 3 h of birth from severe respiratory failure due to extensive lung collapse. Thinning of the alveolar septa at birth was impaired in HIF-2 $\alpha$ <sup>-/-</sup> due to impaired differentiation of epithelial cells, which also then produced less surfactant phospholipids, SP-A, SP-B and SP-D (47). Vascular development in these HIF-2 $\alpha$ <sup>-/-</sup> mice was normal in the pseudoglandular and canalicular stages (when VEGF levels were comparable to WT mice) however a subtle deficit in vascularization of the alveolar septa was detected in HIF-2 $\alpha$ <sup>-/-</sup> mice, which coincided with the time when VEGF increased in WT but not knockout mice. Alveolar capillaries also failed to remodel properly in HIF-2 $\alpha$ <sup>-/-</sup> mice and were not located close to the alveolar lumen as in WT mice (47).

#### ***1.6.6 VEGF and epithelial cells***

Immunoreactivity for VEGFR2 has been demonstrated in distal lung epithelial cells of human fetal lung tissue, and addition of exogenous VEGF to human fetal lung explants resulted in increased epithelium volume density and lumen volume density in the tissues (24). Cellular proliferation of distal airway epithelial cells, SP-A mRNA and protein and SP-C mRNA also increased with administration of VEGF, suggesting that VEGF may be an important autocrine growth factor in the developing human fetal lung (24). Studies by Compornolle and colleagues later showed that VEGFR2 was present in type II

pneumocytes as well as microvessels, and that administration of an anti-VEGFR2 antibody to mouse fetuses at E 17.5 prevented the normal thinning of alveolar septa and disappearance of PAS<sup>+</sup> cells (47). Freshly isolated type II cells also expressed VEGFR-2 and responded to VEGF by increasing the expression of SP-B and SP-C (47). After intra-amniotic administration of VEGF, prematurely delivered mice had significantly higher aerated lung area, decreased alveolar septal thickness, fewer PAS<sup>+</sup> cells/mm alveolus and increased surfactant production compared to saline treated litters (47). These studies suggest an important role for VEGF in epithelial cell differentiation and maturation in the lung.

#### **1.7 EXTRACELLULAR MATRIX AND MATRIX METALLOPROTEINASES**

The extracellular matrix (ECM) is an important component of the lung. During the lung development, ECM macromolecules must be precisely deposited and subsequently remodeled. The basement membrane is a specialized form of ECM deposited as thin sheets underlying epithelial and mesenchymal cells and surrounding vascular spaces (102). Formation of the bronchial tree by repetitive branching, enlargement of the peripheral air sacs, septation, vascularization and angiogenesis all require basement membrane turnover to accommodate growth (50). It is likely that both epithelial cells and fibroblasts participate in the basement membrane formation in fetal rat lung (144). Type IV collagen forms a major component of the basement membrane, along with laminins, perlecan and entactin, nidogen and various other components (50).

It has previously been demonstrated that appropriate ECM composition is an essential element for normal development of the lung. Administration of  $\beta$ -aminopropionitrile to

neonatal rats interferes with the cross-linking of elastin and collagen, by specific inhibition of lysyl oxidase. This inhibition results in enlarged alveolar ducts and modestly enlarged alveoli that are diminished in number when compared with control animals (98). Collagen is an essential component in the regulation of early lung branching. Branching of lung rudiments is impaired using inhibitors of collagen production, such as *cis*-hydroxyproline, azetadine-2-carboxylic acid, and 2,2'-dipyridyl (50).

### ***1.7.1 Matrix metalloproteinases***

As lung development requires the coordinated deposition and degradation of the ECM it follows that there are enzymes to facilitate this degradation. Matrix metalloproteinases (MMPs) are a family of zinc-dependent enzymes whose physiologic and pathologic importance is to modulate the ECM in such diverse roles as embryonic development, in the ovarian cycle, or in inflammatory diseases such as rheumatoid arthritis or fibrosis of the liver. They can be divided into two structurally independent groups, namely secreted MMPs and membrane-type MMPs (MT-MMPs). There are, at present, 25 vertebrate MMPs and 22 human homologues (153). Secreted MMPs include collagenases (interstitial collagenase, or MMP-1; neutrophil collagenase or MMP-8; and rodent interstitial collagenase or MMP-13), gelatinases (gelatinase-A or MMP-2; gelatinase-B or MMP-9). Stromolysins (stromolysin-1 or MMP-3; stromolysin-2 or MMP-10, stromolysin-3 or MMP-11) and other MMPs (matrilysin, or MMP-7; metalloelastase or MMP-12). Four MT-MMPs have been cloned MT1-MMP (MMP-14), MT2-MMP (MMP-15), MT3-MMP (MMP-16) and MT4-MMP (MMP-17) (127).

MMP-2 and MMP-9 are type IV collagenases that degrade basement membrane components and elastin. It has been firmly established that MMPs are required for angiogenesis (127). MMP-2 deficient mice develop normally, with no gross anatomical abnormalities, however they display a significantly slower (approximately 15 %) growth rate (85). It has, however, recently been demonstrated that 15 % of newborn MMP-2<sup>-/-</sup> mice gasp for breath and in all mice the lungs have abnormally large alveolar spaces, fewer septations, and thinner interstitial tissue than control litter mates (97). MMP-9 deficient mice, although they develop to term and survive normally after birth, exhibit an abnormal pattern of skeletal growth plate ossification secondary to reduced angiogenesis (168).

Specific endogenous inhibitors, the tissue inhibitors of metalloproteinases (TIMPs), reduce the proteolytic activities of MMPs. Four TIMPs have been described, named TIMPs 1, 2, 3 and 4 in order of discovery. TIMPs form a 1:1 stoichiometric complex with all activated MMPs with which they become covalently linked. However TIMP-1 also binds pro-MMP-9 and TIMP-2 also binds pro-MMP-2 (135).

MMP regulation can also occur at the transcriptional level (through altered gene expression) and at the level of activation of the secreted proenzyme (by proteolytic exposure of the Zn<sup>2+</sup> binding site). MMP-2 and MMP-9 differ in their mode of activation, as pro-MMP-2 is activated at the cell surface by MT1-MMP in a reaction involving TIMP-2 (Figure 1.5), whereas activation of MMP-9 occurs by plasminogen-dependant and independent mechanisms (103, 104).

### **1.7.2 MMPs and alveolar development**

Type IV collagen is a major component of the basement membranes of cells (114) and late fetal development in rats is associated with increased type-IV collagen degrading activity (50). In the postnatal rat lung total collagen synthesis increases rapidly at d 6 and then plateaus until about d 22, type IV collagen degradation is low throughout the postnatal period but peaks on d 11 (11).

In the rabbit lung MMP-2 (and MMP-9, though results were not significant) exhibited increased gelatinolytic activity as the lung developed, between E 23 (canalicular stage) and d 1 (alveolar stage) (69), and during the alveolar stage both MMP-2 and MMP-9 were detected in alveolar epithelial cells (69). Interestingly MT1-MMP was found to increase late in development at d 1, suggesting that it may act to increase MMP-2 activity at this time, as the activation ratio of MMP-2 also increased during lung development (69). MMP-2 mRNA in the mouse lung has been demonstrated, by *in situ* hybridization, to be predominately expressed by mesenchymal cells in association with the epithelium, whilst bronchial epithelial cells are negative (141).

### **1.7.3 MMPs and hyperoxia**

Hyperoxia has been shown to regulate MMPs in the lungs of adult and neonatal rats and rabbits. Adult rats exposed to 85 % O<sub>2</sub> had increased levels of MMP-2 and MMP-9 activities in both broncho-alveolar lavage fluid and type II cells (133). An upregulation of MMP-2 and -9 activity and mRNA (by *in situ* hybridization) is also seen in adult rats exposed to 100 % O<sub>2</sub> for 60 h (134). In the newborn rat pup, 85 % O<sub>2</sub> from d 1 to d 6 caused increased type IV collagenase mRNA and activity (55), and previous studies from

our laboratory found that exposing rat pups to hyperoxia caused an increase in MMP-2 and -9 activity (138).

#### ***1.7.4 TIMPS and alveolar development***

TIMP-2 immunoreactivity was detected in epithelial cells, endothelial cells, mesothelial cells and mesenchymal cells during the glandular stage of rabbit lung development (69). By the E 23 TIMP-2 protein was restricted to epithelial and some mesenchymal cells, and during the alveolar stage TIMP-2 was localized mainly to the epithelial cells of the airways and alveoli (69).

Neonatal rabbits exposed to 100 % O<sub>2</sub> for 96 h showed a fivefold increase in TIMP mRNA (82) and in adult rats exposed to 85 % O<sub>2</sub> an increase in TIMP-1 mRNA levels but no changes in TIMP-2 mRNA were observed (133).

### **1.8 LEUKOTRIENES**

Leukotrienes (LTs) are potent bioactive lipids derived from the 5-lipoxygenase (5-LO) pathway of arachidonic acid (AA) metabolism. They are known to be involved in a variety of inflammatory diseases such as asthma and rheumatoid arthritis (19, 128). There are two classes of leukotrienes originating from different processing of the common precursor LTA<sub>4</sub>; the pathway of leukotriene synthesis is shown in Figure 1.5. LTB<sub>4</sub> is produced predominantly by neutrophils and macrophages and is a potent chemotactic and chemokinetic agent for leukocytes (66). LTB<sub>4</sub> also stimulates a number of leukocyte functions, including aggregation, stimulation of ion fluxes, superoxide anion production and adherence (66). The cysteinyl-leukotrienes (also known as cysteinyl leukotrienes) were originally known as slow reacting substances of anaphylaxis, due to their role in



anaphylactic-induced bronchoconstriction. Cysteinyl-LTs are produced principally by eosinophils, mast cells and macrophages. LTD<sub>4</sub> has been shown to increase vascular permeability throughout the respiratory tract in the guinea pig (21). The best-known functions of the cysteinyl-LTs are smooth muscle cell constriction, smooth muscle cell proliferation and hypertrophy and bronchial hyperresponsiveness (19). In addition to production by white blood cells, endothelial cells and smooth muscle cells can convert LTA<sub>4</sub> produced by granulocytes and macrophages into LTB<sub>4</sub> and/or LTC<sub>4</sub> (which can then be further metabolized into LTD<sub>4</sub> and LTE<sub>4</sub>) (38, 61).

Leukotrienes are not stored in the cell, but are synthesized upon appropriate stimulation (140). *De novo* synthesis of LTs from leukocytes requires a complex series of reactions (Figure 1.5). The initial step involves the release of the substrate arachidonic acid (AA), from membrane lipids within the nuclear envelope, by cytosolic (c) phospholipase A<sub>2</sub> (PLA<sub>2</sub>). Translocation of the enzyme 5-lipoxygenase (5-LO) from the cytosol (peripheral blood leukocytes) or nucleus (alveolar macrophages) (45) is stimulated when levels of intracellular Ca<sup>2+</sup> increase as a result of cellular activation (165). 5-lipoxygenase-activating protein (FLAP) is also found associated with the nuclear membrane (175, 176) (though some is also attached to the endoplasmic reticulum (176)); it is thought to function as a substrate transfer protein, through binding of arachidonic acid (110). 5-LO causes the lipoxygenation of AA at carbon atom 5 to produce 5(*S*)-hydroperoxy-6-*trans*-8,11,14-*cis*-eicosatetraenoic acid (5-HPETE) and the ensuing dehydration of 5-HPETE to the unstable epoxide LTA<sub>4</sub> (140). The subsequent hydrolysis of LTA<sub>4</sub> to LTB<sub>4</sub> is initiated by the enzyme LTA<sub>4</sub> hydrolase. The alternate route for processing of LTA<sub>4</sub> leads to the

formation of the cysteinyl-LTs, LTC<sub>4</sub>, LTD<sub>4</sub> and LTE<sub>4</sub>. LTC<sub>4</sub> is formed from LTA<sub>4</sub> by the catalyst LTC<sub>4</sub> synthase. LTC<sub>4</sub> is normally rapidly metabolized by enzymatic cleavage of successive amino acids from the glutathione side chain, forming LTD<sub>4</sub> and LTE<sub>4</sub>.

The role of leukotrienes as inflammatory mediators has been shown by 5-LO deficient mice which are more resistant to platelet activating factor-induced shock and show a marked reduction in the ear inflammatory response to exogenous AA (37, 71). Similar results are seen in the FLAP<sup>-/-</sup> mouse (33).

Two G-protein-coupled receptors with seven transmembrane-spanning domains specific for LTB<sub>4</sub> have been found and named BLT<sub>1</sub> and BLT<sub>2</sub>. BLT<sub>1</sub> is predominantly found in leukocytes, whereas BLT<sub>2</sub> is ubiquitously expressed in various tissues (73). Through studies on knockout mice, BLT<sub>1</sub> has been shown to be essential for the physiological effects of LTB<sub>4</sub> (as described earlier) (78, 156). More recent evidence suggests that peroxisomal proliferator-activated receptor- $\alpha$  (PPAR- $\alpha$ ) can also bind and be activated by LTB<sub>4</sub> (56). The actions of the cysteinyl-LTs are mediated by two receptors, CysLT<sub>1</sub> and CysLT<sub>2</sub>, which show varying affinity for the cysteinyl-LTs; CysLT<sub>1</sub> binds LTD<sub>4</sub> preferentially, followed by LTC<sub>4</sub> then LTE<sub>4</sub>, while CysLT<sub>2</sub> binds LTC<sub>4</sub> and LTD<sub>4</sub> equally well, with a lower affinity for LTE<sub>4</sub> (73).

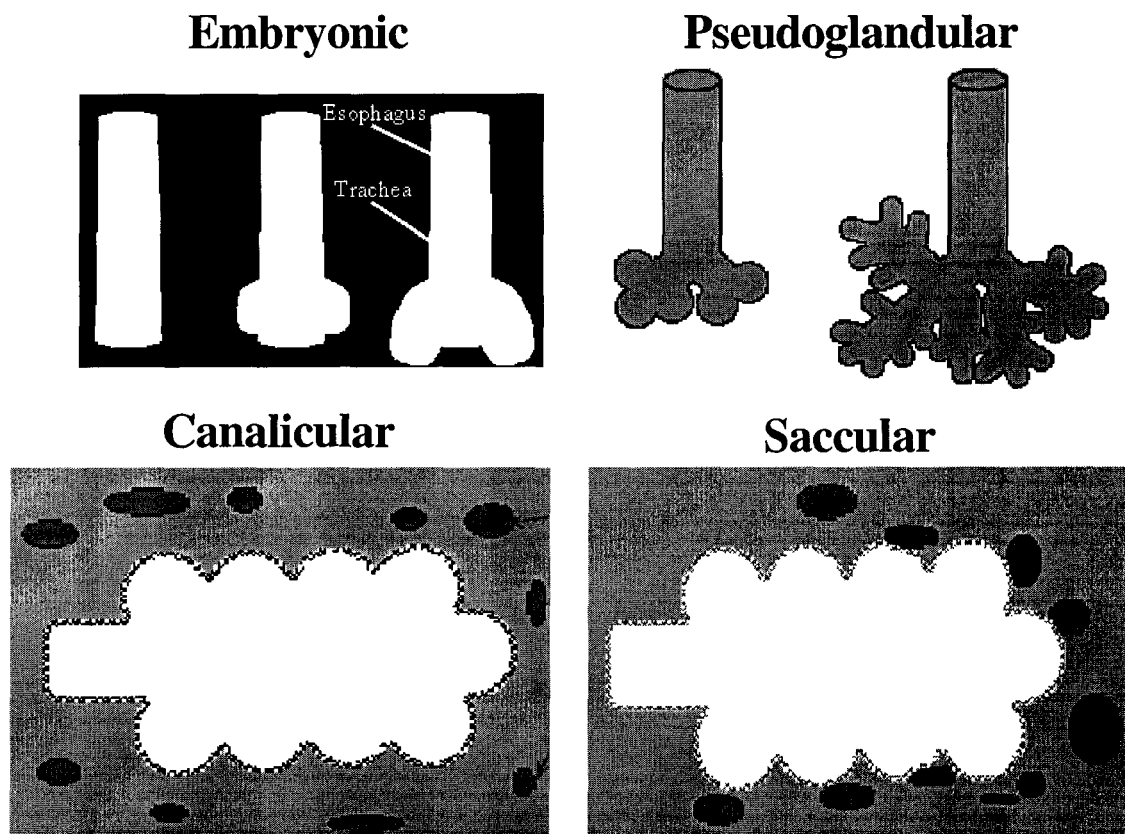
### ***1.8.1 Leukotrienes and hyperoxia***

LTs have previously been shown to respond to a hyperoxic environment. In adult rats exposed to > 97 % O<sub>2</sub> for 60 h LTB<sub>4</sub> increased significantly in lavage fluid, when compared to normoxic control rats (157). In the same experiments administration of AA861, a 5-LO inhibitor, reduced the increase in LTB<sub>4</sub> as well as the increased number

of neutrophils which is seen when rats are exposed to O<sub>2</sub>. Further, after 72 h of O<sub>2</sub> exposure, treatment with AA861 reduced the mortality of rats from 85 % to 20 %, suggesting that the increase in LTB<sub>4</sub> is responsible for accumulation of neutrophils in the lung and that the neutrophil recruitment contributes to the lung injury during O<sub>2</sub> breathing (157). Cysteinyl-LTs have also been shown to respond to oxygen radicals in an experiment where young pigs were administered hypoxanthine-xanthine oxidase (which generates oxygen metabolites) and a 2.1-fold increase in LT release was observed (146).

Our laboratory has provided strong evidence for the involvement of cysteinyl-LTs in the inhibition of alveolar development seen when newborn rats are exposed to high O<sub>2</sub> concentrations. When newborn rats were placed in > 95 % O<sub>2</sub> from d 4 to d 14, there was a significant increase in cysteinyl-LT output on d 14 from lung slices of animals exposed to O<sub>2</sub> compared with air-exposed pups (22). Further, when either the 5-LO inhibitor, MK-0591, or the LTD<sub>4</sub> receptor inhibitor, Wy-50295, was administered during the hyperoxic-exposure, cysteinyl-LT output was significantly lowered. In the same experiments hyperoxia was shown to severely retard the development of the alveoli, and treatment with either of the inhibitors prevented this inhibited alveolarization, providing evidence that hyperoxia-induced cysteinyl-LTs may mediate O<sub>2</sub>-induced inhibition of alveolarization (22). Interestingly, subsequent experiments showed a critical window for both hyperoxic exposure and LTs. Pups exposed to O<sub>2</sub> from d 4 to d 9 had more profound inhibition of alveolarization on d 14, when compared to exposed to O<sub>2</sub> from d 1 to d 4 or d 9 to d 14 (113). O<sub>2</sub> exposure from d 4 to d 9 also significantly stimulated cysteinyl-LT production at d 9 but levels returned to normal by d 14. Inhibition of LTs with MK-0591

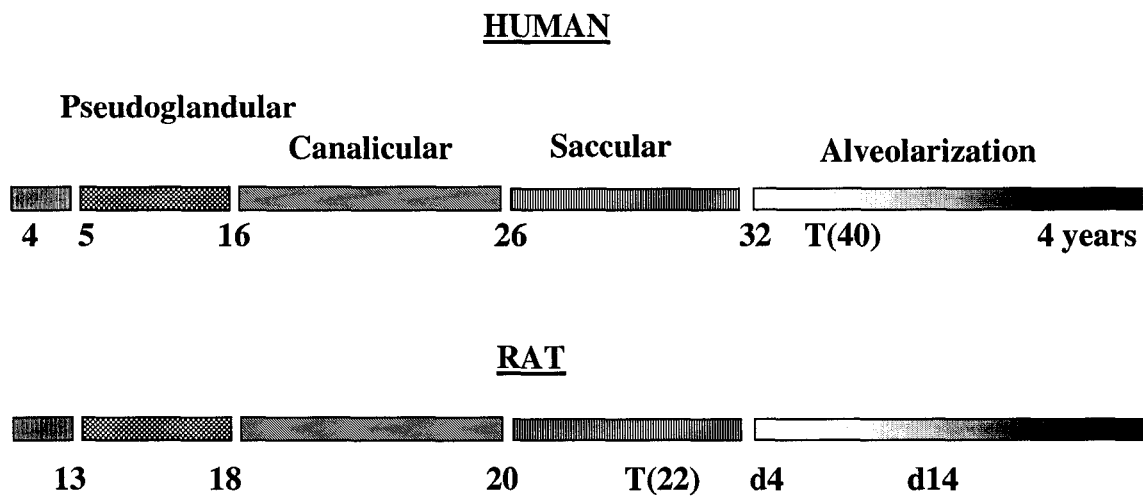
from d 3 to d 9 or d 9 to d 14, during O<sub>2</sub> exposure from d 4 to d 14, prevented the inhibition of alveolarization seen in vehicle treated O<sub>2</sub> exposed lungs, suggesting that the alveoli are sensitive to LTs shortly before and after d 9 (113).



---

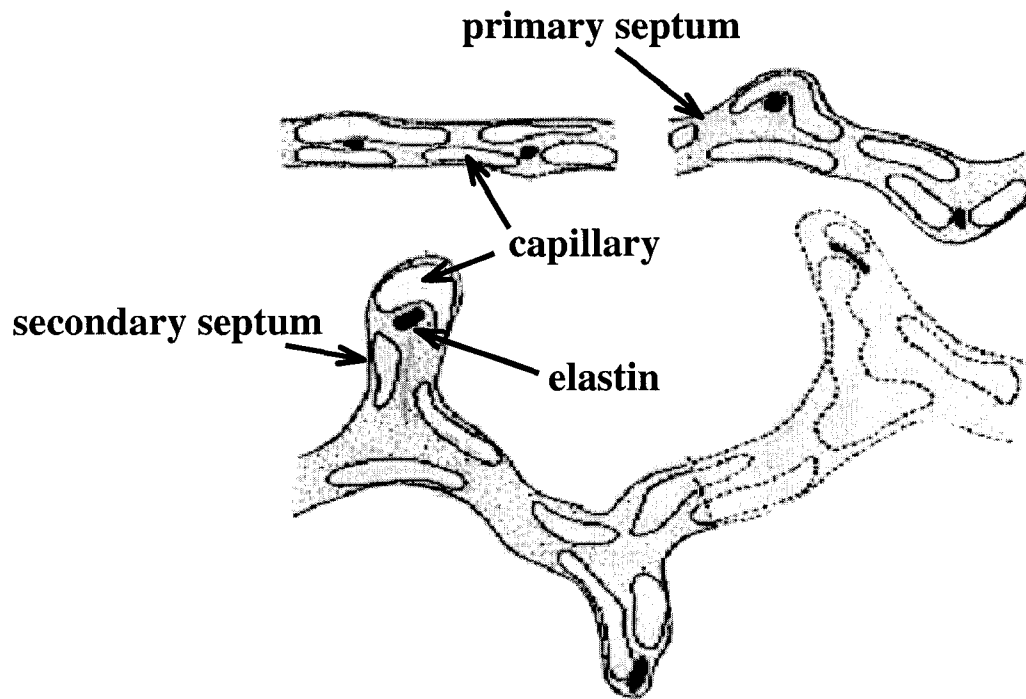
**Figure 1.1** Stages of branching morphogenesis.

A schematic of the stages of lung development as described in the text.




---

**Figure 1.2    Timing of the stages of development of the human and rat lung.**



---

**Figure 1.3** Septation of saccules.

Process whereby mature secondary septa divide a saccule to form an alveolus. Described in detail in the text. Figure adapted from reference 29.





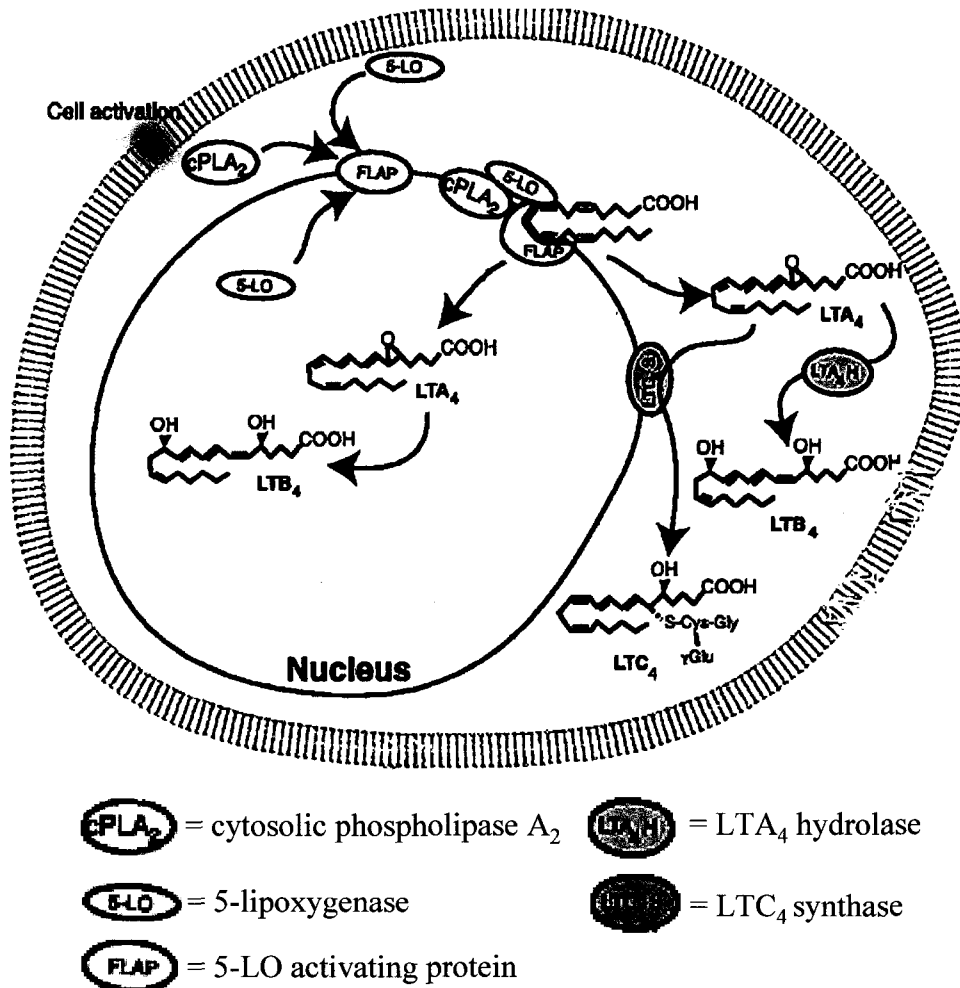


**Figure 1.5** Leukotriene synthesis pathway.

Intra-cellular pathways of leukotriene synthesis. A detailed description is provided in and in the text. Adapted from Funk CD, *Science* 294(5548):1871-5, 2001

## **1.9 REFERENCES**

1. **Acarregui, M. J., S. T. Penisten, K. L. Goss, K. Ramirez, and J. M. Snyder.** Vascular endothelial growth factor gene expression in human fetal lung in vitro. *Am J Respir Cell Mol Biol* 20: 14-23., 1999.
2. **Adamson, C. S.** Development of Lung Structure. In: *The Lung: Scientific Foundations*, edited by J. B. W. R G Crystal, E R Weibel, P J Barnes. New York: Lippencott Raven, 1997, p. 993.
3. **Adamson, I. Y., and D. H. Bowden.** Derivation of type 1 epithelium from type 2 cells in the developing rat lung. *Lab Invest* 32: 736-45., 1975.
4. **Adamson, I. Y., and D. H. Bowden.** The type 2 cell as progenitor of alveolar epithelial regeneration. A cytodynamic study in mice after exposure to oxygen. *Lab Invest* 30: 35-42., 1974.
5. **Adamson, I. Y., and G. M. King.** Sex differences in development of fetal rat lung. II. Quantitative morphology of epithelial-mesenchymal interactions. *Lab Invest* 50: 461-8., 1984.
6. **Akeno, N., M. F. Czyzyk-Krzeska, T. S. Gross, and T. L. Clemens.** Hypoxia induces vascular endothelial growth factor gene transcription in human osteoblast-like cells through the hypoxia-inducible factor- 2alpha. *Endocrinology* 142: 959-62., 2001.
7. **Albertine, K. H., G. P. Jones, B. C. Starcher, J. F. Bohnsack, P. L. Davis, S. C. Cho, D. P. Carlton, and R. D. Bland.** Chronic lung injury in preterm lambs. Disordered respiratory tract development. *Am J Respir Crit Care Med* 159: 945-58., 1999.
8. **Alcorn, D. G., T. M. Adamson, J. E. Maloney, and P. M. Robinson.** A morphologic and morphometric analysis of fetal lung development in the sheep. *Anat Rec* 201: 655-67., 1981.
9. **Ames, B. N., M. K. Shigenaga, and T. M. Hagen.** Oxidants, antioxidants, and the degenerative diseases of aging. *Proc Natl Acad Sci U S A* 90: 7915-22., 1993.
10. **Amy, R. W., D. Bowes, P. H. Burri, J. Haines, and W. M. Thurlbeck.** Postnatal growth of the mouse lung. *J Anat* 124: 131-51., 1977.
11. **Arden, M. G., and I. Y. Adamson.** Collagen degradation during postnatal lung growth in rats. *Pediatr Pulmonol* 14: 95-101., 1992.

12. **Asikainen, T. M., K. O. Raivio, M. Saksela, and V. L. Kinnula.** Expression and developmental profile of antioxidant enzymes in human lung and liver. *Am J Respir Cell Mol Biol* 19: 942-9., 1998.
13. **Auten, R. L., Jr., S. N. Mason, D. T. Tanaka, K. Welty-Wolf, and M. H. Whorton.** Anti-neutrophil chemokine preserves alveolar development in hyperoxia-exposed newborn rats. *Am J Physiol Lung Cell Mol Physiol* 281: L336-44., 2001.
14. **Awonusonu, F., S. Srinivasan, J. Strange, W. Al-Jumaily, and M. C. Bruce.** Developmental shift in the relative percentages of lung fibroblast subsets: role of apoptosis postseptation. *Am J Physiol* 277: L848-59., 1999.
15. **Bacic, M., N. A. Edwards, and M. J. Merrill.** Differential expression of vascular endothelial growth factor (vascular permeability factor) forms in rat tissues. *Growth Factors* 12: 11-5, 1995.
16. **Bancalari, E., and A. Gonzalez.** Clinical Course and Lung Function Abnormalities During Development of Neonatal Chronic Lung Disease. In: *Chronic Lung Disease in Early Infancy*, edited by R. D. a. C. Bland, J.J. New York: Marcel Dekker, 2001, p. 41.
17. **Berg, J. T., J. E. White, and M. F. Tsan.** Response of alveolar macrophage-depleted rats to hyperoxia. *Exp Lung Res* 21: 175-85., 1995.
18. **Bhatt, A. J., G. S. Pryhuber, H. Huyck, R. H. Watkins, L. A. Metlay, and W. M. Maniscalco.** Disrupted pulmonary vasculature and decreased vascular endothelial growth factor, Flt-1, and TIE-2 in human infants dying with bronchopulmonary dysplasia. *Am J Respir Crit Care Med* 164: 1971-80., 2001.
19. **Bisgaard, H.** Role of leukotrienes in asthma pathophysiology. *Pediatr Pulmonol* 30: 166-76., 2000.
20. **Blanco, L. N., and L. Frank.** The formation of alveoli in rat lung during the third and fourth postnatal weeks: effect of hyperoxia, dexamethasone, and deferoxamine. *Pediatr Res* 34: 334-40., 1993.
21. **Bochnowicz, S., and D. C. Underwood.** Dose-dependent mediation of leukotriene D4-induced airway microvascular leakage and bronchoconstriction in the guinea pig. *Prostaglandins Leukot Essent Fatty Acids* 52: 403-11., 1995.
22. **Boros, V., J. S. Burghardt, C. J. Morgan, and D. M. Olson.** Leukotrienes are indicated as mediators of hyperoxia-inhibited alveolarization in newborn rats. *Am J Physiol* 272: L433-41., 1997.
23. **Brody, J. S., S. Lahiri, M. Simpson, E. K. Motoyama, and T. Velasquez.** Lung elasticity and airway dynamics in Peruvian natives to high altitude. *J Appl Physiol* 42: 245-51., 1977.

24. **Brown, K. R., K. M. England, K. L. Goss, J. M. Snyder, and M. J. Acarregui.** VEGF induces airway epithelial cell proliferation in human fetal lung in vitro. *Am J Physiol Lung Cell Mol Physiol* 281: L1001-10., 2001.
25. **Bucher, J. R., and R. J. Roberts.** The development of the newborn rat lung in hyperoxia: a dose-response study of lung growth, maturation, and changes in antioxidant enzyme activities. *Pediatr Res* 15: 999-1008., 1981.
26. **Burghardt, J. S., V. Boros, D. F. Biggs, and D. M. Olson.** Lipid mediators in oxygen-induced airway remodeling and hyperresponsiveness in newborn rats. *Am J Respir Crit Care Med* 154: 837-42., 1996.
27. **Burri, P. H.** Fetal and postnatal development of the lung. *Annu Rev Physiol* 46: 617-28, 1984.
28. **Burri, P. H.** Postnatal growth and maturation of the lung. *Chest* 67: 2S-3S., 1975.
29. **Burri, P. H.** The postnatal growth of the rat lung. 3. Morphology. *Anat Rec* 180: 77-98., 1974.
30. **Burri, P. H.** Structural Aspects of Prenatal and Postnatal Development and Growth of the Lung. In: *Lung Growth and Development*, edited by J. A. McDonald. New York: Marcel Dekker Int., 1997, p. 1.
31. **Burri, P. H., J. Dbaly, and E. R. Weibel.** The postnatal growth of the rat lung. I. Morphometry. *Anat Rec* 178: 711-30., 1974.
32. **Burri, P. H., and M. R. Tarek.** A novel mechanism of capillary growth in the rat pulmonary microcirculation. *Anat Rec* 228: 35-45., 1990.
33. **Byrum, R. S., J. L. Goulet, R. J. Griffiths, and B. H. Koller.** Role of the 5-lipoxygenase-activating protein (FLAP) in murine acute inflammatory responses. *J Exp Med* 185: 1065-75., 1997.
34. **Caduff, J. H., L. C. Fischer, and P. H. Burri.** Scanning electron microscope study of the developing microvasculature in the postnatal rat lung. *Anat Rec* 216: 154-64., 1986.
35. **Carmeliet, P., V. Ferreira, G. Breier, S. Pollefeyt, L. Kieckens, M. Gertsenstein, M. Fahrig, A. Vandenhoeck, K. Harpal, C. Eberhardt, C. Declercq, J. Pawling, L. Moons, D. Collen, W. Risau, and A. Nagy.** Abnormal blood vessel development and lethality in embryos lacking a single VEGF allele. *Nature* 380: 435-9., 1996.
36. **Chandel, N. S., D. S. McClintock, C. E. Feliciano, T. M. Wood, J. A. Melendez, A. M. Rodriguez, and P. T. Schumacker.** Reactive oxygen species generated at mitochondrial complex III stabilize hypoxia-inducible factor-1alpha during hypoxia: a mechanism of O<sub>2</sub> sensing. *J Biol Chem* 275: 25130-8., 2000.

37. **Chen, X. S., J. R. Sheller, E. N. Johnson, and C. D. Funk.** Role of leukotrienes revealed by targeted disruption of the 5- lipoxygenase gene. *Nature* 372: 179-82., 1994.
38. **Claesson, H. E., and J. Haeggstrom.** Human endothelial cells stimulate leukotriene synthesis and convert granulocyte released leukotriene A4 into leukotrienes B4, C4, D4 and E4. *Eur J Biochem* 173: 93-100., 1988.
39. **Clark, J. M., and C. J. Lambertsen.** Pulmonary oxygen toxicity: a review. *Pharmacol Rev* 23: 37-133., 1971.
40. **Coalson, J. J.** Pathology of Chronic Lung Disease of Early Infancy. In: *Chronic Lung Disease in Early Infancy*, edited by R. D. a. C. Bland, J.J. New York: Marcel Dekker, 2001, p. 85.
41. **Coalson, J. J., T. J. Kuehl, M. B. Escobedo, J. L. Hilliard, F. Smith, K. Meredith, D. M. Null, Jr., W. Walsh, D. Johnson, and J. L. Robotham.** A baboon model of bronchopulmonary dysplasia. II. Pathologic features. *Exp Mol Pathol* 37: 335-50., 1982.
42. **Coalson, J. J., V. Winter, and R. A. deLemos.** Decreased alveolarization in baboon survivors with bronchopulmonary dysplasia. *Am J Respir Crit Care Med* 152: 640-6., 1995.
43. **Coalson, J. J., V. T. Winter, D. R. Gerstmann, S. Idell, R. J. King, and R. A. Delemos.** Pathophysiologic, morphometric, and biochemical studies of the premature baboon with bronchopulmonary dysplasia. *Am Rev Respir Dis* 145: 872-81., 1992.
44. **Coalson, J. J., V. T. Winter, T. Siler-Khodr, and B. A. Yoder.** Neonatal chronic lung disease in extremely immature baboons. *Am J Respir Crit Care Med* 160: 1333-46., 1999.
45. **Coffey, M., M. Peters-Golden, J. C. Fantone, 3rd, and P. H. Sporn.** Membrane association of active 5-lipoxygenase in resting cells. Evidence for novel regulation of the enzyme in the rat alveolar macrophage. *J Biol Chem* 267: 570-6., 1992.
46. **Collins, M. H., J. Kleinerman, A. C. Moessinger, A. H. Collins, L. S. James, and W. A. Blanc.** Morphometric analysis of the growth of the normal fetal guinea pig lung. *Anat Rec* 216: 381-91., 1986.
47. **Compernelle, V., K. Brusselmans, T. Acker, P. Hoet, M. Tjwa, H. Beck, S. Plaisance, Y. Dor, E. Keshet, F. Lupu, B. Nemery, M. Dewerchin, P. Van Veldhoven, K. Plate, L. Moons, D. Collen, and P. Carmeliet.** Loss of HIF-2alpha and inhibition of VEGF impair fetal lung maturation, whereas treatment with VEGF prevents fatal respiratory distress in premature mice. *Nat Med* 10: 10, 2002.
48. **Corne, J., G. Chupp, C. G. Lee, R. J. Homer, Z. Zhu, Q. Chen, B. Ma, Y. Du, F. Roux, J. McArdle, A. B. Waxman, and J. A. Elias.** IL-13 stimulates vascular

endothelial cell growth factor and protects against hyperoxic acute lung injury. *J Clin Invest* 106: 783-91., 2000.

49. **Crapo, J. D., B. E. Barry, H. A. Foscue, and J. Shelburne.** Structural and biochemical changes in rat lungs occurring during exposures to lethal and adaptive doses of oxygen. *Am Rev Respir Dis* 122: 123-43., 1980.

50. **Crouch, E. C., R. C. Macham, R. M. Davila, and D. Noguchi.** Collagens and Elastic Fiber Proteins in Lung Development. In: *Lung Growth and Development*, edited by J. A. McDonald. New York: Marcel Dekker Int., 1997, p. 327.

51. **D'Angio, C. T., C. J. Johnston, T. W. Wright, C. K. Reed, and J. N. Finkelstein.** Chemokine mRNA alterations in newborn and adult mouse lung during acute hyperoxia. *Exp Lung Res* 24: 685-702., 1998.

52. **D'Angio, C. T., W. M. Maniscalco, R. M. Ryan, N. E. Avissar, K. Basavegowda, and R. A. Sinkin.** Vascular endothelial growth factor in pulmonary lavage fluid from premature infants: effects of age and postnatal dexamethasone. *Biol Neonate* 76: 266-73., 1999.

53. **deMello, D. E., D. Sawyer, N. Galvin, and L. M. Reid.** Early fetal development of lung vasculature. *Am J Respir Cell Mol Biol* 16: 568-81., 1997.

54. **Deng, H., S. N. Mason, and R. L. Auten, Jr.** Lung inflammation in hyperoxia can be prevented by antichemokine treatment in newborn rats. *Am J Respir Crit Care Med* 162: 2316-23., 2000.

55. **Devaskar, U. P., W. Taylor, R. Govindrajan, M. Malicdem, S. Heyman, and D. E. deMello.** Hyperoxia induces interstitial (type I) and increases type IV collagenase mRNA expression and increases type I and IV collagenolytic activity in newborn rat lung. *Biol Neonate* 66: 76-85, 1994.

56. **Devchand, P. R., H. Keller, J. M. Peters, M. Vazquez, F. J. Gonzalez, and W. Wahli.** The PPARalpha-leukotriene B4 pathway to inflammation control. *Nature* 384: 39-43., 1996.

57. **DiFiore, J. W., D. O. Fauza, R. Slavin, and J. M. Wilson.** Experimental fetal tracheal ligation and congenital diaphragmatic hernia: a pulmonary vascular morphometric analysis. *J Pediatr Surg* 30: 917-23; discussion 923-4., 1995.

58. **Dvorak, H. F., L. F. Brown, M. Detmar, and A. M. Dvorak.** Vascular permeability factor/vascular endothelial growth factor, microvascular hyperpermeability, and angiogenesis. *Am J Pathol* 146: 1029-39., 1995.

59. **Ema, M., S. Taya, N. Yokotani, K. Sogawa, Y. Matsuda, and Y. Fujii-Kuriyama.** A novel bHLH-PAS factor with close sequence similarity to hypoxia-inducible factor 1alpha regulates the VEGF expression and is potentially involved in lung and vascular development. *Proc Natl Acad Sci U S A* 94: 4273-8., 1997.

60. **Favier, J., H. Kempf, P. Corvol, and J. M. Gasc.** Coexpression of endothelial PAS protein 1 with essential angiogenic factors suggests its involvement in human vascular development. *Dev Dyn* 222: 377-88., 2001.
61. **Feinmark, S. J., and P. J. Cannon.** Endothelial cell leukotriene C4 synthesis results from intercellular transfer of leukotriene A4 synthesized by polymorphonuclear leukocytes. *J Biol Chem* 261: 16466-72., 1986.
62. **Ferrara, N.** Vascular endothelial growth factor. *Eur J Cancer* 32A: 2413-22., 1996.
63. **Ferrara, N., K. Houck, L. Jakeman, and D. W. Leung.** Molecular and biological properties of the vascular endothelial growth factor family of proteins. *Endocr Rev* 13: 18-32., 1992.
64. **Fong, G. H., J. Rossant, M. Gertsenstein, and M. L. Breitman.** Role of the Flt-1 receptor tyrosine kinase in regulating the assembly of vascular endothelium. *Nature* 376: 66-70., 1995.
65. **Fong, G. H., L. Zhang, D. M. Bryce, and J. Peng.** Increased hemangioblast commitment, not vascular disorganization, is the primary defect in flt-1 knock-out mice. *Development* 126: 3015-25., 1999.
66. **Ford-Hutchinson, A. W.** Leukotriene B4 in inflammation. *Crit Rev Immunol* 10: 1-12, 1990.
67. **Forsythe, J. A., B. H. Jiang, N. V. Iyer, F. Agani, S. W. Leung, R. D. Koos, and G. L. Semenza.** Activation of vascular endothelial growth factor gene transcription by hypoxia-inducible factor 1. *Mol Cell Biol* 16: 4604-13., 1996.
68. **Freeman, B. A., and J. D. Crapo.** Hyperoxia increases oxygen radical production in rat lungs and lung mitochondria. *J Biol Chem* 256: 10986-92., 1981.
69. **Fukuda, Y., M. Ishizaki, Y. Okada, M. Seiki, and N. Yamanaka.** Matrix metalloproteinases and tissue inhibitor of metalloproteinase-2 in fetal rabbit lung. *Am J Physiol Lung Cell Mol Physiol* 279: L555-61., 2000.
70. **Goldkorn, T., N. Balaban, M. Shannon, V. Chea, K. Matsukuma, D. Gilchrist, H. Wang, and C. Chan.** H<sub>2</sub>O<sub>2</sub> acts on cellular membranes to generate ceramide signaling and initiate apoptosis in tracheobronchial epithelial cells. *J Cell Sci* 111: 3209-20., 1998.
71. **Goulet, J. L., J. N. Snouwaert, A. M. Latour, T. M. Coffman, and B. H. Koller.** Altered inflammatory responses in leukotriene-deficient mice. *Proc Natl Acad Sci U S A* 91: 12852-6., 1994.
72. **Haddad, J. J., R. E. Olver, and S. C. Land.** Antioxidant/pro-oxidant equilibrium regulates HIF-1 $\alpha$  and NF-kappa B redox sensitivity. Evidence for

inhibition by glutathione oxidation in alveolar epithelial cells. *J Biol Chem* 275: 21130-9., 2000.

73. **Haeggstrom, J. Z., and A. Wetterholm.** Enzymes and receptors in the leukotriene cascade. *Cell Mol Life Sci* 59: 742-53., 2002.

74. **Halder, J. B., X. Zhao, S. Soker, B. C. Paria, M. Klagsbrun, S. K. Das, and S. K. Dey.** Differential expression of VEGF isoforms and VEGF(164)-specific receptor neuropilin-1 in the mouse uterus suggests a role for VEGF(164) in vascular permeability and angiogenesis during implantation. *Genesis* 26: 213-24., 2000.

75. **Hall, S. M., A. A. Hislop, C. M. Pierce, and S. G. Haworth.** Prenatal origins of human intrapulmonary arteries: formation and smooth muscle maturation. *Am J Respir Cell Mol Biol* 23: 194-203., 2000.

76. **Halliwell, B., and J. M. Gutteridge.** Role of free radicals and catalytic metal ions in human disease: an overview. *Methods Enzymol* 186: 1-85, 1990.

77. **Han, R. N., S. Buch, I. Tseu, J. Young, N. A. Christie, H. Frndova, S. J. Lye, M. Post, and A. K. Tanswell.** Changes in structure, mechanics, and insulin-like growth factor-related gene expression in the lungs of newborn rats exposed to air or 60% oxygen. *Pediatr Res* 39: 921-9., 1996.

78. **Haribabu, B., M. W. Verghese, D. A. Steeber, D. D. Sellars, C. B. Bock, and R. Snyderman.** Targeted disruption of the leukotriene B(4) receptor in mice reveals its role in inflammation and platelet-activating factor-induced anaphylaxis. *J Exp Med* 192: 433-8., 2000.

79. **Haworth, S.** Development of Vessels. In: *Chronic Lung Disease in Early Infancy*, edited by C. Lefant. New York: Marcel Dekker, 2001.

80. **Healy, A. M., L. Morgenthau, X. Zhu, H. W. Farber, and W. V. Cardoso.** VEGF is deposited in the subepithelial matrix at the leading edge of branching airways and stimulates neovascularization in the murine embryonic lung. *Dev Dyn* 219: 341-52., 2000.

81. **Hiratsuka, S., O. Minowa, J. Kuno, T. Noda, and M. Shibuya.** Flt-1 lacking the tyrosine kinase domain is sufficient for normal development and angiogenesis in mice. *Proc Natl Acad Sci U S A* 95: 9349-54., 1998.

82. **Horowitz, S., D. L. Shapiro, J. N. Finkelstein, R. H. Notter, C. J. Johnston, and D. J. Quible.** Changes in gene expression in hyperoxia-induced neonatal lung injury. *Am J Physiol* 258: L107-11., 1990.

83. **Houck, K. A., D. W. Leung, A. M. Rowland, J. Winer, and N. Ferrara.** Dual regulation of vascular endothelial growth factor bioavailability by genetic and proteolytic mechanisms. *J Biol Chem* 267: 26031-7., 1992.



84. **Husain, A. N., N. H. Siddiqui, and J. T. Stocker.** Pathology of arrested acinar development in postsurfactant bronchopulmonary dysplasia. *Hum Pathol* 29: 710-7., 1998.
85. **Itoh, T., T. Ikeda, H. Gomi, S. Nakao, T. Suzuki, and S. Itohara.** Unaltered secretion of beta-amyloid precursor protein in gelatinase A (matrix metalloproteinase 2)-deficient mice. *J Biol Chem* 272: 22389-92., 1997.
86. **Jakkula, M., T. D. Le Cras, S. Gebb, K. P. Hirth, R. M. Tuder, N. F. Voelkel, and S. H. Abman.** Inhibition of angiogenesis decreases alveolarization in the developing rat lung. *Am J Physiol Lung Cell Mol Physiol* 279: L600-7., 2000.
87. **Jeltsch, M., A. Kaipainen, V. Joukov, X. Meng, M. Lakso, H. Rauvala, M. Swartz, D. Fukumura, R. K. Jain, and K. Alitalo.** Hyperplasia of lymphatic vessels in VEGF-C transgenic mice. *Science* 276: 1423-5., 1997.
88. **Jingjing, L., Y. Xue, N. Agarwal, and R. S. Roque.** Human Muller cells express VEGF183, a novel spliced variant of vascular endothelial growth factor. *Invest Ophthalmol Vis Sci* 40: 752-9., 1999.
89. **Jobe, A. H., and E. Bancalari.** Bronchopulmonary dysplasia. *Am J Respir Crit Care Med* 163: 1723-9., 2001.
90. **Jobe, A. J.** The new BPD: an arrest of lung development. *Pediatr Res* 46: 641-3., 1999.
91. **Joukov, V., K. Pajusola, A. Kaipainen, D. Chilov, I. Lahtinen, E. Kukk, O. Saksela, N. Kalkkinen, and K. Alitalo.** A novel vascular endothelial growth factor, VEGF-C, is a ligand for the Flt4 (VEGFR-3) and KDR (VEGFR-2) receptor tyrosine kinases. *Embo J* 15: 290-98., 1996.
92. **Kasahara, Y., R. M. Tuder, L. Taraseviciene-Stewart, T. D. Le Cras, S. Abman, P. K. Hirth, J. Waltenberger, and N. F. Voelkel.** Inhibition of VEGF receptors causes lung cell apoptosis and emphysema. *J Clin Invest* 106: 1311-9., 2000.
93. **Kauffman, S. L., P. H. Burri, and E. R. Weibel.** The postnatal growth of the rat lung. II. Autoradiography. *Anat Rec* 180: 63-76., 1974.
94. **Kelley, J.** Cytokines of the lung. *Am Rev Respir Dis* 141: 765-88., 1990.
95. **Kempson, S.** Energy and Cellular Metabolism. In: *Human Physiology*, edited by R. Rhoades and R. Pflanzner. Florida: Saunders College Publishing, 1992, p. 199.
96. **Kendall, R. L., and K. A. Thomas.** Inhibition of vascular endothelial cell growth factor activity by an endogenously encoded soluble receptor. *Proc Natl Acad Sci U S A* 90: 10705-9., 1993.

97. **Kheradmand, F., K. Rishi, and Z. Werb.** Signaling through the EGF receptor controls lung morphogenesis in part by regulating MT1-MMP-mediated activation of gelatinase A/MMP2. *J Cell Sci* 115: 839-48., 2002.
98. **Kida, K., and W. M. Thurlbeck.** The effects of beta-aminopropionitrile on the growing rat lung. *Am J Pathol* 101: 693-710., 1980.
99. **Klagsbrun, M., and P. A. D'Amore.** Regulators of angiogenesis. *Annu Rev Physiol* 53: 217-39, 1991.
100. **Laitinen, M., I. Zachary, G. Breier, T. Pakkanen, T. Hakkinen, J. Luoma, H. Abedi, W. Risau, M. Soma, M. Laakso, J. F. Martin, and S. Yla-Herttuala.** VEGF gene transfer reduces intimal thickening via increased production of nitric oxide in carotid arteries. *Hum Gene Ther* 8: 1737-44., 1997.
101. **Le Cras, T. D., D. H. Kim, S. Gebb, N. E. Markham, J. M. Shannon, R. M. Tudor, and S. H. Abman.** Abnormal lung growth and the development of pulmonary hypertension in the Fawn-Hooded rat. *Am J Physiol* 277: L709-18., 1999.
102. **Leblond, C. P., and S. Inoue.** Structure, composition, and assembly of basement membrane. *Am J Anat* 185: 367-90., 1989.
103. **Lijnen, H. R., J. Silence, G. Lemmens, L. Frederix, and D. Collen.** Regulation of gelatinase activity in mice with targeted inactivation of components of the plasminogen/plasmin system. *Thromb Haemost* 79: 1171-6., 1998.
104. **Lijnen, H. R., B. Van Hoef, F. Lupu, L. Moons, P. Carmeliet, and D. Collen.** Function of the plasminogen/plasmin and matrix metalloproteinase systems after vascular injury in mice with targeted inactivation of fibrinolytic system genes. *Arterioscler Thromb Vasc Biol* 18: 1035-45., 1998.
105. **Lindahl, P., L. Karlsson, M. Hellstrom, S. Gebre-Medhin, K. Willetts, J. K. Heath, and C. Betsholtz.** Alveogenesis failure in PDGF-A-deficient mice is coupled to lack of distal spreading of alveolar smooth muscle cell progenitors during lung development. *Development* 124: 3943-53., 1997.
106. **Lines, A., K. Haegadorn, and D. M. Olson.** Dexamethasone and Retinoic Acid alter VEGF in the Neonatal Rat Lung. *in preparation*., 2002.
107. **Lingen, M. W.** Role of leukocytes and endothelial cells in the development of angiogenesis in inflammation and wound healing. *Arch Pathol Lab Med* 125: 67-71., 2001.
108. **Maeda, S., S. Suzuki, T. Suzuki, M. Endo, T. Moriya, M. Chida, T. Kondo, and H. Sasano.** Analysis of intrapulmonary vessels and epithelial-endothelial interactions in the human developing lung. *Lab Invest* 82: 293-301., 2002.

109. **Maglione, D., V. Guerriero, G. Viglietto, P. Delli-Bovi, and M. G. Persico.** Isolation of a human placenta cDNA coding for a protein related to the vascular permeability factor. *Proc Natl Acad Sci U S A* 88: 9267-71., 1991.
110. **Mancini, J. A., C. Li, and P. J. Vickers.** 5-Lipoxygenase activity in the human pancreas. *J Lipid Mediat* 8: 145-50., 1993.
111. **Maniscalco, W. M., R. H. Watkins, C. T. D'Angio, and R. M. Ryan.** Hyperoxic injury decreases alveolar epithelial cell expression of vascular endothelial growth factor (VEGF) in neonatal rabbit lung. *Am J Respir Cell Mol Biol* 16: 557-67., 1997.
112. **Maniscalco, W. M., R. H. Watkins, J. N. Finkelstein, and M. H. Campbell.** Vascular endothelial growth factor mRNA increases in alveolar epithelial cells during recovery from oxygen injury. *Am J Respir Cell Mol Biol* 13: 377-86., 1995.
113. **Manji, J. S., C. J. O'Kelly, W. I. Leung, and D. M. Olson.** Timing of hyperoxic exposure during alveolarization influences damage mediated by leukotrienes. *Am J Physiol Lung Cell Mol Physiol* 281: L799-806., 2001.
114. **Martin, G. R., and R. Timpl.** Laminin and other basement membrane components. *Annu Rev Cell Biol* 3: 57-85, 1987.
115. **Martinez, A., W. Tausch, and P. Dargaville.** Epidemiology of Bronchopulmonary Dysplasia. In: *Chronic Lung Disease in Early Infancy*, edited by R. D. a. C. Bland, J.J. New York: Marcel Dekker, 2001, p. 21.
116. **Massaro, D., and G. D. Massaro.** Dexamethasone accelerates postnatal alveolar wall thinning and alters wall composition. *Am J Physiol* 251: R218-24., 1986.
117. **Massaro, D., N. Teich, and G. D. Massaro.** Postnatal development of pulmonary alveoli: modulation in rats by thyroid hormones. *Am J Physiol* 250: R51-5., 1986.
118. **Massaro, D., N. Teich, S. Maxwell, G. D. Massaro, and P. Whitney.** Postnatal development of alveoli. Regulation and evidence for a critical period in rats. *J Clin Invest* 76: 1297-305., 1985.
119. **Massaro, G. D., and D. Massaro.** Postnatal treatment with retinoic acid increases the number of pulmonary alveoli in rats. *Am J Physiol* 270: L305-10., 1996.
120. **Massaro, G. D., J. Olivier, C. Dzikowski, and D. Massaro.** Postnatal development of lung alveoli: suppression by 13% O<sub>2</sub> and a critical period. *Am J Physiol* 258: L321-7., 1990.
121. **Massaro, G. D., J. Olivier, and D. Massaro.** Short-term perinatal 10% O<sub>2</sub> alters postnatal development of lung alveoli. *Am J Physiol* 257: L221-5., 1989.

122. **McGrath-Morrow, S. A., and J. Stahl.** Apoptosis in neonatal murine lung exposed to hyperoxia. *Am J Respir Cell Mol Biol* 25: 150-5., 2001.
123. **Merkus, P. J., A. A. ten Have-Opbroek, and P. H. Quanjer.** Human lung growth: a review. *Pediatr Pulmonol* 21: 383-97., 1996.
124. **Miquerol, L., B. L. Langille, and A. Nagy.** Embryonic development is disrupted by modest increases in vascular endothelial growth factor gene expression. *Development* 127: 3941-6., 2000.
125. **Mortola, J. P., C. A. Morgan, and V. Virgona.** Respiratory adaptation to chronic hypoxia in newborn rats. *J Appl Physiol* 61: 1329-36., 1986.
126. **Muratore, C. S., H. T. Nguyen, M. M. Ziegler, and J. M. Wilson.** Stretch-induced upregulation of VEGF gene expression in murine pulmonary culture: a role for angiogenesis in lung development. *J Pediatr Surg* 35: 906-12; discussion 912-3., 2000.
127. **Murphy, G., V. Knauper, S. Cowell, R. Hembry, H. Stanton, G. Butler, J. Freije, A. M. Pendas, and C. Lopez-Otin.** Evaluation of some newer matrix metalloproteinases. *Ann N Y Acad Sci* 878: 25-39., 1999.
128. **Musser, J. H., and A. F. Kreft.** 5-lipoxygenase: properties, pharmacology, and the quinolinyl(bridged)aryl class of inhibitors. *J Med Chem* 35: 2501-24., 1992.
129. **Neufeld, G., T. Cohen, N. Shraga, T. Lange, O. Kessler, and Y. Herzog.** The neuropilins: multifunctional semaphorin and VEGF receptors that modulate axon guidance and angiogenesis. *Trends Cardiovasc Med* 12: 13-9., 2002.
130. **Ng, Y. S., R. Rohan, M. E. Sunday, D. E. Demello, and P. A. D'Amore.** Differential expression of VEGF isoforms in mouse during development and in the adult. *Dev Dyn* 220: 112-21., 2001.
131. **Northway, W. H., Jr.** Historical perspective of Bronchopulmonary Dysplasia. In: *Chronic Lung Disease in Early Infancy*, edited by R. D. a. C. Bland, J.J. New York: Marcel Dekker, 2001, p. 1.
132. **Olofsson, B., K. Pajusola, A. Kaipainen, G. von Euler, V. Joukov, O. Saksela, A. Orpana, R. F. Pettersson, K. Alitalo, and U. Eriksson.** Vascular endothelial growth factor B, a novel growth factor for endothelial cells. *Proc Natl Acad Sci U S A* 93: 2576-81., 1996.
133. **Pardo, A., R. Barrios, V. Maldonado, J. Melendez, J. Perez, V. Ruiz, L. Segura-Valdez, J. I. Sznajder, and M. Selman.** Gelatinases A and B are up-regulated in rat lungs by subacute hyperoxia: pathogenetic implications. *Am J Pathol* 153: 833-44., 1998.
134. **Pardo, A., M. Selman, K. Ridge, R. Barrios, and J. I. Sznajder.** Increased expression of gelatinases and collagenase in rat lungs exposed to 100% oxygen. *Am J Respir Crit Care Med* 154: 1067-75., 1996.

135. **Pepper, M. S.** Role of the matrix metalloproteinase and plasminogen activator-plasmin systems in angiogenesis. *Arterioscler Thromb Vasc Biol* 21: 1104-17., 2001.
136. **Pepper, M. S., N. Ferrara, L. Orci, and R. Montesano.** Vascular endothelial growth factor (VEGF) induces plasminogen activators and plasminogen activator inhibitor-1 in microvascular endothelial cells. *Biochem Biophys Res Commun* 181: 902-6., 1991.
137. **Poltorak, Z., T. Cohen, R. Sivan, Y. Kandelis, G. Spira, I. Vlodaysky, E. Keshet, and G. Neufeld.** VEGF145, a secreted vascular endothelial growth factor isoform that binds to extracellular matrix. *J Biol Chem* 272: 7151-8., 1997.
138. **Radomski, A., G. Sawicki, D. M. Olson, and M. W. Radomski.** The role of nitric oxide and metalloproteinases in the pathogenesis of hyperoxia-induced lung injury in newborn rats. *Br J Pharmacol* 125: 1455-62., 1998.
139. **Randell, S. H., R. R. Mercer, and S. L. Young.** Neonatal hyperoxia alters the pulmonary alveolar and capillary structure of 40-day-old rats. *Am J Pathol* 136: 1259-66., 1990.
140. **Reid, G. K., S. Kargman, P. J. Vickers, J. A. Mancini, C. Leveille, D. Ethier, D. K. Miller, J. W. Gillard, R. A. Dixon, and J. F. Evans.** Correlation between expression of 5-lipoxygenase-activating protein, 5-lipoxygenase, and cellular leukotriene synthesis. *J Biol Chem* 265: 19818-23., 1990.
141. **Reponen, P., C. Sahlberg, P. Huhtala, T. Hurskainen, I. Thesleff, and K. Tryggvason.** Molecular cloning of murine 72-kDa type IV collagenase and its expression during mouse development. *J Biol Chem* 267: 7856-62., 1992.
142. **Risau, W.** Mechanisms of angiogenesis. *Nature* 386: 671-4., 1997.
143. **Roeckl, W., D. Hecht, H. Sztajer, J. Waltenberger, A. Yayon, and H. A. Weich.** Differential binding characteristics and cellular inhibition by soluble VEGF receptors 1 and 2. *Exp Cell Res* 241: 161-70., 1998.
144. **Rolland, G., J. Xu, A. K. Tanswell, and M. Post.** Ontogeny of extracellular matrix gene expression by rat lung cells at late fetal gestation. *Biol Neonate* 73: 112-20, 1998.
145. **Rozycki, H. J., P. G. Comber, and T. F. Huff.** Cytokines and oxygen radicals after hyperoxia in preterm and term alveolar macrophages. *Am J Physiol Lung Cell Mol Physiol* 282: L1222-8., 2002.
146. **Sanderud, J., M. Kumlin, E. Granstrom, and O. D. Saugstad.** Effects of oxygen radicals on cysteinyl leukotriene metabolism and pulmonary circulation in young pigs. *Eur Surg Res* 27: 117-26, 1995.
147. **Schittny, J. C., V. Djonov, A. Fine, and P. H. Burri.** Programmed cell death contributes to postnatal lung development. *Am J Respir Cell Mol Biol* 18: 786-93., 1998.

148. **Schreck, R., P. Rieber, and P. A. Baeuerle.** Reactive oxygen intermediates as apparently widely used messengers in the activation of the NF-kappa B transcription factor and HIV-1. *Embo J* 10: 2247-58., 1991.
149. **Shah, M., K. Bry, and M. Hallman.** Protective effect of exogenous transferrin against hyperoxia: a study on premature rabbits. *Pediatr Pulmonol* 24: 429-37., 1997.
150. **Shalaby, F., J. Rossant, T. P. Yamaguchi, M. Gertsenstein, X. F. Wu, M. L. Breitman, and A. C. Schuh.** Failure of blood-island formation and vasculogenesis in Flk-1-deficient mice. *Nature* 376: 62-6., 1995.
151. **Shima, D. T., A. P. Adamis, N. Ferrara, K. T. Yeo, T. K. Yeo, R. Allende, J. Folkman, and P. A. D'Amore.** Hypoxic induction of endothelial cell growth factors in retinal cells: identification and characterization of vascular endothelial growth factor (VEGF) as the mitogen. *Mol Med* 1: 182-93., 1995.
152. **Srinivasan, G., E. N. Bruce, P. K. Houtz, and M. C. Bruce.** Dexamethasone-induced changes in lung function are not prevented by concomitant treatment with retinoic acid. *Am J Physiol Lung Cell Mol Physiol* 283: L275-87., 2002.
153. **Sternlicht, M. D., and Z. Werb.** How matrix metalloproteinases regulate cell behavior. *Annu Rev Cell Dev Biol* 17: 463-516, 2001.
154. **Stevenson, D. K., L. L. Wright, J. A. Lemons, W. Oh, S. B. Korones, L. A. Papile, C. R. Bauer, B. J. Stoll, J. E. Tyson, S. Shankaran, A. A. Fanaroff, E. F. Donovan, R. A. Ehrenkranz, and J. Verter.** Very low birth weight outcomes of the National Institute of Child Health and Human Development Neonatal Research Network, January 1993 through December 1994. *Am J Obstet Gynecol* 179: 1632-9., 1998.
155. **Sutter, C. H., E. Laughner, and G. L. Semenza.** Hypoxia-inducible factor 1alpha protein expression is controlled by oxygen-regulated ubiquitination that is disrupted by deletions and missense mutations. *Proc Natl Acad Sci U S A* 97: 4748-53., 2000.
156. **Tager, A. M., J. H. Dufour, K. Goodarzi, S. D. Bercury, U. H. von Andrian, and A. D. Luster.** BLTR mediates leukotriene B(4)-induced chemotaxis and adhesion and plays a dominant role in eosinophil accumulation in a murine model of peritonitis. *J Exp Med* 192: 439-46., 2000.
157. **Taniguchi, H., F. Taki, K. Takagi, T. Satake, S. Sugiyama, and T. Ozawa.** The role of leukotriene B4 in the genesis of oxygen toxicity in the lung. *Am Rev Respir Dis* 133: 805-8., 1986.
158. **Tanswell, A. K., and B. A. Freeman.** Pulmonary antioxidant enzyme maturation in the fetal and neonatal rat. II. The influence of maternal iron supplements upon fetal lung catalase activity. *Pediatr Res* 18: 871-4., 1984.

159. **Taylor, R. N., D. I. Lebovic, D. Hornung, and M. D. Mueller.** Endocrine and paracrine regulation of endometrial angiogenesis. *Ann N Y Acad Sci* 943: 109-21., 2001.
160. **Thannickal, V. J., and B. L. Fanburg.** Reactive oxygen species in cell signaling. *Am J Physiol Lung Cell Mol Physiol* 279: L1005-28., 2000.
161. **Tian, H., R. E. Hammer, A. M. Matsumoto, D. W. Russell, and S. L. McKnight.** The hypoxia-responsive transcription factor EPAS1 is essential for catecholamine homeostasis and protection against heart failure during embryonic development. *Genes Dev* 12: 3320-4., 1998.
162. **Tian, H., S. L. McKnight, and D. W. Russell.** Endothelial PAS domain protein 1 (EPAS1), a transcription factor selectively expressed in endothelial cells. *Genes Dev* 11: 72-82., 1997.
163. **Tischer, E., R. Mitchell, T. Hartman, M. Silva, D. Gospodarowicz, J. C. Fiddes, and J. A. Abraham.** The human gene for vascular endothelial growth factor. Multiple protein forms are encoded through alternative exon splicing. *J Biol Chem* 266: 11947-54., 1991.
164. **Tschanz, S. A., B. M. Damke, and P. H. Burri.** Influence of postnatally administered glucocorticoids on rat lung growth. *Biol Neonate* 68: 229-45, 1995.
165. **Ueda, N., S. Yamamoto, J. A. Oates, and A. R. Brash.** Stereoselective hydrogen abstraction in leukotriene A4 synthesis by purified 5-lipoxygenase of porcine leukocytes. *Prostaglandins* 32: 43-8., 1986.
166. **Unemori, E. N., N. Ferrara, E. A. Bauer, and E. P. Amento.** Vascular endothelial growth factor induces interstitial collagenase expression in human endothelial cells. *J Cell Physiol* 153: 557-62., 1992.
167. **Veness-Meehan, K. A., F. G. Bottone, Jr., and A. D. Stiles.** Effects of retinoic acid on airspace development and lung collagen in hyperoxia-exposed newborn rats. *Pediatr Res* 48: 434-44., 2000.
168. **Vu, T. H., J. M. Shipley, G. Bergers, J. E. Berger, J. A. Helms, D. Hanahan, S. D. Shapiro, R. M. Senior, and Z. Werb.** MMP-9/gelatinase B is a key regulator of growth plate angiogenesis and apoptosis of hypertrophic chondrocytes. *Cell* 93: 411-22., 1998.
169. **Waltenberger, J., L. Claesson-Welsh, A. Siegbahn, M. Shibuya, and C. H. Heldin.** Different signal transduction properties of KDR and Flt1, two receptors for vascular endothelial growth factor. *J Biol Chem* 269: 26988-95., 1994.
170. **Wang, H., and J. A. Keiser.** Vascular endothelial growth factor upregulates the expression of matrix metalloproteinases in vascular smooth muscle cells: role of flt-1. *Circ Res* 83: 832-40., 1998.

171. **Watkins, R. H., C. T. D'Angio, R. M. Ryan, A. Patel, and W. M. Maniscalco.** Differential expression of VEGF mRNA splice variants in newborn and adult hyperoxic lung injury. *Am J Physiol* 276: L858-67., 1999.
172. **Weibel, E. R.** Development of Vasculature. In: *The Lung: Scientific Foundations*, edited by J. B. W. R G Crystal, E R Weibel, P J Barnes. New York: Lippencott Raven, 1997.
173. **Weiss, M. J., and P. H. Burri.** Formation of interalveolar pores in the rat lung. *Anat Rec* 244: 481-9., 1996.
174. **Wood, M. W., F. J. Seidler, and T. A. Slotkin.** Immediate decline in DNA synthesis in neonatal rat lung caused by exposure to 100% oxygen. *Res Commun Chem Pathol Pharmacol* 80: 323-8., 1993.
175. **Woods, J. W., M. J. Coffey, T. G. Brock, Singer, II, and M. Peters-Golden.** 5-Lipoxygenase is located in the euchromatin of the nucleus in resting human alveolar macrophages and translocates to the nuclear envelope upon cell activation. *J Clin Invest* 95: 2035-46., 1995.
176. **Woods, J. W., J. F. Evans, D. Ethier, S. Scott, P. J. Vickers, L. Hearn, J. A. Heibein, S. Charleson, and Singer, II.** 5-lipoxygenase and 5-lipoxygenase-activating protein are localized in the nuclear envelope of activated human leukocytes. *J Exp Med* 178: 1935-46., 1993.
177. **Yang, F., J. J. Coalson, H. H. Bobb, J. D. Carter, J. Banu, and A. J. Ghio.** Resistance of hypotransferrinemic mice to hyperoxia-induced lung injury. *Am J Physiol* 277: L1214-23., 1999.
178. **Zachary, I., A. Mathur, S. Yla-Herttuala, and J. Martin.** Vascular protection: A novel nonangiogenic cardiovascular role for vascular endothelial growth factor. *Arterioscler Thromb Vasc Biol* 20: 1512-20., 2000.
179. **Zeng, X., S. E. Wert, R. Federici, K. G. Peters, and J. A. Whitsett.** VEGF enhances pulmonary vasculogenesis and disrupts lung morphogenesis in vivo. *Dev Dyn* 211: 215-27., 1998.



It is obvious from the literature that there are still many questions to be answered in relation to the development of the alveoli and inhibition of this development due to hyperoxia. It is an essential area of research as it has many implications for the premature newborn, which is exposed to a relative hyperoxic environment before its lungs are mature enough to deal with it. Even room air to a premature newborn is hyperoxic, and O<sub>2</sub> therapies designed to rescue the infant compounds the problem and can lead to adverse changes in lung morphology and the overall health of the newborn.

The overall objective of these studies was, therefore, to increase the understanding of how the lung develops, through determining changes in mediators of alveolarization that occur when alveolar development is disrupted by a hyperoxic environment.

Three possible mediators of alveolarization or hyperoxic-inhibited alveolarization were examined:

The first, VEGF, is a potent angiogenic factor. As inhibition of angiogenesis has been previously shown to cause inhibited alveolarization, we hypothesized that hyperoxic-exposure of rat pups during the development of the alveoli would decrease the mRNA expression and protein levels of VEGF and its receptors.

MMP-2 and MMP-9 are enzymes often associated with inflammation. Exposure of newborn rats to hyperoxia causes an inflammatory response and lung damage. Therefore

the hypothesis that increased O<sub>2</sub> levels would increase the expression and activity of MMP-2 and MMP-9 was tested.

The final potential mediators of hyperoxic-inhibited alveolarization examined were the LTs. The cysteinyl-LTs had been previously shown to mediate O<sub>2</sub>-inhibited septation; in these experiments we hypothesized that this increase in LTs occurred through an increase in one of the enzymes responsible for LT synthesis, 5-LO, and its activating protein, FLAP. We further examined the location of these factors in the lungs of rat pups exposed to hyperoxia

**3.1 ANIMALS**

Sprague-Dawley albino rat pups (Charles River Laboratories, St. Constant, Quebec, Canada) of both sexes were used. Dams were received into the Health Sciences Animal Laboratory Service Department of the University of Alberta on E 13 and kept under veterinary supervision. The approval of the University of Alberta Animal Care Committee was obtained and the guidelines of the Canadian Council of Animal Care were followed in all experimental procedures. Dams were maintained on regular laboratory rodent pellets and water *ad libitum* and kept on a 12 h light/dark cycle.

**3.1.1 *O<sub>2</sub> Exposure***

The day pups were delivered was designated d 0. On d 2 pups from two parallel litters were mixed and 10 pups were randomly selected and placed with each dam. On the morning of d 4 dams were switched to the other set of pups and cages were placed into 0.14 m<sup>3</sup> Plexiglas exposure chambers containing > 95 % O<sub>2</sub> (oxygen/hyperoxia) or 21 % O<sub>2</sub> (room air/normoxia), as previously published (1, 2, 4). Oxygen concentrations were monitored daily (Ventronic oxygen analyzer no. 5517, Temecula, CA, USA). The oxygen and the room air were filtered through barium hydroxide lime (Baralyme, Chemeton Medical Division, St. Louis, MO, USA) to keep CO<sub>2</sub> levels below 0.5 %, and through charcoal to remove odors. Temperature and humidity were maintained at 26 °C and 75 - 80 % respectively. The chambers were opened for < 15 min daily in which time the pups

were placed in clean cages and the dams were switched between air and O<sub>2</sub> groups. A schematic of the oxygen-exposure protocol is shown in Figure 3.1, and an example of the structural effects of O<sub>2</sub> on development using this protocol is shown in Figure 3.2.

### ***3.1.2 Preparation of lung samples***

Pups from each exposure group were removed from the dams and brought to laboratory on d 4, 6, 9, 12 and 14. The pups were kept warm by keeping them in groups covered with rags and they were killed as quickly as possible to minimize stress. Pups were killed with an intraperitoneal overdose of pentobarbital sodium (100 mg / kg Euthanyl; MIC Pharmaceuticals, Cambridge, ON, Canada).

For mRNA and Western blotting experiments the vasculature of the lung was washed by perfusion with 5 ml of ice-cold phosphate buffered saline which was slowly injected into the right ventricle. The lungs were then removed and snap frozen in liquid nitrogen before being stored at - 80 °C.

Previous to extraction of RNA or protein, the lungs were ground in liquid nitrogen with a pestle and mortar, poured (in the liquid nitrogen) into pre-cooled plastic test tubes and placed on dry ice. Stoppers were placed in test tubes after the liquid nitrogen had evaporated off to eliminate pressure build up in the tubes.

## **3.2 REVERSE TRANSCRIPTION (RT) AND REAL-TIME QUANTITATIVE POLYMERASE CHAIN REACTION (PCR)**

Total RNA was isolated using TRIzol reagent according to the manufacturer's instructions (Life Technologies, Burlington, Ontario, Canada). Briefly, 1 ml of Trizol was

added to about 1 g of tissue and homogenized on ice for 20 s using a polytron homogenizer set at '7'. Chloroform (200  $\mu$ l) was added and samples were shaken and then centrifuged at 4 °C at 12,000 x g for 15 min. The top layer (containing the RNA) was removed to a new eppendorf, 500  $\mu$ l of isopropanol was added and the RNA was precipitated at - 80 °C for 15 min. The supernatant was removed and the RNA pellet was washed with 75 % ethanol, then dried for 5 min before being dissolved in 100  $\mu$ l of TE buffer (10mM Tris-HCl, 1 mM EDTA, pH 7.0).

The samples were further treated with DNase 1 (DNA-free<sup>TM</sup>, Ambion Inc, Austin, Texas) to ensure that no DNA contamination existed. To 100  $\mu$ l of RNA, 10  $\mu$ l of 10x DNase and 2  $\mu$ l of DNase 1 were added, the reaction was then incubated at 37 °C for 1 h. DNase Inactivation Reagent (10  $\mu$ l) was added, and the RNA was mixed and then incubated at room temperature for 2 min. The samples were centrifuged for 1 min and the supernatant was removed.

To quantitate the amount of RNA per sample, 5  $\mu$ l of each sample was added to 495  $\mu$ l TE buffer and the wavelengths at 260 nm and 280 nm were measured. The quantity of RNA was calculated by the following equation; RNA concentration = spectrophotometric conversion (40  $\mu$ g/ml for 1 cm path length in a quartz cuvette) x absorbance at 260 nm ( $A_{260}$ ) x dilution factor. The quality of the RNA was assessed by electrophoresis of samples on a 1 % agarose gel containing 0.5  $\mu$ g/ml ethidium bromide and then visualization of the 28 S and 18 S ribosomal RNA bands under UV light. The RNA was stored in aliquots of 10  $\mu$ l at a concentration 2  $\mu$ g/ $\mu$ l in the - 80 °C freezer.

### **3.2.1 Reverse Transcription (RT)**

Total RNA (100 ng) was added to a reaction mixture containing 100 ng random nanomers (Stratagene, La Jolla, CA), 1x cDNA first-strand buffer, 500 mM DTT, 0.4 U/ $\mu$ l RNase Inhibitor, 1 mM each deoxyNTPs and 0.75 U/ $\mu$ l Superscript II reverse transcriptase (Gibco BRL, Life Technologies, Burlington, Ontario, Canada) in a 60  $\mu$ l volume. Negative RT (no reverse transcriptase enzyme) and no-template (no RNA) controls were also included. The RT thermal cycle was 25 °C for 10 min, 50 °C for 45 min, 85 °C for 5 min and was performed in 96 well plates on the iCycler iQ system (Bio-Rad Laboratories, Hercules, California).

### **3.2.2 Real-time PCR**

For real-time PCR two methods of detection were used; the first used SYBR-green which fluoresces when incorporated into double stranded DNA, the second used a molecular beacon which fluoresces when it binds to a specific complementary sequence on the cDNA. Both these methods are explained in Figure 3.3. The primers, fluorescent beacons and method of detection used for each gene of interest are shown in Table 3.1. Primers were purchased from Sigma Genosys (Oakville, Ontario, Canada) and the fluorescent molecular beacons from Stratagene (La Jolla, CA). The primers were optimized for annealing temperature and RT RNA concentration by assessing PCR products (on 1 % agarose gels containing 0.5  $\mu$ g/ml ethidium bromide) from reactions with varying RNA concentrations and varying annealing temperatures, respectively. The correct product size was also confirmed at this time by running a DNA base pair marker on the gel. The PCR products obtained from each of the primer sets used are shown in

Figure 3.4. The correct sequence of the cDNA was confirmed by sequencing by the DNA core laboratory (3 rd Floor Medical Sciences Building).

The PCR mixture (50  $\mu$ l total volume) consisted of 0.2  $\mu$ M of each primer, 0.2  $\mu$ M of each molecular beacon (if used, refer to Table 3.1), 10x PCR buffer (including SYBR green if used, refer to Table 3.1) (Perkin Elmer-Applied Biosystems, Warrington, UK), 1.9 mM MgCl<sub>2</sub>, 0.2 mM each dNTPs, 0.04 U/ $\mu$ l Taq polymerase (Gibco BRL, Life Technologies, Burlington, Ontario, Canada) and 2  $\mu$ l cDNA. Amplification and detection were performed using the iCycler iQ real-time PCR detection system (Bio-Rad Laboratories, Hercules, California) with the following cycle profile for all primer sets: 50 °C for 2 min, 95 °C for 10 min and 45 cycles of 95 °C for 15 s, 56 °C for 1 min 72 °C for 30 s.

### ***3.2.3 Analysis of real time PCR results***

The cDNA of d 4 animals was pooled and used as a control group to allow analysis between PCR plates. A standard curve was generated using d 4 starting concentrations of RNA (i.e. before RT reaction) of 800 ng, 400 ng, 200 ng, 100 ng, 50 ng, 25 ng and 12.5 ng and the slope of this curve calculated. All results also were normalized to cyclophilin, a cytoskeletal protein, which is expressed constitutively in all tissues and did not change during these experiments; mean =  $2.13 \pm 0.13$  relative fluorescent units. Cyclophilin quantification was performed by separate PCR reactions using SYBR-green or, when a fluorescently labeled beacon was used, in the same reaction as the gene of interest. Quantification was performed by determining the threshold cycle ( $C_T$ ), which is the cycle where the fluorescence of a sample rises appreciably above the background fluorescence.

The  $C_T$  is proportional to the amplified starting copy number of cDNA (or RNA). Figure 3.5 shows an example of the  $C_T$  and results obtained from a typical real-time PCR reaction. All reactions were performed in triplicate and a no-template reaction was included for each plate. The quantity of mRNA was calculated by normalizing the  $C_T$  of genes of interest to the  $C_T$  of the housekeeping protein cyclophilin of the same RNA probe, according to the following formula:  $(E_{\text{gene of interest}})^{\Delta CT_{\text{gene of interest}} (CT_{\text{control}} - CT_{\text{sample}})} / (E_{\text{cyclophilin}})^{\Delta CT_{\text{cyc}} (CT_{\text{control}} - CT_{\text{sample}})}$ , where E is the efficiency of the reaction and was calculated as,  $E = 10^{-1 / \text{slope of standard curve}}$  and the control was the pooled d 4 samples with 100 ng starting concentration of RNA (5).

### 3.3 PROTEIN ANALYSIS

#### 3.3.1 *Protein extraction*

The ground, frozen tissue samples (about 1 g each) were homogenized for 20 s in 1 ml lysis buffer containing 50mM Tris-HCl, 3mM Sucrose, 0.1% Triton X-100 and 1mM Protease Inhibitor Cocktail (Calbiochem-Novabiochem Corporation, La Jolla, CA, USA). Samples were transferred into 1.5 ml tubes and centrifuged at 5,000 x g at 4 °C for 20 min and the supernatant was removed, aliquoted and stored at - 80 °C. The protein content was estimated using a Micro BCA Protein Assay Reagent Kit (Pierce, Rockford, Illinois, USA). The samples were diluted 1 / 20, 1 / 50 and 1 / 100 in lysis buffer to ensure that readings within the limits of the standard curve (0 – 15 µg of bovine serum albumin / well) were obtained. On a 96 well plate, 100 µl of standard or sample plus 400 µl H<sub>2</sub>O, then 500 µl of the prepared BCA reagent was added to each well. The plates were incubated at 60 °C for 1 h, then cooled before the samples were measured on a plate



reader at 562 nm. The optical density was then compared to the standard curve and the amount of protein per well (i.e. per 100  $\mu$ l, adjusted for dilution) was calculated.

### 3.3.2 *Western Immunoblotting*

The presence and relative abundance of proteins were determined using Western immunoblotting as described by Laemmli (3). Aliquots from lung homogenates (prepared as described under protein extraction) were diluted in lysis buffer and 6x reducing loading buffer (Tris-Cl 0.5 M,  $\beta$ -mercaptoethanol, 87 % glycerol, 10 % SDS, 1 % bromophenol blue) to give a 1x solution of loading buffer. The protein (40 $\mu$ g/well) was loaded into polyacrylamide gels; 6 % for VEGF, 15 % for VEGFR1 and VEGFR2, 12 % for MMP-2 and MMP-9, 5-LO and FLAP. The proteins were separated by electrophoresis at 100 V for 1.5 h in electrophoresis buffer (using 1:5 dilution of a 5x buffer containing 0.5 M Tris base, 1.92 M glycine, 0.5 % SDS) and then transferred onto nitrocellulose membranes (Bio-Rad, Mississauga, Ontario, Canada) for 1 h at 80 V at 4 °C using a buffer containing 25 mM Tris base, 150 mM glycine and 20 % (v/v) methanol. The membranes were blocked for non-specific binding using a 7 % skimmed milk solution in TBS - 0.1% Tween (10 mM Tris-Cl, 150 mM NaCl, 0.1 % (v/v) Tween 20). The membranes were incubated with primary antibodies as in Table 3.2 diluted in a 5 % skimmed milk solution (as above) for 2 h at room temperature. Membranes were rinsed 3 x, washed 6 x 15 min on a shaker in TBS - 0.1% Tween and then incubated for 1 h with a peroxidase conjugated secondary antibody (see Table 3.2) diluted to 1:3000 in a 5 % skimmed milk solution (Jackson ImmunoResearch, Bio/Can Scientific, Mississauga, Ontario, Canada). The washing protocol was repeated with TBS - 0.15% Tween. After

repeated washing, the membranes were incubated with 2 ml of enhanced chemiluminescence reagent for 2 min (Amersham Pharmacia Biotech, UK) and then placed in a Fluor-X Max Imager (Bio-rad, Mississauga, Ontario, Canada) where the image was captured. Bands were analyzed by densitometric analysis using the Fluor-X Max software. Individual bands were selected and the density of colour of each band was automatically calculated.

### **3.4 STATISTICAL ANALYSES**

Western immunoblotting and gelatinase zymography results were calculated as a ratio to d 4 values for comparison, and PCR results used d 4 lungs as control values. All results were normally distributed and were analyzed by two-way analysis of variance (ANOVA), where variance was distributed according to treatment and time. When a significant F value was found, Tukey's post hoc test was used to determine significance. For morphometric analysis, a student's t-test was performed between the treated and untreated groups. A Spearman Rank Order test was used to assess correlations between data. Statistical significance was achieved at  $p < 0.05$ .

### 3.5 REFERENCES

1. **Boros, V., J. S. Burghardt, C. J. Morgan, and D. M. Olson.** Leukotrienes are indicated as mediators of hyperoxia-inhibited alveolarization in newborn rats. *Am J Physiol* 272: L433-41., 1997.
2. **Burghardt, J. S., V. Boros, D. F. Biggs, and D. M. Olson.** Lipid mediators in oxygen-induced airway remodeling and hyperresponsiveness in newborn rats. *Am J Respir Crit Care Med* 154: 837-42., 1996.
3. **Laemmli, U. K.** Cleavage of structural proteins during the assembly of the head of bacteriophage T4. *Nature* 227: 680-5., 1970.
4. **Manji, J. S., C. J. O'Kelly, W. I. Leung, and D. M. Olson.** Timing of hyperoxic exposure during alveolarization influences damage mediated by leukotrienes. *Am J Physiol Lung Cell Mol Physiol* 281: L799-806., 2001.
5. **Pfaffl, M. W.** A new mathematical model for relative quantification in real-time RT-PCR. *Nucleic Acids Res* 29: E45-E45., 2001.

Gene of interest	Forward Primer	Reverse Primer	SYBR-green	Fluorescent beacon
Cyclophilin	TCACCCACACTGTGCCCATCTACGA	GGATGCCACAGGATTCCATAACCA	-	CAGGCTGCGAGCTGT TTGCAGACAAAAGTTC CAAAGACAGCAGCCTG
VEGF	TGCACTGGACCCTGGCTTTAC	CGGCAGTAGCTTCGCTGGTAG	yes	
VEGFR1	CTCGTTAGAGATTTGGAAGCGC	GCAGGGACACCTCTAGCTTGAC	-	CAGCTGGTCAAAACC TCAGTGACCACGAGC ACGCTG
VEGFR2	TAGCTGTCGCTCTGTGGTTCTG	CCTGCAAGTAATCTGAAGGGTT	-	CAGGCTGGCCTGGCG ATTCCCTCCATCCACC CCAGCCTG
HIF-2 $\alpha$	TTGCGGGGGTTGTAGATG	ACTTGGACGCTCTGCCTATG	yes	
MMP-2	ATCTGGTGTCTCCCTTACGG	GTGCAGTGATGTCCGACAAC	yes	
MMP-9	GGCAAGGATGGTCTACTGGC	GACGCACATCTCTCCTGCCG	-	CGCGATCCACTTCGA CGACGACGAGITGTG GTGATCGCG
TIMP-1	GAAATCATCGAGACCACCTT	AACCGGATATCTGTGGCATT	yes	
TIMP-2	CCCTGTGACACGCTTAGCAT	TGGTGCCCATGATGCTCTT	yes	

**Table 3.1 Primers and Fluorescent Beacons used for real-time PCR**

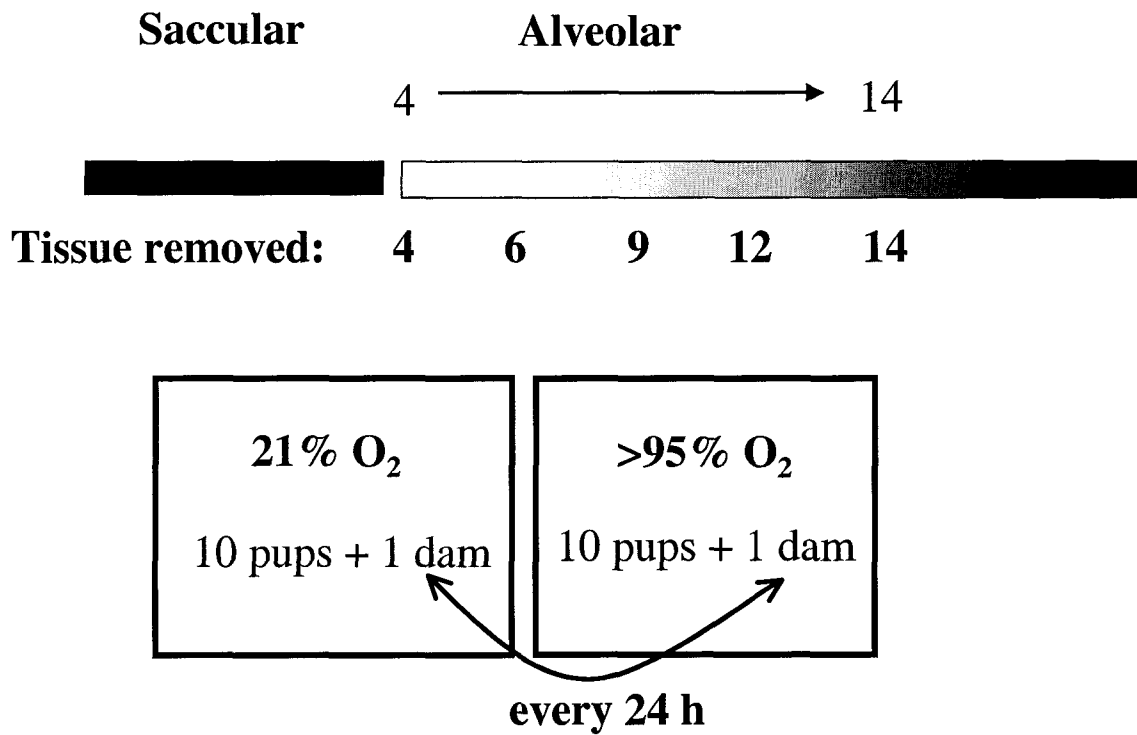
All primers and beacons are written 5' to 3'. Fluorescent beacons have Texas Red attached to the 5' end and the quencher DABCYL attached to the 3' end.

Protein of interest	Raised in	Western blot dilution	Source	Secondary Antibody
VEGFR1	rabbit	1:500	Alpha Diagnostics	goat anti rabbit
VEGFR2	rabbit	1:500	Alpha Diagnostics	goat anti rabbit
MMP-2	rabbit	1:500	Sigma-Aldrich	goat anti rabbit
MMP-9	rabbit	1:500	Sigma-Aldrich	goat anti rabbit
5-LO	rabbit	1:200	gift from Merck-Frost	goat anti rabbit
FLAP	rabbit	1:300	gift from Merck-Frost	goat anti rabbit

---

**Table 3.2 Antibodies used for Western Immunoblotting Experiments**

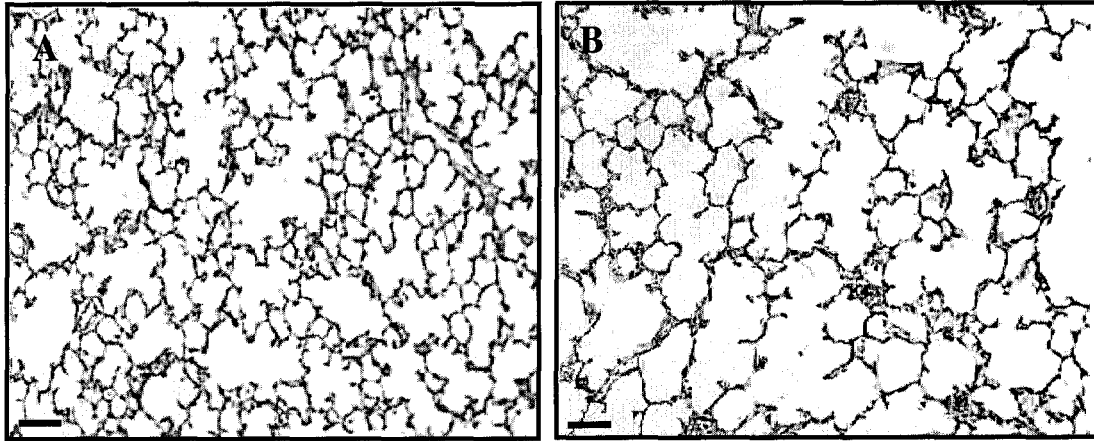
All secondary antibodies for Western Immunoblotting were peroxidase conjugated and were purchased from Jackson ImmunoResearch (Bio/Can Scientific, Mississauga, Ontario).




---

**Figure 3.1**    **Scheme showing the hyperoxic-exposure protocol.**

Rat pups were exposed to air or > 95 % O<sub>2</sub> from d 4 to d 14 during the period of alveolarization. Lungs were removed on days 4, 6, 9, 12 and 14. Dams were switched between the room air and hyperoxic environments every 24 hours.



---

**Figure 3.2** Representative photomicrograph of the effect of (A) air and (B) O<sub>2</sub> on the morphometry of rat lungs at d 14.

Rat pups were exposed to air (A) or > 95 % O<sub>2</sub> (B) from d 4 to d 14. On d 14 lungs were removed and fixed and lung slices were stained with Haematoxylin and Eosin. The airspaces in (B) are larger and a more simple shape than in (A). The bars represent 200 μm.

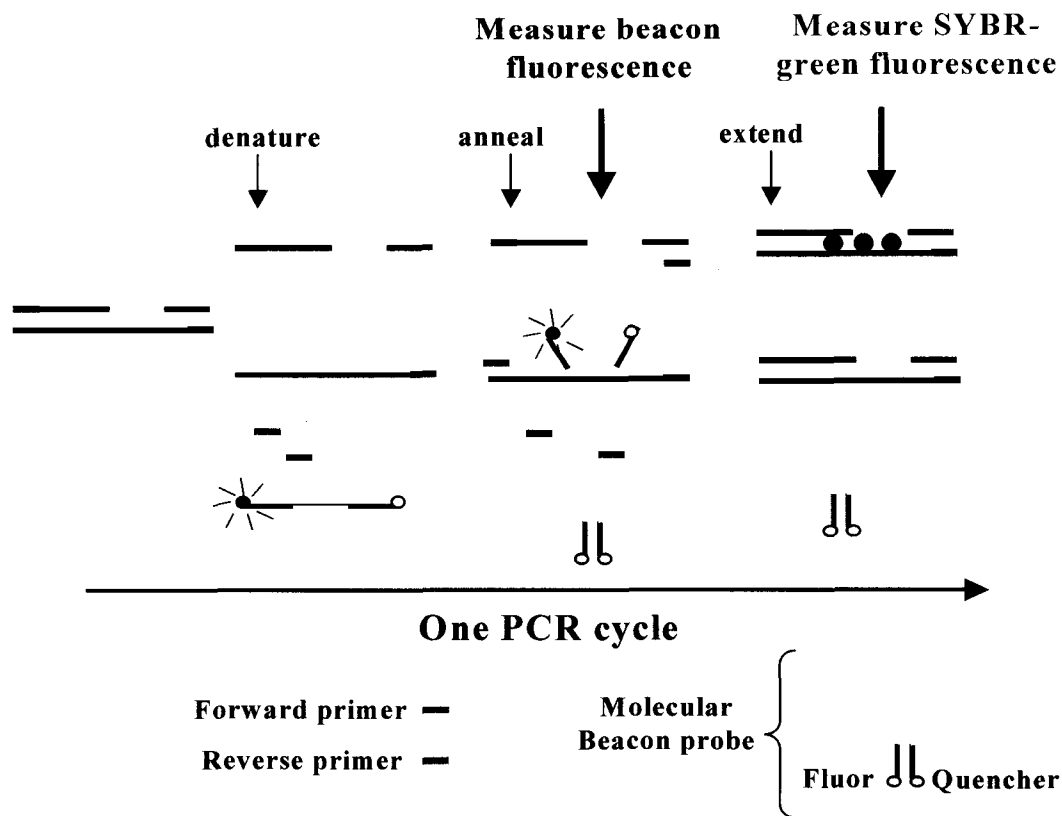


**Figure 3.3 The chemistry of real time PCR.**

A) SYBR-green was included in the reaction. During extension more and more SYBR-green molecules bind to the newly synthesized DNA and the increase in fluorescence can be measured. On denaturation the dye molecules are released and the fluorescence returns to background. B) A molecular beacon was designed to be complementary to a sequence in the middle of the amplicon. During denaturation the beacons assume a random coil formation and fluoresce. As the temperature is decreased stem hybrids form preventing fluorescence. However in the presence of a target, molecular beacons also bind to the amplicons and generate fluorescence. When the temperature is increased for the primer extension step, the molecular beacons dissociate from their targets and the fluorescence is again quenched. A new hybridization takes place in the annealing step of each cycle and the intensity of the resulting fluorescence indicates the amount of accumulated amplicon at the end of the previous cycle.



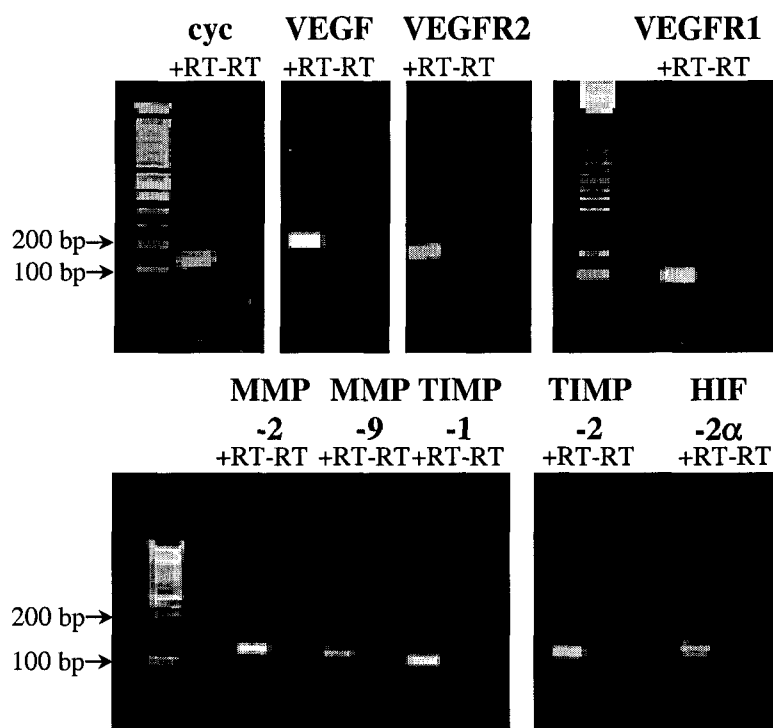


**Figure 3.4** PCR products for each gene of interest.

Products of PCR reactions were run on 1 % agarose gel containing 0.5  $\mu\text{g/ml}$  EtBr. All products were the appropriate size (+RT) and the reactions containing no reverse transcriptase (-RT) showed no bands.

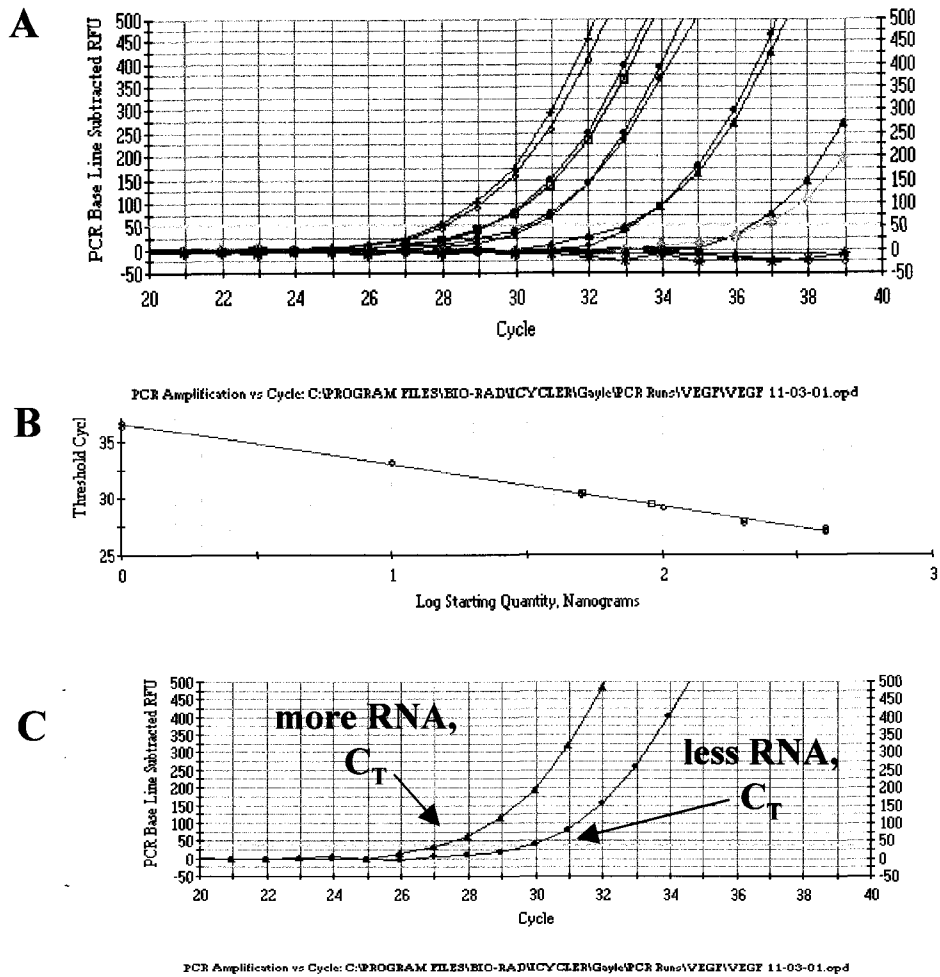


**Figure 3.5** Example of the results obtained from a real-time PCR reaction.

- A) A standard curve was generated from pooled d 4 samples. B) The threshold cycles ( $C_T$ ) values obtained from A were plotted against the log of the starting quantity of RNA. C) An example of a 2.8 cycle increase in  $C_T$ , which corresponds to a decrease in RNA.

## **CHAPTER 4. EFFECTS OF HYPEROXIA ON VEGF, ITS RECEPTORS AND HIF-2 $\alpha$ IN THE NEWBORN RAT LUNG**

---

A version of this manuscript has been submitted to the American Journal of Physiology – Lung Cell and Molecular Physiology.

### **4.1 INTRODUCTION**

Hyperoxic injury in developing lungs leads to microvascular damage, diminished epithelial cell proliferation and arrest of alveolarization. In 1983 Roberts *et al.* (26) studied the effect of 6 days of exposure of neonatal rats to > 95 % O<sub>2</sub> (26) on the microvasculature of the lung and showed a decreased density of small and large capillaries in the lung. Hyperoxia during the neonatal period in rats also interferes with the process of septation; alveolar number and internal surface area are decreased and the parenchymal airspace is enlarged (4, 20, 29).

Vascular endothelial growth factor (VEGF) is a key regulator of lung development. It acts through two distinct tyrosine kinase receptors, VEGFR1 (Flt-1) and VEGFR2 (KDR/flk-1) and is essential for endothelial cell differentiation as well as the sprouting of new capillaries from preexisting vessels (angiogenesis) (10, 25). Angiogenesis has been shown to be necessary for the development of the alveoli in the newborn rat. Jakkula *et al.* (13) administered inhibitors of endothelial cell proliferation (thalidomide and fumagillin) to rat pups between d 3 and d 14 and demonstrated decreased capillary

density along with inhibited septation of the lungs. In the same study VEGF action was blocked by the VEGFR2 receptor blocker SU-5416 and similar results were observed (13). Further evidence that VEGF and angiogenesis are associated with the development of the alveoli comes from a study showing that pulmonary cell stretch which stimulates capillary and alveolar septal growth in an *in vitro* system, upregulated VEGF mRNA and protein expression (23).

VEGF and its receptors have previously been shown to respond to oxygen in neonatal animals. Maniscalco *et al.*, showed that neonatal rabbits exposed to 100 % O<sub>2</sub> for 9 days had decreased VEGF mRNA abundance, decreased alveolar epithelial cell VEGF expression, and decreased VEGF immunostaining (18). In later work it was demonstrated that the reduction in VEGF mRNA was mainly due to a decrease in expression of the VEGF<sub>189</sub> splice variant (30). However, Watkins and colleagues actually showed an increase in lavage fluid VEGF protein on d 4, d 6 and d 8 during exposure of neonatal rabbits to 100 % O<sub>2</sub> and only a decrease after 9 days of hyperoxia. It has further been demonstrated that the expression of VEGF and its receptors are decreased after exposure to > 95 % O<sub>2</sub> for 48 hours in the adult rat, but nothing is known of the response of VEGF receptors to hyperoxia in neonatal rabbits or rats (16).

The transduction of an O<sub>2</sub> signal to the level of gene expression requires the nuclear translocation and activation of redox-responsive transcription factors over specific ranges of pO<sub>2</sub>. VEGF expression is induced when most cell types are exposed to hypoxia as a result of increased transcriptional activation and mRNA stabilization of hypoxia-inducible factor-1 $\alpha$  (HIF-1 $\alpha$ ) (27). HIF-2 $\alpha$  (or HIF-1 $\alpha$ -like factor) has close sequence

similarity to HIF-1 $\alpha$  (8), however the modes of expression of HIF-1 $\alpha$  and HIF-2 $\alpha$  vary greatly as HIF-2 $\alpha$  is abundantly expressed in the adult lung in the normoxic state whereas HIF-1 $\alpha$  is ubiquitous at much lower O<sub>2</sub> levels (8). HIF-2 $\alpha$  was found to be highly expressed in vascular endothelial cells in the lung around parturition, while the low levels of HIF-1 $\alpha$  during gestation did not change. It is therefore postulated that HIF-2 $\alpha$  regulates VEGF expression under normoxic conditions and during lung and vascular development. Recent experiments further demonstrated that loss of HIF-2 $\alpha$  impaired lung maturation as well as creating a subtle deficit in vascularization of the alveolar septa (6).

There may be differences in lung maturation between the rat and the rabbit; dexamethasone has been shown to inhibit septation in the neonatal rat, however recent data shows that there is no difference in lung structure after administration of dexamethasone to neonatal rabbits (17, 21). No experiments have as yet addressed the effects of O<sub>2</sub> on VEGF expression or protein levels in the neonatal rat lung or VEGF receptor expression or levels in any model of inhibited alveolar development. The initial aim of these experiments, therefore, was to determine changes in VEGF, VEGFR1 and VEGFR2 mRNA expression and protein levels, both during the normal period of alveolar development in the neonatal rat lung and during exposure to a hyperoxic environment. Additionally we studied one of the potential regulators of VEGF expression in this system, HIF-2 $\alpha$ , which has been previously shown to respond to high oxygen concentrations.

## 4.2 METHODS

Sprague-Dawley albino rat pups were exposed to O<sub>2</sub> as described in Methods. Reverse Transcription and Real-Time Quantitative PCR were performed for HIF-2 $\alpha$ , VEGF, VEGFR1 and VEGFR2. VEGFR1 and VEGFR2 relative protein levels were analyzed by Western immunoblotting. All these techniques and the primers and antibodies used are described in the Methods Section.

### 4.2.1 *VEGF Immunoassay*

VEGF protein levels were assessed by immunoassay. Samples were prepared as in Methods section (2.3.1). The VEGF assay was performed using the Quantikine® M, mouse VEGF Immunoassay kit (R&D Systems Inc., Minneapolis, MN) according to manufacture's instructions. This assay recognizes both the 165 and 121 amino acid residue forms of VEGF and has 70 % cross-reactivity with recombinant rat VEGF. The starting sample concentration was 2  $\mu$ g total protein /  $\mu$ l and samples were diluted 5-fold in Calibrator Diluent RD5T before analysis. A standard curve of supplied mouse VEGF standard was generated; 500 pg/ml, 250 pg/ml, 125 pg/ml, 62.5 pg/ml, 31.2 pg/ml, 15.6 pg/ml and 7.8 pg/ml by serial dilutions in Calibrator Diluent RD5T. Assay Diluent RD1N (50  $\mu$ l) was added to each well with a repeat pipettor, then 50  $\mu$ l of Standard (leading to a curve of 25, 12.5, 6.25, 3.125, 1.563, 0.78, 0.39 pg/well), sample or mouse VEGF Control were added to appropriate wells in triplicate and incubated at room temperature for 2 h. The wells were emptied by inverting and banging the plate on absorbent towels, and wells were washed with Wash Buffer using a squirt bottle. The washing was repeated for a total of 5 times. Mouse VEGF conjugate (100  $\mu$ l) was added to each well and the

plate was incubated at room temperature for 2 h. The washing step was repeated as before and 100  $\mu$ l of Substrate Solution was then added to each well and the plate was incubated at room temperature for 30 min in the dark. The reaction was stopped by addition of 100  $\mu$ l of Stop Solution and the plate was tapped to ensure mixing. The optical density of each well was determined on a microplate reader set to 450 nm. Sample concentrations were determined from the standard curve, measured as pg/well. These results were then adjusted for a 5-fold dilution, and the starting concentration of 2  $\mu$ g/ $\mu$ l, so that final results were expressed as pg VEGF /  $\mu$ l total lung protein.

### **4.3 RESULTS**

#### **4.3.1 VEGF**

Changes in total mRNA levels for the angiogenic growth factor, VEGF, were examined. The primers used for the real-time PCR analysis amplified a sequence that was common to all VEGF splice variants. Expression of total VEGF mRNA tended to increase slightly between d 6 and d 12 in the animals raised in room air (Fig. 4.1 A), this increase reached significance by d 14 ( $p < 0.05$ ) where values were twice those of d 6 air-exposed pups. Exposure to oxygen abolished the increase in mRNA levels seen in the normoxic pups, so that O<sub>2</sub>-exposed pups exhibited significantly lower VEGF mRNA levels than those from lungs of normoxic pups on d 12 and d 14 ( $p < 0.001$ ) (Fig. 4.1 A).

An increase, similar to that of the total VEGF mRNA, was seen in VEGF protein mass between d 4 and d 12 ( $p < 0.05$ ), this increase was maintained through d 14 at  $0.61 \pm 0.04$  pg /  $\mu$ g total lung protein in normoxic pups (Fig. 4.1 B). Contrary to the inhibition seen in total VEGF mRNA, O<sub>2</sub> exposure resulted in a biphasic effect on VEGF protein levels,

stimulating an increase from d 4 ( $0.41 \pm 0.03$  pg /  $\mu$ g protein) to d 9 ( $0.57 \pm 0.03$  pg /  $\mu$ g protein) ( $p < 0.001$ ), then a decrease on day 12 to lower than normoxic control values,  $0.40 \pm 0.06$  pg /  $\mu$ g compared to  $0.59 \pm 0.02$  pg /  $\mu$ g total lung protein respectively ( $p < 0.001$ ). This trend was maintained on d 14, though values were not significant at this age (Fig. 4.1 B).

#### 4.3.2 VEGFR1

We were interested in investigating whether O<sub>2</sub>-exposure had an effect on the VEGF receptor mRNA expression or protein levels. VEGFR1 mRNA increased from d 6 to d 14 when levels were three times higher than those of the d 6 group ( $p < 0.05$ ) (Fig. 4.2 A). Rat pups exposed to hyperoxia inhibited this age-dependent increase in VEGFR1 mRNA as levels remained similar to d 6 throughout the course of the experiment. This resulted in VEGFR1 mRNA levels of O<sub>2</sub>-exposed group being significantly lower than the air-exposed group on d 9, d 12 and d 14 ( $p < 0.001$ ) (Fig. 4.2 A).

Contrary to mRNA expression, protein levels of VEGFR1 did not change significantly between d 6 and d 14 in normoxic-exposed pups (Fig. 4.2 B). However, exposure of rat pups to a hyperoxic environment did cause a significant decrease in overall VEGFR1 protein levels ( $p < 0.05$  between air and O<sub>2</sub>-exposed groups) (Fig. 4.2 B). A significant interaction between group (air/O<sub>2</sub>) and postnatal day (age) was not observed.

#### 4.3.3 VEGFR2

Message transcribing for VEGFR2 protein increased between d 9 and d 14 in animals exposed to a normoxic environment, so that by d 14 mRNA levels were 2.3 times those on d 6 ( $p < 0.05$ ) (Fig. 4.3 A). Exposure to O<sub>2</sub> had a significant effect by d 12 when



VEGFR2 mRNA levels decreased to half the d 6 air values, and were only 27 % of the mRNA levels of the d 12 air-exposed pups ( $p < 0.001$ ). The effect of oxygen-exposure was even greater by d 14, when mRNA levels from the O<sub>2</sub> group were merely 8 % of the air group ( $p < 0.001$ ) (Fig. 4.3 A).

Protein levels for VEGFR2 in the normoxic-raised pups did not demonstrate the increase observed for VEGFR2 mRNA (Fig. 4.3 B). However, exposure to O<sub>2</sub> did have a similar effect of decreasing protein levels. VEGFR2 protein levels of the hyperoxic-exposed pups were 60 % of those from the air-exposed group by d 12 ( $p < 0.001$ ); this decrease was maintained through to d 14 ( $p < 0.001$ ) (Fig. 4.3 B).

#### **4.3.4 HIF-2 $\alpha$**

To identify a possible mechanism whereby VEGF mRNA is decreased after exposure of rat pups to hyperoxia, O<sub>2</sub>-induced changes in mRNA for the transcription factor HIF-2 $\alpha$  were determined. HIF-2 $\alpha$  mRNA followed a similar pattern to that of VEGF. There was an age-dependent increase in HIF-2 $\alpha$  mRNA between d 9 and d 14, with d 14 values increasing to 2.4 times those on d 9 ( $p < 0.05$ ) (Fig. 4.4 A). Again similarly to total VEGF mRNA levels, O<sub>2</sub>-exposure inhibited the increase in HIF-2 $\alpha$  mRNA seen in the control animals; there was a significant difference between air and O<sub>2</sub> groups on d 12 and d 14 ( $p < 0.001$ ) (Fig. 4.4 A). By d 14 mRNA levels of hyperoxic-exposed pups were 62 % of those in the normoxic-exposed animals ( $p < 0.001$ ) (Fig. 4.4 A). There was a strong correlation between VEGF mRNA and HIF-2 $\alpha$  mRNA in the normoxic pups, the correlation coefficient was 0.799 ( $p < 0.001$ ) (Fig. 4.4 B). Interestingly, when the pups

were exposed to a hyperoxic environment, this correlation was lost (correlation coefficient, 0.355).

#### **4.4 DISCUSSION**

In this study we replicated, in the newborn rat, the response of VEGF to hyperoxia as seen in the newborn rabbit. We further extended the current body of knowledge to include the effects of hyperoxia on HIF-2 $\alpha$ , VEGFR1 and VEGFR2. The results of this study demonstrate that VEGF mRNA expression increases during the period of alveolar development and is reduced after exposure of neonatal rats to a hyperoxic environment during this critical time. VEGFR1 and VEGFR2 mRNA and protein were also decreased during exposure to a high-O<sub>2</sub> environment. Expression of HIF-2 $\alpha$  followed a similar pattern to, and correlated strongly with, levels of VEGF mRNA in normoxic-exposed pups. However this correlation was lost after exposure to hyperoxia, suggesting that the low levels of HIF-2 $\alpha$  observed at high O<sub>2</sub> concentrations are not stimulating VEGF expression. To the best of our knowledge this is the first demonstration that HIF-2 $\alpha$  mRNA relative abundance decreases in response to a hyperoxic environment. As it is well established that this hyperoxic-exposure protocol inhibits alveolarization in the rat pup (4, 20) we postulate that signaling through VEGF receptors may be an important mechanism for postnatal lung development and that hyperoxic-inhibition of this pathway may contribute to the observed reduction in septation of the alveoli.

Our work is in agreement with that of Maniscalco and colleagues who showed that neonatal rabbits exposed to 100 % O<sub>2</sub> for 9 days from birth had decreased VEGF mRNA abundance (18), due to a significant decline in VEGF<sub>189</sub> (30). In our experiments

although total VEGF mRNA was decreased due to hyperoxia, VEGF<sub>164</sub> protein levels were found to increase on d 9 before decreasing below normoxic values on d 12. Interestingly, Watkins *et al.* found a similar trend measuring total VEGF protein from lavage fluid of newborn rabbits exposed to 100 % O<sub>2</sub>; they found increased VEGF on d 4, d 6 and d 8 before levels decreased to below those of air-exposed animals on d 9 (30). As total mRNA decreased and protein levels of combined VEGF<sub>164</sub> and VEGF<sub>120</sub> initially increased in our experiments, it is likely that the 188 splice variant was decreased during the first 6 days of hyperoxic-exposure.

VEGF expression is induced when most cell types are exposed to hypoxia as a result of increased transcriptional activation and mRNA stabilization of HIF-1 $\alpha$  and HIF-2 $\alpha$  (1, 27). This study demonstrates increasing levels of HIF-2 $\alpha$  mRNA expression from d 9 to d 14 in the postnatal rat lung, which is in agreement with earlier work showing a concurrent increase in HIF-2 $\alpha$  and VEGF in the neonatal mouse lung between d 5 and d 14 (8). It is unknown how hyperoxia decreases HIF-2 $\alpha$  levels, however HIF-2 $\alpha$  is increased by hypoxia in a similar manner to HIF-1 $\alpha$ , through both hypoxia-dependant stabilization of the protein, or through a multi-step process leading to interaction with CREB-binding protein (7).

In our experiments both VEGFR1 and VEGFR2 were decreased during exposure of the neonatal lung to a high O<sub>2</sub> environment. However these receptors are known to have different modes of action. Targeted disruption of VEGFR1 leads to mice with mature, differentiated endothelial cells but with large, disorganized vessels, thought to result from overproduction of endothelial progenitor cells rather than vascular disorganization (11,

12). It is now thought that VEGFR1 plays a negative regulatory role by binding to VEGF (9). VEGFR2 knockout mice produce neither differentiated endothelial cells nor organized blood vessels and also possess no hematopoietic precursors (25, 28). This receptor is responsible for endothelial mitogenesis and migration, as well as regulating vascular permeability (2). Our results suggest that endothelial cell differentiation and migration, as stimulated through the VEGFR2, as well as endothelial cell maintenance and possibly spatial organization, through VEGFR1, are both necessary for postnatal lung development. However if as suggested above, VEGF<sub>188</sub> is diminished early in the experiments, decreased signaling through VEGFR1 may be an important early result of hyperoxic exposure as VEGF<sub>188</sub> is unable to bind VEGFR2 in its intact form but does bind VEGFR1. This early response could affect different aspects of alveolar development than later in development when all VEGF splice variants appear to be decreased. Indeed events do occur at different critical periods during alveolarization (20); maximal lung cell proliferation occurs during the first half of alveolarization, maximal endothelial cell proliferation peaks on d 7 (15) and the concentration of pulmonary arteries doubles between d 8 and d 11 (22).

It has been shown that VEGFR2, rather than VEGFR1, mediates the advanced lung maturation seen when VEGF is exogenously administered to premature mouse fetuses *in vivo* (6). Further, the VEGFR2 receptor blocker, SU-5416 caused decreased capillary density and inhibited septation, suggesting that angiogenesis occurring by VEGF signaling through VEGFR2 receptor is essential for the maturation of the neonatal lung. As VEGF<sub>189</sub> can be cleaved by urokinase-type plasminogen activator forming a peptide

similar to VEGF<sub>165</sub> which also has similar receptor binding and mitogenic properties (24), the early lower levels of VEGF<sub>188</sub> may decrease signaling through VEGFR2 by this mechanism.

Recent evidence suggests that VEGF affects more than just endothelial cells. Over-expression of VEGF in the developing pulmonary epithelium of transgenic mice not only increased growth of pulmonary vessels but also disrupted branching morphogenesis and inhibited Type I cell differentiation (31). There is also evidence that VEGF may be involved in epithelial cell growth and proliferation in the human fetal lung *in vitro* (5). VEGFR2 protein is found in the distal airway epithelial cells of the midtrimester human lung, and exogenous VEGF added to explants caused increased epithelial proliferation and volume density (5). A recent study by Compemolle *et al.* demonstrated that type II cells expressed VEGFR2 transcripts and responded to VEGF by increasing their production of SP-B and SP-C (6). The same paper demonstrated that, as well as creating a subtle deficit in vascularization of the alveolar septa, loss of HIF-2 $\alpha$  impaired lung maturation (6).

This study has important implications in the pathology of chronic lung disease of prematurity (CLD), which in its severest form develops into bronchopulmonary dysplasia (BPD). The pathology of BPD in recent years suggests that the condition is mainly due to arrested development of the premature lung (14) resulting in a lack of alveolarization and dysmorphic vasculature. Therefore, the process of endothelial differentiation and organization into the alveolar microvasculature may be disrupted after premature birth and injury from oxygen and ventilation. Recently a study by Bhatt *et al.* of premature

human infants dying of BPD, showed a disrupted pulmonary vasculature along with decreased expression of VEGF and VEGFR1 (3). Further work from the same laboratory demonstrated the normal increase in capillary density or the endothelial cell marker PECAM-1 failed to occur in very premature baboons; VEGF and VEGFR1 were again decreased in this model of CLD (19).

We conclude that hyperoxic-exposure during the period of alveolarization in the rat pup causes decreased VEGF levels, possibly through decreased levels of the transcription factor HIF-2 $\alpha$ , as well as decreased VEGF receptor levels. As it is evident that the vascular growth is a fundamental part of normal alveolar development, we speculate that hyperoxic-induced changes in VEGF may be an important element in the pathology of BPD.

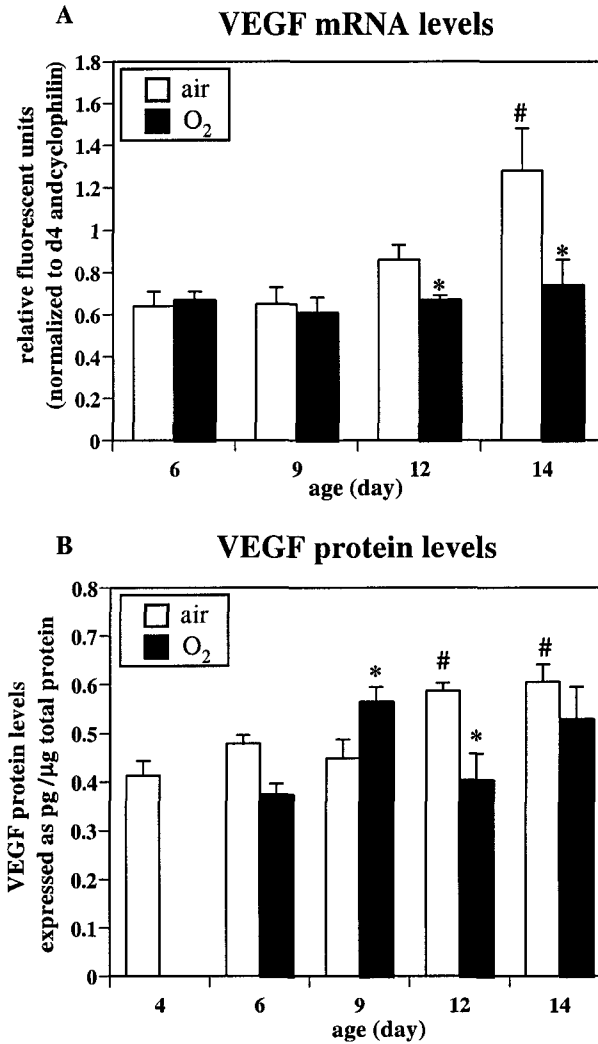


**Figure 4.1 Time course and effects of >95% O<sub>2</sub> from day 4 to 14 on (A) VEGF mRNA expression and (B) VEGF protein levels.**

Time course and effects of >95% O<sub>2</sub> from day 6 to 14 on (A) VEGF mRNA expression and (B) VEGF protein levels. Data are means ± SEM. n=5-6 for lungs/group. Animals were exposed to air (open bars) or O<sub>2</sub> (closed bars). VEGF mRNA increased with advancing age, by d 14 levels were twice those of d 6 pups (p<0.05). O<sub>2</sub> exposure caused a significant decrease in VEGF mRNA expression below that of the air group on d 12 and d 14 (p<0.001). VEGF protein levels also increased with advancing age, with d 12 and d14 levels being higher than those on d 6 (p<0.05). O<sub>2</sub> exposure caused an increase in VEGF protein levels compared to the air group on d 9 (p<0.001). Levels then decreased to below air-exposed animals by d 12 (p<0.001) \* indicates significant difference between air and O<sub>2</sub> pups on the day indicated. # indicates significant difference from d 6 air values.

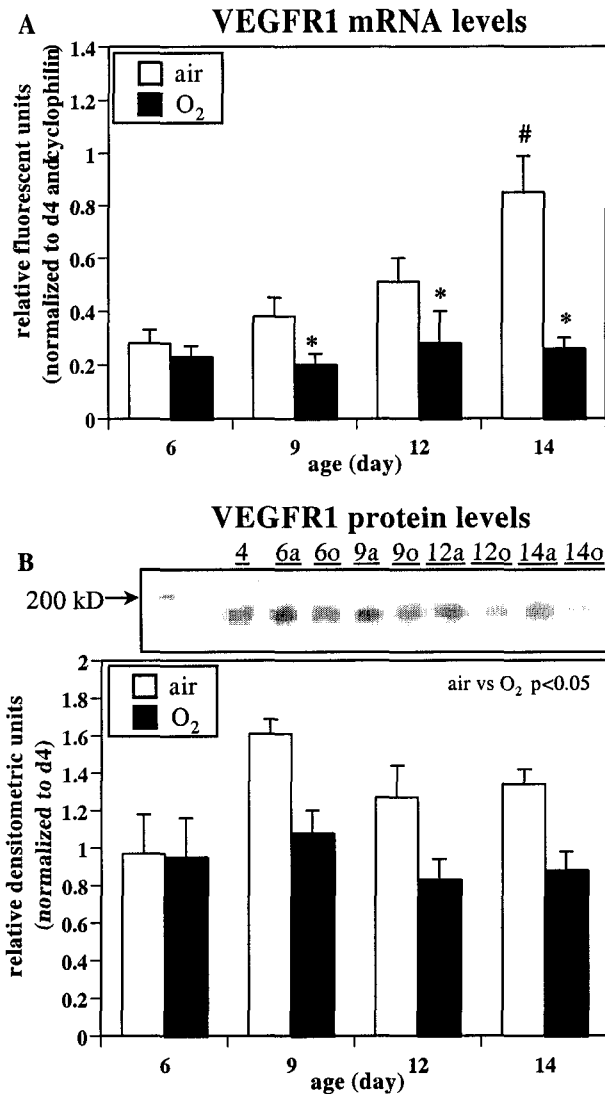


**Figure 4.2 Time course and effects of >95% O<sub>2</sub> from day 6 to 14 on (A) VEGFR1 mRNA expression and (B) VEGFR1 protein levels**

Data are means  $\pm$  SEM. n=5-6 for lungs/group. A representative western blot is shown above the graph indicating the day the lungs were removed and the experimental group; a = air, o = oxygen. VEGFR1 mRNA expression increased with advancing age, by d 14 levels were three times higher than those of d 6 pups ( $p < 0.05$ ). O<sub>2</sub> exposure caused a significant decrease in VEGFR1 mRNA expression below that of the air group on d 9, d 12 and d 14 ( $p < 0.001$ ). VEGFR1 protein levels did not change advancing age. O<sub>2</sub> exposure caused a significant decrease in VEGFR1 protein levels compared to levels from the air-exposed groups ( $p < 0.05$  for O<sub>2</sub> values compared to air values when all days are compared as one group). \* indicates significant difference between air and O<sub>2</sub> pups on the day indicated. # indicates significant difference from d 6 air values.



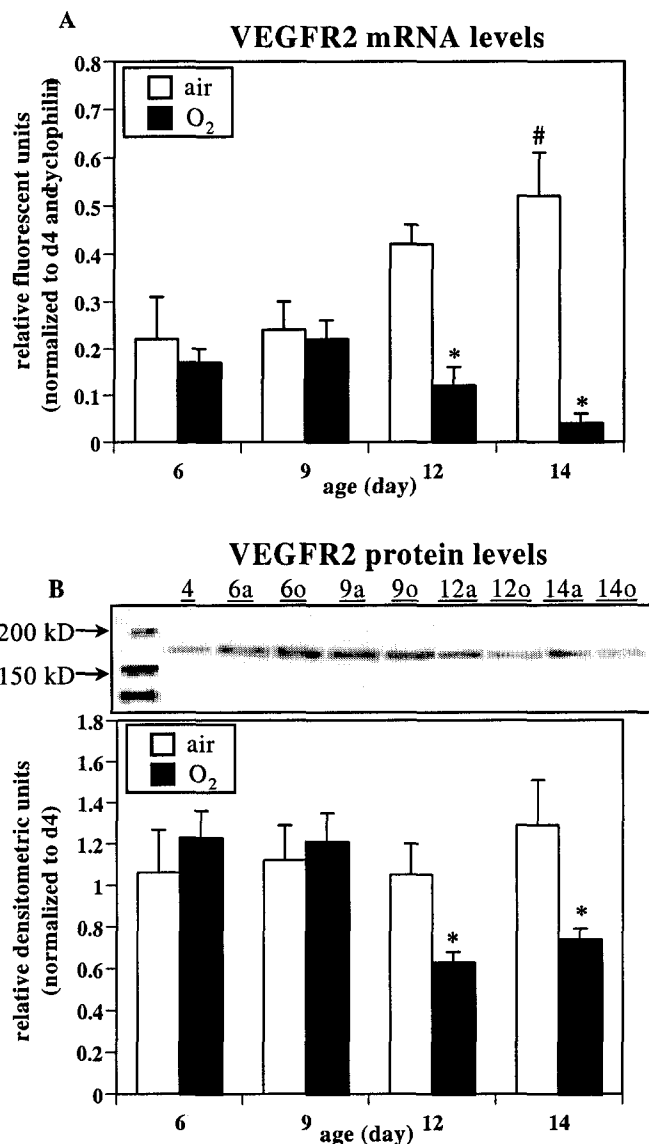


**Figure 4.3** Time course and effects of >95% O<sub>2</sub> from day 4 to 14 on (A) VEGFR2 mRNA expression and (B) VEGFR2 protein levels.

Data are means  $\pm$  SEM. n=5-6 for lungs/group. A representative western blot is shown above the graph indicating the day the lungs were removed and the experimental group; a = air, o = oxygen. VEGFR2 mRNA expression increased with advancing age, by d 14 levels were 2.3 times those of d 6 pups ( $p < 0.05$ ). O<sub>2</sub> exposure caused a significant decrease in VEGFR2 mRNA expression below that of the air group on d 12 and d 14 ( $p < 0.001$ ). VEGFR2 protein levels did not change with advancing age. O<sub>2</sub> exposure caused a decrease in VEGFR2 protein levels compared to the air group on d 12 and d 14 ( $P < 0.001$ ). \* indicates significant difference between air and O<sub>2</sub> pups on the day indicated. # indicates significant difference from d 6 air values.

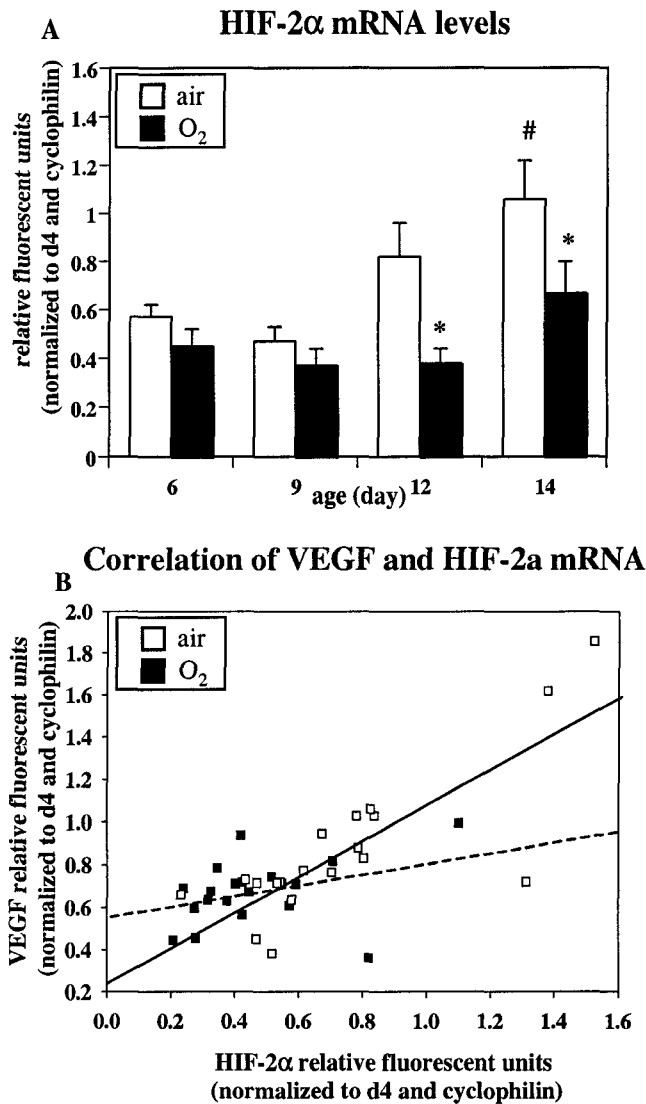


**Figure 4.4 Time course and effects of >95% O<sub>2</sub> from day 6 to 14 on (A) HIF-2 $\alpha$  mRNA expression and (B) correlation between VEGF and HIF-2 $\alpha$  mRNA expression.**

Data are means  $\pm$  SEM. n=5 for lungs/group. HIF-2 $\alpha$  mRNA expression increased with advancing age, by d 14 levels were 2.4 times those of d 9 pups ( $p < 0.05$ ). O<sub>2</sub> exposure caused a significant decrease in HIF-2 $\alpha$  mRNA expression below that of the air group on d 12 and d 14 ( $p < 0.001$ ). There was a strong correlation between VEGF and HIF-2 $\alpha$  mRNA expression in normoxic-exposed pups (solid line, the correlation coefficient was 0.799 ( $p < 0.001$ )). There was no correlation between VEGF and HIF-2 $\alpha$  mRNA expression in hyperoxic-exposed pups (dashed line, the correlation coefficient was 0.355).

#### 4.5 REFERENCES

1. **Akeno, N., M. F. Czyzyk-Krzeska, T. S. Gross, and T. L. Clemens.** Hypoxia induces vascular endothelial growth factor gene transcription in human osteoblast-like cells through the hypoxia-inducible factor-2alpha. *Endocrinology* 142: 959-62., 2001.
2. **Becker, P. M., A. D. Verin, M. A. Booth, F. Liu, A. Birukova, and J. G. Garcia.** Differential regulation of diverse physiological responses to VEGF in pulmonary endothelial cells. *Am J Physiol Lung Cell Mol Physiol* 281: L1500-11., 2001.
3. **Bhatt, A. J., G. S. Pryhuber, H. Huyck, R. H. Watkins, L. A. Metlay, and W. M. Maniscalco.** Disrupted pulmonary vasculature and decreased vascular endothelial growth factor, Flt-1, and TIE-2 in human infants dying with bronchopulmonary dysplasia. *Am J Respir Crit Care Med* 164: 1971-80., 2001.
4. **Boros, V., J. S. Burghardt, C. J. Morgan, and D. M. Olson.** Leukotrienes are indicated as mediators of hyperoxia-inhibited alveolarization in newborn rats. *Am J Physiol* 272: L433-41., 1997.
5. **Brown, K. R., K. M. England, K. L. Goss, J. M. Snyder, and M. J. Acarregui.** VEGF induces airway epithelial cell proliferation in human fetal lung in vitro. *Am J Physiol Lung Cell Mol Physiol* 281: L1001-10., 2001.
6. **Compernelle, V., K. Brusselmans, T. Acker, P. Hoet, M. Tjwa, H. Beck, S. Plaisance, Y. Dor, E. Keshet, F. Lupu, B. Nemery, M. Dewerchin, P. Van Veldhoven, K. Plate, L. Moons, D. Collen, and P. Carmeliet.** Loss of HIF-2alpha and inhibition of VEGF impair fetal lung maturation, whereas treatment with VEGF prevents fatal respiratory distress in premature mice. *Nat Med* 10: 10, 2002.
7. **Ema, M., K. Hirota, J. Mimura, H. Abe, J. Yodoi, K. Sogawa, L. Poellinger, and Y. Fujii-Kuriyama.** Molecular mechanisms of transcription activation by HLF and HIF1alpha in response to hypoxia: their stabilization and redox signal-induced interaction with CBP/p300. *Embo J* 18: 1905-14., 1999.
8. **Ema, M., S. Taya, N. Yokotani, K. Sogawa, Y. Matsuda, and Y. Fujii-Kuriyama.** A novel bHLH-PAS factor with close sequence similarity to hypoxia-inducible factor 1alpha regulates the VEGF expression and is potentially involved in lung and vascular development. *Proc Natl Acad Sci U S A* 94: 4273-8., 1997.
9. **Ferrara, N.** Role of vascular endothelial growth factor in regulation of physiological angiogenesis. *Am J Physiol Cell Physiol* 280: C1358-66., 2001.
10. **Ferrara, N., and S. Bunting.** Vascular endothelial growth factor, a specific regulator of angiogenesis. *Curr Opin Nephrol Hypertens* 5: 35-44., 1996.
11. **Fong, G. H., J. Rossant, M. Gertsenstein, and M. L. Breitman.** Role of the Flt-1 receptor tyrosine kinase in regulating the assembly of vascular endothelium. *Nature* 376: 66-70., 1995.
12. **Fong, G. H., L. Zhang, D. M. Bryce, and J. Peng.** Increased hemangioblast commitment, not vascular disorganization, is the primary defect in flt-1 knock-out mice. *Development* 126: 3015-25., 1999.
13. **Jakkula, M., T. D. Le Cras, S. Gebb, K. P. Hirth, R. M. Tudor, N. F. Voelkel, and S. H. Abman.** Inhibition of angiogenesis decreases alveolarization in the developing rat lung. *Am J Physiol Lung Cell Mol Physiol* 279: L600-7., 2000.

14. **Jobe, A. H., and E. Bancalari.** Bronchopulmonary dysplasia. *Am J Respir Crit Care Med* 163: 1723-9., 2001.
15. **Kauffman, S. L., P. H. Burri, and E. R. Weibel.** The postnatal growth of the rat lung. II. Autoradiography. *Anat Rec* 180: 63-76., 1974.
16. **Klekamp, J. G., K. Jarzecka, and E. A. Perkett.** Exposure to hyperoxia decreases the expression of vascular endothelial growth factor and its receptors in adult rat lungs. *Am J Pathol* 154: 823-31., 1999.
17. **Kovar, J., P. D. Sly, and K. E. Willet.** Inhaled Corticosteroids And Early Postnatal Lung Development. *American Thoracic Society 2002, 98th International Conference, Atlanta, Georgia, 2002.*
18. **Maniscalco, W. M., R. H. Watkins, C. T. D'Angio, and R. M. Ryan.** Hyperoxic injury decreases alveolar epithelial cell expression of vascular endothelial growth factor (VEGF) in neonatal rabbit lung. *Am J Respir Cell Mol Biol* 16: 557-67., 1997.
19. **Maniscalco, W. M., R. H. Watkins, G. S. Pryhuber, A. Bhatt, C. Shea, and H. Huyck.** Angiogenic factors and alveolar vasculature: development and alterations by injury in very premature baboons. *Am J Physiol Lung Cell Mol Physiol* 282: L811-23., 2002.
20. **Manji, J. S., C. J. O'Kelly, W. I. Leung, and D. M. Olson.** Timing of hyperoxic exposure during alveolarization influences damage mediated by leukotrienes. *Am J Physiol Lung Cell Mol Physiol* 281: L799-806., 2001.
21. **Massaro, D., N. Teich, S. Maxwell, G. D. Massaro, and P. Whitney.** Postnatal development of alveoli. Regulation and evidence for a critical period in rats. *J Clin Invest* 76: 1297-305., 1985.
22. **Meyrick, B., and L. Reid.** Pulmonary arterial and alveolar development in normal postnatal rat lung. *Am Rev Respir Dis* 125: 468-73., 1982.
23. **Muratore, C. S., H. T. Nguyen, M. M. Ziegler, and J. M. Wilson.** Stretch-induced upregulation of VEGF gene expression in murine pulmonary culture: a role for angiogenesis in lung development. *J Pediatr Surg* 35: 906-12; discussion 912-3., 2000.
24. **Plouet, J., F. Moro, S. Bertagnolli, N. Coldeboeuf, H. Mazarguil, S. Clamens, and F. Bayard.** Extracellular cleavage of the vascular endothelial growth factor 189-amino acid form by urokinase is required for its mitogenic effect. *J Biol Chem* 272: 13390-6., 1997.
25. **Risau, W.** Mechanisms of angiogenesis. *Nature* 386: 671-4., 1997.
26. **Roberts, R. J., K. M. Weesner, and J. R. Bucher.** Oxygen-induced alterations in lung vascular development in the newborn rat. *Pediatr Res* 17: 368-75., 1983.
27. **Semenza, G. L.** HIF-1 and human disease: one highly involved factor. *Genes Dev* 14: 1983-91., 2000.
28. **Shalaby, F., J. Rossant, T. P. Yamaguchi, M. Gertsenstein, X. F. Wu, M. L. Breitman, and A. C. Schuh.** Failure of blood-island formation and vasculogenesis in Flk-1-deficient mice. *Nature* 376: 62-6., 1995.
29. **Thibeault, D. W., S. Mabry, and M. Rezaiekhlig.** Neonatal pulmonary oxygen toxicity in the rat and lung changes with aging. *Pediatr Pulmonol* 9: 96-108, 1990.

30. **Watkins, R. H., C. T. D'Angio, R. M. Ryan, A. Patel, and W. M. Maniscalco.** Differential expression of VEGF mRNA splice variants in newborn and adult hyperoxic lung injury. *Am J Physiol* 276: L858-67., 1999.
31. **Zeng, X., S. E. Wert, R. Federici, K. G. Peters, and J. A. Whitsett.** VEGF enhances pulmonary vasculogenesis and disrupts lung morphogenesis in vivo. *Dev Dyn* 211: 215-27., 1998.

## **CHAPTER 5.            THE EFFECTS OF HYPEROXIA ON MATRIX METALLOPROTEINASES -2 AND -9 IN THE NEWBORN RAT LUNG**

---

### ***5.1 INTRODUCTION***

Lung alveoli are formed when immature saccules subdivide into functional gas-exchange units through formation of secondary septa (8, 9). The process of septation involves budding from the primary septum (saccular wall), formation of a double-capillary network, elongation of septa, coalescence of vessels to form a single capillary layer, and thinning of the septal walls (8, 9). Exposure of neonatal rats to hyperoxia during alveolarization interferes with the process of septation; alveolar number and internal surface area are decreased and the parenchymal airspace is enlarged (3, 26, 38). These parameters persist up to day (d) 40 (31). Hyperoxia during the neonatal period also disrupts lung connective tissue, alters elastic fiber structure and concentration (4), and causes an inflammatory reaction characterized by interalveolar edema, and proteinosis (3, 7, 26). Chronic inflammation of the neonatal lung leads to fibrosis and thickening of the septa (3, 26).

Matrix metalloproteinases (MMPs) are a group of enzymes that have a specialized function in extracellular matrix (ECM) turnover. MMPs regulate many processes associated with development, such as branching morphogenesis, angiogenesis and ECM

degradation, as well as inflammatory processes and wound healing (40). MMP-2 and MMP-9, also called gelatinases-A and -B respectively, both cleave gelatin, type IV and V collagen and elastin. Types IV, V and VII collagens are associated with the basement membranes (11). MMP-2 and MMP-9 exhibit increased gelatinolytic activities as the fetal lung develops (15), and during the postnatal lung growth stage both MMP-2 and MMP-9 are detected in alveolar epithelial cells (15). MMP-2 deficient mice develop normally, with no gross anatomical abnormalities, however they display a significantly slower growth rate (approximately 15 %) (18). Conversely, MMP-9 deficient mice, while developing to term and surviving normally after birth, exhibit an abnormal pattern of skeletal growth plate vascularization and ossification (39).

MMPs are tightly regulated by the tissue inhibitors of metalloproteinases (TIMPs). Two of the four TIMP family members, TIMP-1 and TIMP-2, are capable of inhibiting the activity of all MMPs and play a key role in maintaining the balance between ECM deposition and degradation (13). Low levels of TIMP-2 are also necessary for MT(membrane-type)1-MMP-mediated activation of MMP-2 (21).

Hyperoxia has previously been shown to regulate MMPs. Adult rats exposed to 85 % O<sub>2</sub> had increased levels of MMP-2 and MMP-9 activities in both bronchoalveolar lavage fluid and type II cells (29). In the newborn rat pup, 85 % O<sub>2</sub> from d 1 to d 6 caused increased type IV collagenase mRNA and activity (12). Further, in a previous study from our laboratory (30), exposing rat pups to hyperoxia from birth caused an increase in MMP-2 and MMP-9 activity at d 14. However in a recent publication in which neonatal rats were exposed to > 90 % O<sub>2</sub> from d 1 to d 10, MMP-2 and MMP-9 activity showed a

biphasic effect where levels were initially increased above normoxic values and then fell to below hyperoxic levels by d 6 and d 8 respectively (6).

During the d 4 to d 14 period in the rat pup a series of events occur, which combine to form the mature alveolar structures. Maximal septation and cell proliferation occur at the initiation of alveolarization (41) and maximal endothelial cell proliferation peaks on d 7 (20). However the concentration of pulmonary arteries is unchanged from birth to d 8 and then doubles between d 8 and d 11 (28). Further, a 20 % reduction in the number of fibroblasts is seen near the end of the period of alveolarization (17). As this complex series of events occurs throughout alveolar development, we wanted to comprehensively study the pattern of mRNA expression, protein levels and activity of MMP-2 and MMP-9 at various time-points during this period. We hypothesized that MMP-2 and MMP-9 would increase during the period of alveolar development. As there is some discrepancy about the results of hyperoxia on MMPs in the newborn rat lung we also examined the effects of hyperoxia from d 4 to d 14 and hypothesized that normal levels of MMP-2 and MMP-9 would be elevated. As hyperoxia was found to decrease MMP-2 and MMP-9, contrary to our original hypothesis, we inhibited MMPs in pups in a normoxic environment and hypothesized that alveolar development would be inhibited.

## **5.2 MATERIALS AND METHODS**

Sprague-Dawley albino rat pups were exposed to O<sub>2</sub> as described in Methods. Reverse Transcription and Real-Time Quantitative PCR were performed for MMP-2, MMP-9,



TIMP-1 and TIMP-2. Western Immunoblotting was carried out to determine protein levels of MMP-2 and MMP-9.

### **5.2.1 Gelatinase Zymography**

The relative gelatinolytic activity of MMP-2 and MMP-9 was determined by gelatinase zymography. Samples were prepared as described in Methods section (2.3.1). Aliquots of lung sample were diluted in a non-reducing loading buffer (Tris-Cl pH 6.8, 36 % glycerol, 10 % SDS, bromophenol blue). The protein samples (40 µg) were loaded into 7.5 % polyacrylamide gels containing 0.2 % gelatin and the proteins were separated by electrophoresis at 100 V at 4 °C for 2 h in electrophoresis buffer (using 1:5 dilution of a 5x buffer containing 0.5 M Tris base, 1.92 M glycine, 0.5 % SDS). The gels were washed in 2.5 % Triton-X 100 (3 x 20 min) at room temperature and then incubated overnight (16 - 18 h) at 37 °C in a 50 mM Tris-Cl buffer, pH 7.6, supplemented with 0.15 M NaCl, 5 mM CaCl<sub>2</sub> and 0.05 % NaN<sub>3</sub>. The gels were removed and stained in 0.05 % Coomassie Brilliant Blue G-250 in a mixture of methanol: acetic acid: water (2.5:1:6.5) for 1 h, then destained in 4 % ethanol and 8 % acetic acid for 4 - 5 h. The gels were analyzed as for Western Immunoblotting. As a negative control, 100 µM 1,10 phenanthroline monohydrate, a metalloproteinase inhibitor, was added to the incubating buffer of a test zymography gel. This completely inhibited any gelatinolytic activity, so that the gel had no digested areas whatsoever.

### **5.2.2 MMP inhibition**

Rat pups raised in room air were administered 20 mg / kg doxycycline (Sigma-Aldrich, Oakville, Ontario, Canada) diluted in 0.9 % saline to 4 mg / ml so that each rat was

administered 10 µl / 2 g of total weight, or equal volume of vehicle (0.9 % saline) by gavage, twice daily (8.00 and 20.00) from d 4 to d 14.

#### 5.2.2.1 *In situ zymography*

An 8 % polyacrylamide gel with 50 mM Tris-Cl pH 7.4, 5 mM CaCl<sub>2</sub> and 1 % gelatin was placed flat in a humid chamber, coated with 1 ml zymography incubation buffer (as above) and unfixed cryosections of lung tissue on slides were placed directly onto surface. The gel was incubated at 37 °C overnight (18 h). The slides were removed and the gels were placed in zymography incubating buffer for 16 h at 37 °C. The gel was stained and destained as for gelatinase zymography. MMPs in the lung digested an area which was white against the blue background of the gel.

#### 5.2.2.2 *Lung morphometry*

Rat pups were killed on d 14 with an overdose of pentobarbitol sodium (as in Methods 2.1.2). The trachea was exposed and a canula was inserted into the trachea and tied in place as for IHC. A solution of 2.5 % glutaraldehyde was allowed to flow into the lungs through the canula at a constant pressure of 20 cm water for 2 h. The trachea was then ligated with thread and the lungs were excised from the chest cavity and immersed in glutaraldehyde for 24 h. Lung volumes were measured by displacement of the fixative solution by suspending the lungs in the solution and measuring the change in the weight, so that the volume increase is registered as weight gain (33). Previous experiments (3) have calculated minimal shrinkage using this technique (0-2 %), so data were not corrected.

After fixation, transverse sections of the inferior portion of the left lung were embedded in paraffin. Tissue slices 3  $\mu\text{m}$  thick were cut throughout the entire sections and stained with Gomori-trichromaldehyde fuscine. The slides were initially examined to eliminate sections with evidence of inadequate preparation.

Light-level morphometric assessment of the lung parenchymal tissue was performed in a blinded fashion on coded slides from 8 animals in each group. Six randomly selected fields were examined from the inferior section of the left lung. Images of histological specimens observed with the microscope (Olympus Optical Co., Japan) were captured via a 'SPOT' digital camera (Diagnostic Instruments Inc., Michigan, USA). The measurements and calculations were performed with Image-Pro Plus (Media Cybernetics Inc., Del Mar, CA, USA) image analysis software.

The parenchymal tissue includes alveolar septa, alveolar ducts, respiratory bronchiolar tissue, and blood vessels with a diameter  $< 10 \mu\text{m}$  and their contents. The volume density of parenchymal tissue was calculated as  $[\text{field area (FA)} - \text{airspace area} / \text{FA}] \times 100$  from each analyzed field. The mean septal thickness ( $\text{Th}_{\text{sept}}$ ) was calculated from the parenchymal tissue area and the length of the gas-exchange surface.

A value for the mean alveolar diameter ( $\text{Da}$ ) was generated from the image software and was used to calculate the mean volume of airspace units  $(\text{Da}^3 \times \pi) / 3$ . To detect the structural changes in alveolar airspace the perimeter-to-airspace ratio ( $P/A$ ), an indication of the shape of the alveoli, was calculated from each field. A lower ratio indicates a simple, more rounded structure (i.e. less septa protruding into the airspace).

The internal surface area of the lung available for respiratory exchange was calculated from the formula  $(4 \times \text{lung volume}) / D_a$  (adapted from (42)). These data were normalized to 100 g of body weight and used as specific internal surface area (SISA).

### 5.3 **RESULTS**

#### 5.3.1 ***MMP mRNA levels***

Expression of message for MMP-2 did not change significantly between d 6 and d 14 in the animals raised in room air (Fig. 5.1 A). Exposure to oxygen resulted in levels of mRNA consistently greater ( $p < 0.05$  between air and O<sub>2</sub> groups) than levels expressed from lungs of normoxic pups (Fig. 5.1 A).

Mean MMP-9 mRNA expression levels increased slightly (though not significantly) between d 6 and d 14 in animals exposed to room air (Fig. 5.1 B). Rat pups from the hyperoxic environment expressed significantly lower levels of mRNA for MMP-9 than the normoxic pups on each experimental day ( $p < 0.05$  between air and O<sub>2</sub> on each individual day). Levels of mRNA from pups exposed to O<sub>2</sub> were more than 2.5-fold lower than levels of normoxic pups on d 6; this decrease was maintained throughout the experimental period (Fig. 5.1 B).

#### 5.3.2 ***MMP protein and activity levels***

Two bands were observed for MMP-2 by western immunoblotting (Fig. 5.2 A), one representing the 'pro' form of the protein at 72 kD and one representing the active (cleaved) form of the protein at 62 kD. In all experiments the pro-form was in greater

abundance than the active form. Western immunoblotting for MMP-9 revealed only one band at 92 kD, corresponding to the proMMP-9 (Fig. 5. 2 B).

Using gelatinase zymography, three bands corresponding to proMMP-9 (92 kD), proMMP-2 (72 kD) and active MMP-2 (62 kD), were observed for all days and treatment groups (Fig. 5.2 C). It is possible to view the *in vivo* 'pro' form of both MMP-2 and MMP-9 using zymography as the SDS in the gels causes a conformational change in the pro- forms so that they actively degrade gelatin *in vitro*.

### 5.3.3 *ProMMP 2*

There was a small (though not significant) increase in proMMP-2 protein mass from d 4 up to d 14 in the lungs of normoxic pups, so that protein levels were 111 % of d 4 values by d 14 (Fig. 5.3 A). O<sub>2</sub> exposure resulted in a trend for greater protein levels on d 6, 9 and 12, however this trend did not reach significance (Fig. 5.3 A). Activity levels of proMMP-2 did not change between d 4 and d 14 in the normoxic group and, similarly to protein levels, exposure to O<sub>2</sub> caused an increase above normoxic levels on all days, however this trend again did not reach significant values (Fig. 5.3 B).

### 5.3.4 *Active MMP-2*

There was a small, transient decrease in protein levels of the active form of MMP-2 on d 12 ( $p < 0.05$  compared to d 6 and d 9) however by d 14 protein had returned to similar levels to d 6 and d 9. Exposure to O<sub>2</sub> caused a significant decrease in 62 kD MMP-2 protein levels for the group as a whole ( $p < 0.05$  between air and O<sub>2</sub> groups) (Fig. 5.4 A). Activity levels of the active form of MMP-2 in the normoxic animal group did not change significantly during the experimental period. Oxygen exposure caused a

significant inhibition of 62 kD MMP-2 activity for the group as a whole ( $p < 0.05$  between air and O<sub>2</sub> groups) (Fig. 5.4 B).

### 5.3.5 *Pro-MMP-9*

Protein levels of proMMP-9 did not change during the experimental period (d 4 to d 14) in the pups exposed to room air. Hyperoxic exposure, however, caused a rapid decrease in proMMP-9 mean protein levels by d 6, returning to air levels on d 9, and decreasing again on d 12 and d 14 ( $p < 0.001$  between air and O<sub>2</sub> groups on d 6, d 12 and d 14). By d 14 there was a marked reduction to 92 % of d 4 values (Fig. 5.5 A). ProMMP-9 activity levels increased slightly (though not significantly) between d 4 and d 9 (to 112 % of d 4 levels) in the lungs of rat pups raised in room air, which was maintained up to d 14 (Fig. 5.5 B). In rat pups exposed to > 95 %, O<sub>2</sub> levels were decreased for the group as a whole ( $p < 0.05$  between air and O<sub>2</sub> groups).

### 5.3.6 *MMP inhibition*

As it was obvious from the experiments reported above that MMP-2 and MMP-9 activities were decreased during hyperoxic inhibition of alveolarization, and were likely involved in the formation of alveoli, the effect of MMP inhibition on the lungs of pups raised in normoxia was subsequently examined. Administration of the pan-MMP inhibitor, doxycycline, caused an observable decrease in MMP-2 and MMP-9 activity on d 14 as measured by *in situ* gelatinase zymography (n=3, results not shown). Doxycycline caused a small reduction in body weight by d 14; 28.6±0.6 g for control pups versus 26.6±0.4 g for treated pups ( $p < 0.05$ ). No significant reduction in lung volume on d 14

was observed,  $1.65 \pm 0.05$  ml for control pups versus  $1.68 \pm 0.05$  ml for doxycycline treated pups. This resulted in lung/body weight ratios that were similar (0.058 versus 0.063).

Representative photomicrographs of lung parenchyma from each of the experimental groups are depicted in Fig. 5.6. Compared with vehicle-treated animals, the rats treated with doxycycline from d 4 to d 14 had larger and more simplified alveolar airspaces.

These visual impressions were confirmed and quantified by the morphometric data (Table 5.1). A well accepted morphometric technique (3) was used in these experiments to calculate changes resulting from treatment with doxycycline compared to vehicle-administered control animals. Treatment with doxycycline from d 4 to d 14 caused an increase ( $p < 0.05$ ) in the calculated volume of the airspace unit ( $V_{\text{aspunit}}$ ) from  $0.64 \pm 0.04 \mu\text{m}^3 \times 10^5$  in control animals to  $1.67 \pm 0.1 \mu\text{m}^3 \times 10^5$  in doxycycline treated animals. The differences observed with respect to  $V_{\text{aspunit}}$  are mirrored by the parenchymal to airspace ratio ( $P/A$ ). The animals treated with doxycycline showed evidence of simplified alveoli as indicated by a decreased  $P/A$  from  $0.11 \pm 0.003$  to  $0.07 \pm 0.001$  ( $p < 0.05$ ).

A decreased lung surface area, as measured by specific internal surface area (SISA) was also observed in the MMP inhibited group; control pups had a mean SISA of  $6155.9 \pm 199.8 \text{ cm}^2 / 100 \text{ g}$  whereas pups treated with doxycycline had a mean SISA of  $4761.7 \pm 185.4 \text{ cm}^2 / 100 \text{ g}$ . The relative amount of lung parenchymal tissue, as assessed by  $V_p$  (volume of parenchyma) ( $34.4 \pm 0.1 \%$  in controls) decreased in response to doxycycline treatment to  $27.4 \pm 0.3 \%$  ( $p < 0.001$ ). The thickness of the septal walls,  $Th_{\text{sept}}$ , did not change significantly between the experimental groups.

### 5.3.7 *TIMP mRNA levels*

Our original hypothesis predicted that MMPs would increase in the presence of hyperoxia, but all our data, including the inhibited alveolarization with doxycycline administration, suggested the opposite. We therefore decided to measure mRNA levels of two endogenous inhibitors of MMP activity; TIMP-1 and TIMP-2. For these experiments we hypothesized that hyperoxia would increase levels of TIMP-1 mRNA, which would be consistent with previous data and provide a possible explanation for the observed decrease in MMP-2 activity. As the expression of TIMP-2 is largely constitutive (13), we did not expect hyperoxia to have any effect on its mRNA levels.

Expression of message for TIMP-1 did not change significantly between d 6 and d 14 in the animals raised in room air (Fig. 5.7 A). Exposure to oxygen did not cause any change in TIMP-1 mRNA levels until d 14 when O<sub>2</sub> increased levels to 1.7 times the levels expressed from lungs of normoxic pups ( $p < 0.05$ ) (Fig. 5.7 A).

Mean TIMP-2 mRNA expression levels increased slightly (though not significantly) between d 6 and d 14 in animals exposed to room air (Fig. 5.7 B). Rat pups from the hyperoxic environment expressed similar levels of mRNA to the normoxic pups on all experimental days (Fig. 5.7 B).

## 5.4 DISCUSSION

In this study we have demonstrated that MMP-2 and MMP-9 mRNA expression, mass and activity are unchanged during the period of alveolar development of the postnatal rat lung. This is likely due to MMPs increasing in late fetal (15) or earlier in postnatal life,



before our experimental period which started on d 4. Further, contrary to our original hypothesis, we have shown that MMP-2 activity and MMP-9 mRNA, mass and activity are all reduced during the inhibited alveolarization observed when rat pups are exposed to a hyperoxic environment from d 4 to d 14 (3, 26). We went on to inhibit MMP activity in rat pups in a normoxic environment from d 4 to d 14 and dramatically inhibited alveolar development, as assessed by morphometric techniques. As our results demonstrated an unexpected response of MMPs to hyperoxia, we further determined the pattern of TIMP expression in response to O<sub>2</sub>. We found that TIMP-1 mRNA did indeed increase with O<sub>2</sub>-exposure on d 14, which may account for the decreased activity of MMP-2 observed in our experiments (13). TIMP-2 did not change during the experimental period or with oxygen treatment. Our data highlight the capability of MMP-2 and MMP-9 to play an integral role in the process of alveolar development in the newborn rat lung.

As hyperoxia has such a large impact on lung development, it is clear that the observed decrease seen in MMP-2 and MMP-9 is one of many factors affecting alveolarization. Hyperoxia may also decrease cell proliferation, generate reactive oxygen species, increase leukotriene production, activate transcription factors such as NF- $\kappa$ B, and directly or indirectly regulate many growth factors (2, 3, 7).

Previous work from our laboratory and another showed that exposure of newborn rat pups to O<sub>2</sub> increased MMP activity. However the differences seen in our experiments are likely due to the difference in the timing of the hyperoxic exposure. In experiments by Devasker and colleagues, > 85 % O<sub>2</sub> administered to rat pups between d 1 and d 6 increased type IV collagenase (12). This was largely during the saccular stage and into

the early alveolarization stage prior to many events key to alveolar development. Recent experiments by Buckley *et al.* actually showed an interesting effect, where rat pups exposed to hyperoxia had increasing levels of MMP-2 and MMP-9 activity from d 0 to d 2 and d 4 respectively, activity levels then decreased to below those of normoxic animals (6). As these experiments were again studied during the saccular and early alveolar stage of development, this may explain discrepancies between their results and those presented in this paper. Further, in a study from our laboratory (30), exposing rat pups to hyperoxia from birth caused an increase in gelatinase activity after 14 days of hyperoxia, as opposed to a maximum 10 days exposure in this study. The newborn lungs may have either started a repair response or mounted a greater inflammatory response with the longer exposure to oxygen, which could explain an increased level of activity for MMP-2 and MMP-9. Indeed, Buckley *et al.* (5) demonstrated that hyperoxia-induced MMP-9, measured *in vitro*, parallels the time course of *in vivo* repair in a model of migrating cultured type II alveolar epithelial cells. Importantly, we also observed an increase in MMP-2 and MMP-9 activity after recovery from hyperoxia, using the protocol described in this paper and measuring activities on d 28 (unpublished observations).

MMP regulation can occur at the transcriptional level, at the level of activation of the secreted proenzyme (by proteolytic exposure of the zinc binding site), or by inhibition of activity by TIMPs. MMP-2 and MMP-9 differ in their mode of activation, as pro-MMP-2 is activated at the cell surface by MT1-MMP and TIMP-2, whereas activation of MMP-9 occurs by plasminogen-dependant and independent mechanisms (23). Our results show that in this model hyperoxia regulates MMP-2 and MMP-9 through different

mechanisms. Expression of the mRNA encoding MMP-2 or protein levels did not change throughout the course of the experiments, although activity was decreased during exposure to hyperoxia. This decreased activity was possibly due to inhibition from the increased levels of TIMP-1 mRNA. Conversely, MMP-9 appeared to be regulated by hyperoxia at the level of gene expression.

As our studies revealed a potential role for MMP-2 and MMP-9 in the process of alveolarization, we tested the hypothesis that MMPs were essential during normal development by administration of doxycycline. This is a member of the tetracycline family which non-selectively inhibits MMPs by binding to the active zinc sites (36) and also by binding to an inactive calcium site which causes conformational change and loss of enzymatic activity (24). Doxycycline, when administered orally, has been shown to decrease collagenase and gelatinase protein and activity levels in cartilage (35). In our studies gelatinase activity was reduced and lung morphometry at d14 was inhibited. This arrested alveolar development was similar to that seen due to O<sub>2</sub>-exposure, with larger, simplified airspaces when compared to vehicle-treated control animals. These results are in agreement with recent work by Franco *et al.* (14) who observed that instead of improving lipopolysaccharide-induced alveolar growth disorders as they had predicted, doxycycline actually worsened some parameters. Interestingly, neither hyperoxia (3) nor doxycycline administration caused an increase in septal thickness, suggesting a lack of severe inflammation or fibrosis for both these treatments, which concurs with low MMP activity in both models. We recognize that doxycycline inhibits most other members of the MMP family, and has other effects such as regulating cytokines (34), however

doxycycline did lower MMP gelatinase activity and our results are entirely consistent with our observations of decreased MMP activity in the hyperoxic model.

The observed increase in TIMP-1 after exposure to hyperoxia is in agreement with previous studies by Horowitz and colleagues who showed that neonatal rabbits exposed to > 95 % O<sub>2</sub> for 96 h had increased levels of TIMP-1 mRNA (16). Previous studies in the guinea pig have also shown no change in TIMP-2 expression in a model of hyperoxic-induced lung damage in which adult guinea pigs were exposed to 100 % O<sub>2</sub> for 24 and 72 h (27). As TIMP-1 has the ability to inhibit activity of the activated forms of both MMP-2 and MMP-9 (13), increased TIMP-1 may be responsible for the decreased MMP-2 activity observed in our experiments.

Interestingly, a recent publication by Bannikov and colleagues suggests that when the proform of MMP-9 is bound to either gelatin or type-IV collagen-coated surfaces *in vitro*, it acquires activity whilst the proform remains intact (1). This implies that the decreased levels of proMMP-9 seen in our experiments may represent real *in vivo* activity levels.

An important aspect of lung development that is dependent on degradation of the basement membrane, and therefore activity of MMP-2 and MMP-9, is the development of the blood vessels (angiogenesis). For angiogenesis to occur from established vascular channels, a “breaking out” or sprouting of endothelial cells from their ECM investment is necessary. The established vessel is surrounded by a basement membrane composed of collagen type IV, laminin, fibronectin, and other matrix macromolecules. Once this barrier is breached, the proliferating endothelial cells of the new vessel must penetrate the matrix of collagen fibrils, elastin, proteoglycans and many other constituents. Increasing

evidence suggests that MMP-2 and MMP-9 play key roles in this process. MMP-9 is required to initiate angiogenesis in the cartilage growth plate as determined by knockouts (39), and inhibition of the U-PA activity or receptor binding reduces the *in vitro* invasion of human umbilical vascular endothelial cells and formation of capillary-like structures (23).

Angiogenesis has been shown to be involved in alveolar development. Jakkula *et al.* (19) administered thalidomide and fumagillin (inhibitors of angiogenesis) or SU-5416 (a blocker of the R2 receptor for the potent angiogenic growth factor, vascular endothelial growth factor, VEGF) to rat pups between d 3 and d 14, and demonstrated decreased capillary density along with inhibited septation of the lungs. These results suggest that the process of angiogenesis is essential for the maturation of the neonatal lung; it is possible therefore that hyperoxia, through decreasing activity of MMP-2 and MMP-9, is inhibiting angiogenesis and consequently alveolarization. Indeed hyperoxia has previously been shown to inhibit capillary number in the rat pup (32). Further it is possible that VEGF may regulate MMPs in this model as VEGF is decreased during hyperoxic exposure in the neonatal rabbit lung (25) and VEGF administration has previously been shown to increase protein levels and gelatinase activity of MMP-2 (22).

There is conflicting data on the roles of MMPs during altered development of the lungs in the newborn infant. In tracheal aspirates from preterm infants with respiratory distress syndrome no correlations were observed between levels of MMP-9 and the development of bronchopulmonary dysplasia (10). Early reports, however, had shown elevated levels of MMP-9 in tracheal aspirates from preterm infants with respiratory distress syndrome

(37). Our results suggest that MMP-2 and MMP-9 may be intricately involved in the development of the lung, and partly responsible for inhibition of alveolarization caused by hyperoxia in the rat pup. Though future studies on a broader range of MMPs and with more specific blockers of individual MMPs are still necessary, understanding the role of MMPs in alveolar development may have important implications in the treatment of premature infants with newborn chronic lung disease.

Group	n	$V_{\text{aspunit}}$ ( $\mu\text{m}^3 \times 10^5$ )	P/A	$V_p$ (%)	$T_{\text{sept}}$ ( $\mu\text{m}$ )	SISA ( $\text{cm}^2/100\text{g}$ )
Vehicle	8	$0.64 \pm 0.04^*$	$0.11 \pm 0.008^*$	<b><math>20.8 \pm 0.6^*</math></b>	$4.9 \pm 0.07$	$6155 \pm 199^*$
Doxycycline	8	$1.67 \pm 0.10^*$	$0.07 \pm 0.001^*$	$15.9 \pm 0.5^*$	$5.0 \pm 0.17$	$4761 \pm 185^*$

**Table 5.1 Lung morphometry of 14-day-old rat pups treated with 0.9 % saline or doxycycline (20 mg/kg twice daily)**

Values are means  $\pm$  SEM: n, number of rats;  $V_{\text{aspunit}}$ , air space unit volume;  $T_{\text{sept}}$ , septal thickness; SISA, specific internal surface area;  $V_p$ , volume density of parenchymal tissue; P/A, ratio of air space perimeter to area. Within each morphometric parameter \* indicates values that are significantly different from one another ( $P < 0.001$ ).

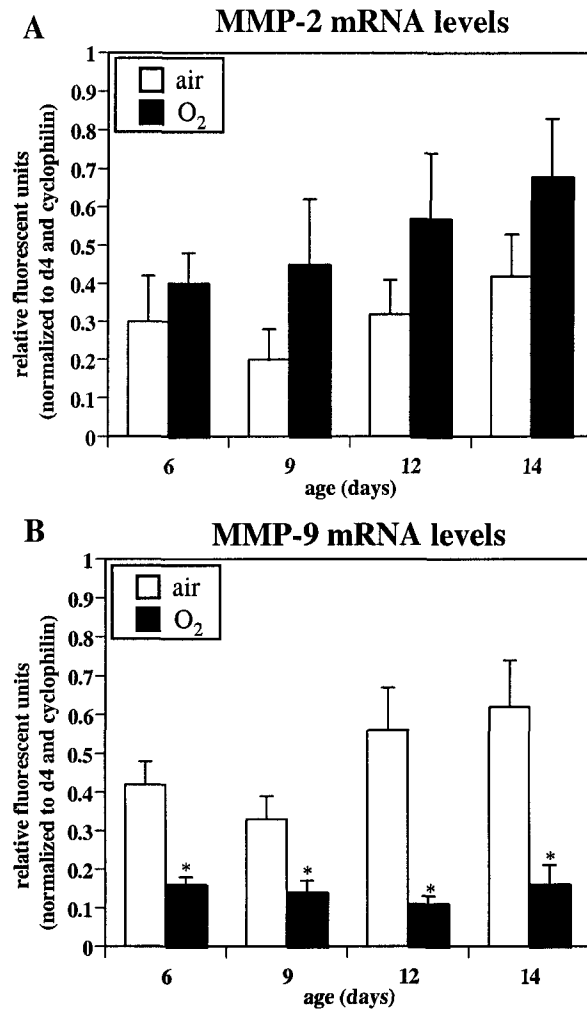


**Figure 5.1 Time course and effects of > 95 % O<sub>2</sub> from d 4 to d 14 on (A) MMP-2 and (B) MMP-9 mRNA expression.**

Data are means  $\pm$  SEM. n=5 for lungs/group. Animals were exposed to air (open bars) or O<sub>2</sub> (closed bars). MMP-2 mRNA levels did not change with advancing age. O<sub>2</sub> exposure caused a significant increase in MMP-2 mRNA expression above that of the air group ( $p < 0.05$  between air and O<sub>2</sub> groups). MMP-9 mRNA levels increased slightly with advancing age. O<sub>2</sub> exposure caused a dramatic decrease in mRNA expression compared to air group ( $p < 0.05$  between air and O<sub>2</sub> groups). \* indicates significant difference between air and O<sub>2</sub> pups on the day indicated.



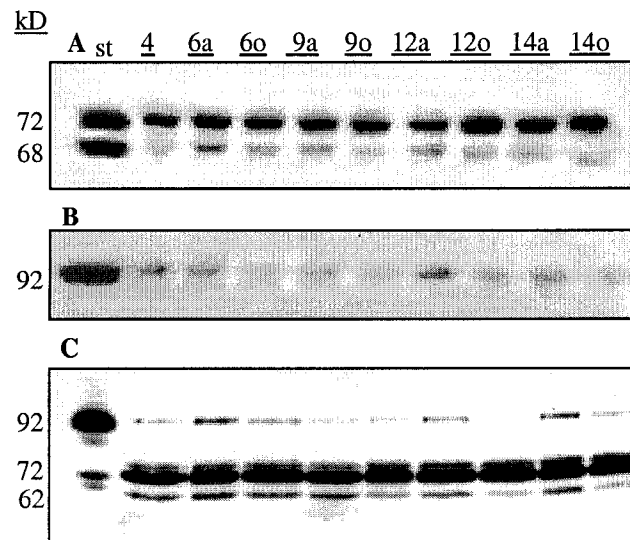


**Figure 5.2 Time course and effects of > 95 % O<sub>2</sub> from d 4 to d 14 on MMP-2 and MMP-9 protein and activity.**

The age of the rat pups, and whether they had been exposed to air (a) or O<sub>2</sub> (o), is given at the top for all three experiments, the first lane in each blot is a control standard. A) representative western blot of MMP-2 protein, a large band, representing the pro form of MMP-2 was observed at 72 kD with the active form of MMP-2 appearing as a fainter, 62 kD band beneath. B) representative western blot of MMP-9, one band was seen at 92 kD, representing the pro form of MMP-9, the active form was not seen by Western blotting. C) representative gelatinase zymography gel (colors were inverted for clarity), similar bands of gelatinolytic activity were observed at 92, 72 and 62 kD.

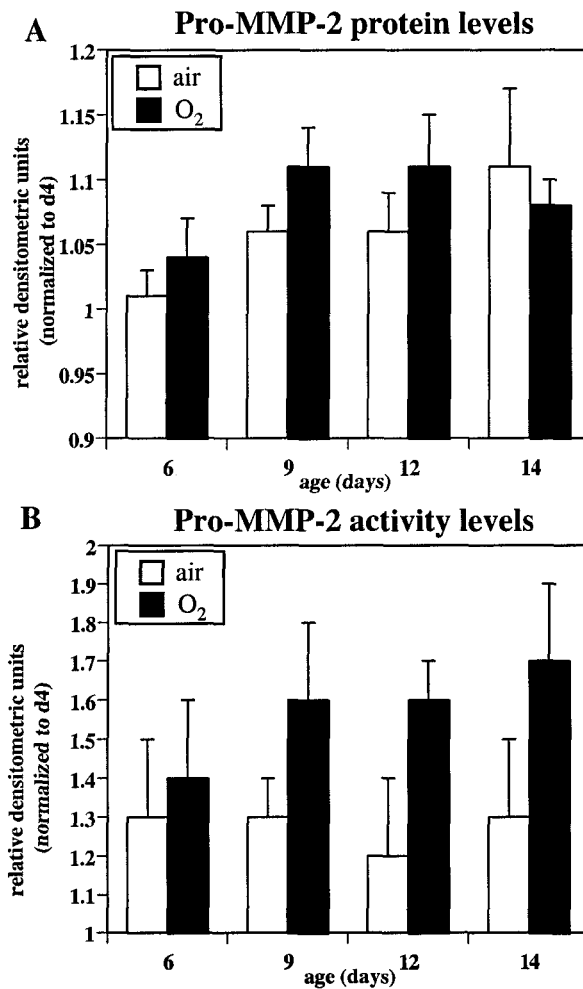


**Figure 5.3** Time course and effects of > 95 % O<sub>2</sub> from d 4 to d 14 on (A) pro-MMP-2 protein levels and (B) pro-MMP-2 activity levels.

Data are means  $\pm$  SEM. n=5-6 for lungs/group. Animals were exposed to air (open bars) or O<sub>2</sub> (closed bars). Pro-MMP-2 protein increased slightly with advancing age. O<sub>2</sub> exposure caused a slight (though not significant) increase in pro-MMP-2 protein levels on d 6, 9 and 12. Pro-MMP-2 activity levels did not change with advancing age. O<sub>2</sub> exposure caused a slight (though not significant) increase in pro-MMP-2 activity levels.

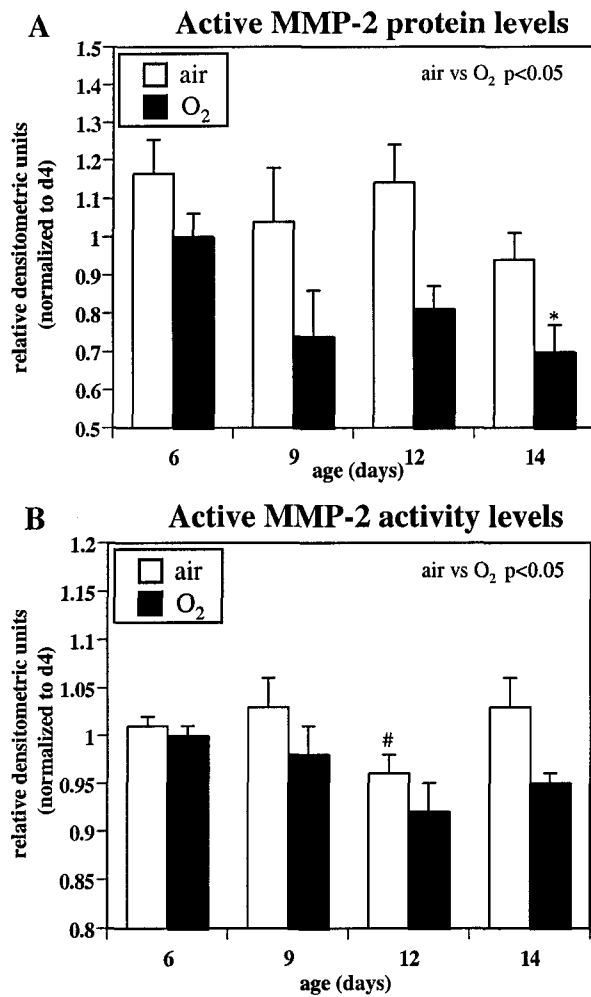


**Figure 5.4 Time course and effects of > 95 % O<sub>2</sub> from d 4 to d 14 on (A) active MMP-2 protein levels and (B) active MMP-2 activity levels.**

Data are means  $\pm$  SEM.  $n=5-7$  for lungs/group. Animals were exposed to air (open bars) or O<sub>2</sub> (closed bars). Active MMP-2 protein levels exhibited a transient decrease on d 12 ( $p<0.05$ ). O<sub>2</sub> exposure caused a significant decrease in active MMP-2 protein levels ( $p<0.05$  between air and O<sub>2</sub> groups). There was no change in active MMP-2 activity on any day examined in the normoxic groups. O<sub>2</sub> exposure caused a significant decrease in active MMP-2 activity levels ( $p<0.05$  between air and O<sub>2</sub> groups). \* indicates significant difference between air and O<sub>2</sub> pups on the day indicated. # indicates significant difference from d 6 air values.

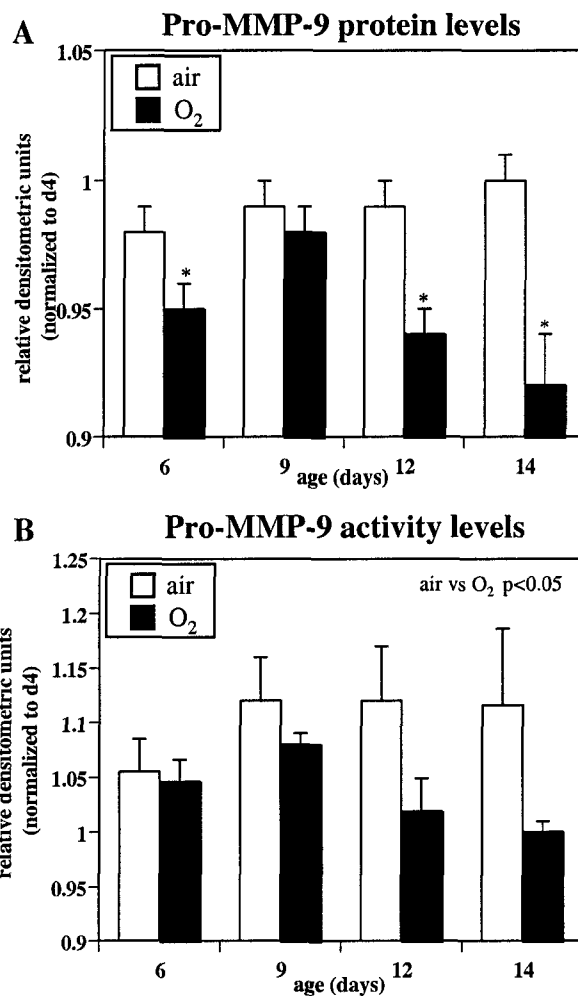
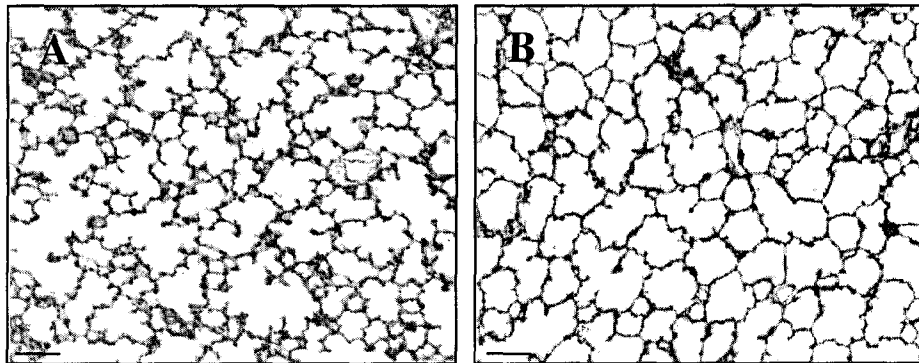


**Figure 5.5 Time course and effects of > 95 % O<sub>2</sub> from d 4 to d 14 on (A) pro-MMP-9 protein levels and (B) pro-MMP-9 activity levels.**

Data are means  $\pm$  SEM. n=5-7 for lungs/group. Animals were exposed to air (open bars) or O<sub>2</sub> (closed bars). Pro-MMP-9 protein did not change with advancing age. O<sub>2</sub> exposure caused a significant decrease in pro-MMP-9 protein levels on d 6, 12 and 14 (p<0.05). Pro-MMP-9 activity levels increased slightly (though not significantly) between d 6 and d 9. O<sub>2</sub> exposure caused a decrease in activity levels for pro-MMP-9 from d 9 onwards (p<0.05 between air and O<sub>2</sub> groups). \* indicates significant difference between air and O<sub>2</sub> pups on the day indicated.



---

**Figure 5.6** Representative photomicrographs of lung parenchyma of 14-day-old rats treated with saline vehicle (A) or doxycycline (B) from d 4 to d 14.

Parenchymal architecture of doxycycline-treated lungs is simpler (fewer and enlarged alveoli). Bar, 100 $\mu$ m.

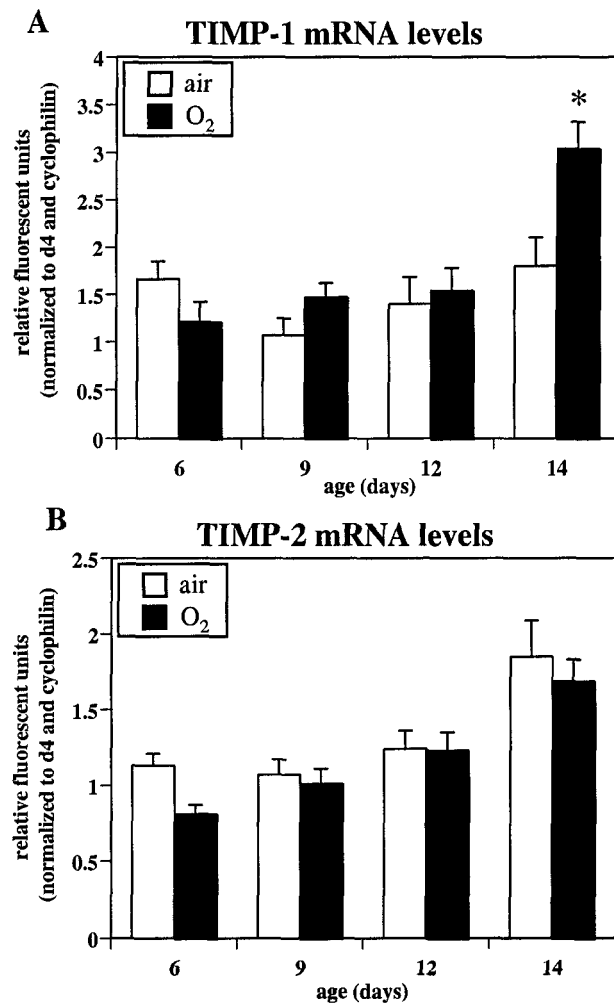


**Figure 5.7** Time course and effects of > 95 % O<sub>2</sub> from d 4 to d 14 on (A) TIMP-1 and (B) TIMP-2 mRNA expression.

Data are means  $\pm$  SEM. n=5 for lungs/group. Animals were exposed to air (open bars) or O<sub>2</sub> (closed bars). TIMP-1 mRNA levels did not change with advancing age. O<sub>2</sub> exposure caused a significant increase in TIMP-1 mRNA expression above that of the air group by d 14 ( $p < 0.05$ ). TIMP-2 mRNA levels increased slightly with advancing age, though this trend did not reach significance. O<sub>2</sub> exposure did not cause a difference in TIMP-2 mRNA levels on any day examined. \* indicates significant difference between air and O<sub>2</sub> pups on the day indicated.

## 5.5 REFERENCES

1. **Bannikov, G. A., T. V. Karelina, I. E. Collier, B. L. Marmer, and G. I. Goldberg.** Substrate binding of gelatinase B induces its enzymatic activity in the presence of intact propeptide. *J Biol Chem* 277: 16022-7., 2002.
2. **Bland, R. D. a. C., J.J.** *Chronic Lung Disease in Early Infancy*. New York: Marcel Dekker, 2001.
3. **Boros, V., J. S. Burghardt, C. J. Morgan, and D. M. Olson.** Leukotrienes are indicated as mediators of hyperoxia-inhibited alveolarization in newborn rats. *Am J Physiol* 272: L433-41., 1997.
4. **Bruce, M. C., R. Pawlowski, and J. F. Tomashefski, Jr.** Changes in lung elastic fiber structure and concentration associated with hyperoxic exposure in the developing rat lung. *Am Rev Respir Dis* 140: 1067-74., 1989.
5. **Buckley, S., B. Driscoll, W. Shi, K. Anderson, and D. Warburton.** Migration and gelatinases in cultured fetal, adult, and hyperoxic alveolar epithelial cells. *Am J Physiol Lung Cell Mol Physiol* 281: L427-34., 2001.
6. **Buckley, S., and D. Warburton.** Dynamics of metalloproteinase-2 and -9, TGF-beta, and uPA activities during normoxic vs. hyperoxic alveolarization. *Am J Physiol Lung Cell Mol Physiol* 283: L747-54., 2002.
7. **Burghardt, J. S., V. Boros, D. F. Biggs, and D. M. Olson.** Lipid mediators in oxygen-induced airway remodeling and hyperresponsiveness in newborn rats. *Am J Respir Crit Care Med* 154: 837-42., 1996.
8. **Burri, P. H.** The postnatal growth of the rat lung. 3. Morphology. *Anat Rec* 180: 77-98., 1974.
9. **Burri, P. H., J. Dbaly, and E. R. Weibel.** The postnatal growth of the rat lung. I. Morphometry. *Anat Rec* 178: 711-30., 1974.
10. **Cederqvist, K., T. Sorsa, T. Tervahartiala, P. Maisi, K. Reunanen, P. Lassus, and S. Andersson.** Matrix metalloproteinases-2, -8, and -9 and TIMP-2 in tracheal aspirates from preterm infants with respiratory distress. *Pediatrics* 108: 686-92., 2001.
11. **Crouch E C, M. G. R., Brody J S, Laurie G W.** Basement Membranes. In: *The Lung: Scientific Foundations*, edited by J. B. W. R G Crystal, E R Weibel, P J Barnes. New York: Lippencott Raven, 1997.
12. **Devaskar, U. P., W. Taylor, R. Govindrajan, M. Malicdem, S. Heyman, and D. E. deMello.** Hyperoxia induces interstitial (type I) and increases type IV collagenase

mRNA expression and increases type I and IV collagenolytic activity in newborn rat lung. *Biol Neonate* 66: 76-85, 1994.

13. **Edwards, D. R., P. P. Beaudry, T. D. Laing, V. Kowal, K. J. Leco, P. A. Leco, and M. S. Lim.** The roles of tissue inhibitors of metalloproteinases in tissue remodelling and cell growth. *Int J Obes Relat Metab Disord* 20 Suppl 3: S9-15., 1996.

14. **Franco, M. L., P. Waszak, G. Banalec, M. Levame, C. Lafuma, A. Harf, and C. Delacourt.** LPS-induced lung injury in neonatal rats: changes in gelatinase activities and consequences on lung growth. *Am J Physiol Lung Cell Mol Physiol* 282: L491-500., 2002.

15. **Fukuda, Y., M. Ishizaki, Y. Okada, M. Seiki, and N. Yamanaka.** Matrix metalloproteinases and tissue inhibitor of metalloproteinase-2 in fetal rabbit lung. *Am J Physiol Lung Cell Mol Physiol* 279: L555-61., 2000.

16. **Horowitz, S., D. L. Shapiro, J. N. Finkelstein, R. H. Notter, C. J. Johnston, and D. J. Quible.** Changes in gene expression in hyperoxia-induced neonatal lung injury. *Am J Physiol* 258: L107-11., 1990.

17. **Hussain, N., F. Wu, C. Christian, and M. J. Kresch.** Hyperoxia inhibits fetal rat lung fibroblast proliferation and expression of procollagens. *Am J Physiol* 273: L726-32., 1997.

18. **Itoh, T., T. Ikeda, H. Gomi, S. Nakao, T. Suzuki, and S. Itohara.** Unaltered secretion of beta-amyloid precursor protein in gelatinase A (matrix metalloproteinase 2)-deficient mice. *J Biol Chem* 272: 22389-92., 1997.

19. **Jakkula, M., T. D. Le Cras, S. Gebb, K. P. Hirth, R. M. Tuder, N. F. Voelkel, and S. H. Abman.** Inhibition of angiogenesis decreases alveolarization in the developing rat lung. *Am J Physiol Lung Cell Mol Physiol* 279: L600-7., 2000.

20. **Kauffman, S. L., P. H. Burri, and E. R. Weibel.** The postnatal growth of the rat lung. II. Autoradiography. *Anat Rec* 180: 63-76., 1974.

21. **Kurschat, P., P. Zigrino, R. Nischt, K. Breitkopf, P. Steurer, C. E. Klein, T. Krieg, and C. Mauch.** Tissue inhibitor of matrix metalloproteinase-2 regulates matrix metalloproteinase-2 activation by modulation of membrane-type 1 matrix metalloproteinase activity in high and low invasive melanoma cell lines. *J Biol Chem* 274: 21056-62., 1999.

22. **Lamoreaux, W. J., M. E. Fitzgerald, A. Reiner, K. A. Hasty, and S. T. Charles.** Vascular endothelial growth factor increases release of gelatinase A and decreases release of tissue inhibitor of metalloproteinases by microvascular endothelial cells in vitro. *Microvasc Res* 55: 29-42., 1998.



23. **Lijnen, H. R., J. Silence, G. Lemmens, L. Frederix, and D. Collen.** Regulation of gelatinase activity in mice with targeted inactivation of components of the plasminogen/plasmin system. *Thromb Haemost* 79: 1171-6., 1998.
24. **Lovejoy, B., A. Cleasby, A. M. Hassell, M. A. Luther, D. Weigl, G. McGeehan, M. H. Lambert, and S. R. Jordan.** Structural analysis of the catalytic domain of human fibroblast collagenase. *Ann N Y Acad Sci* 732: 375-8., 1994.
25. **Maniscalco, W. M., R. H. Watkins, C. T. D'Angio, and R. M. Ryan.** Hyperoxic injury decreases alveolar epithelial cell expression of vascular endothelial growth factor (VEGF) in neonatal rabbit lung. *Am J Respir Cell Mol Biol* 16: 557-67., 1997.
26. **Manji, J. S., C. J. O'Kelly, W. I. Leung, and D. M. Olson.** Timing of hyperoxic exposure during alveolarization influences damage mediated by leukotrienes. *Am J Physiol Lung Cell Mol Physiol* 281: L799-806., 2001.
27. **Melendez, J., V. Maldonado, C. D. Bingle, M. Selman, and A. Pardo.** Cloning and expression of guinea pig TIMP-2. Expression in normal and hyperoxic lung injury. *Am J Physiol Lung Cell Mol Physiol* 278: L737-43., 2000.
28. **Meyrick, B., and L. Reid.** Pulmonary arterial and alveolar development in normal postnatal rat lung. *Am Rev Respir Dis* 125: 468-73., 1982.
29. **Pardo, A., R. Barrios, V. Maldonado, J. Melendez, J. Perez, V. Ruiz, L. Segura-Valdez, J. I. Sznajder, and M. Selman.** Gelatinases A and B are up-regulated in rat lungs by subacute hyperoxia: pathogenetic implications. *Am J Pathol* 153: 833-44., 1998.
30. **Radomski, A., G. Sawicki, D. M. Olson, and M. W. Radomski.** The role of nitric oxide and metalloproteinases in the pathogenesis of hyperoxia-induced lung injury in newborn rats. *Br J Pharmacol* 125: 1455-62., 1998.
31. **Randell, S. H., R. R. Mercer, and S. L. Young.** Neonatal hyperoxia alters the pulmonary alveolar and capillary structure of 40-day-old rats. *Am J Pathol* 136: 1259-66., 1990.
32. **Roberts, R. J., K. M. Weesner, and J. R. Bucher.** Oxygen-induced alterations in lung vascular development in the newborn rat. *Pediatr Res* 17: 368-75., 1983.
33. **Scherle, W.** A simple method for volumetry of organs in quantitative stereology. *Mikroskopie* 26: 57-60., 1970.
34. **Shlopov, B. V., W. R. Lie, C. L. Mainardi, A. A. Cole, S. Chubinskaya, and K. A. Hasty.** Osteoarthritic lesions: involvement of three different collagenases. *Arthritis Rheum* 40: 2065-74., 1997.

35. **Smith, G. N., Jr., L. P. Yu, Jr., K. D. Brandt, and W. N. Capello.** Oral administration of doxycycline reduces collagenase and gelatinase activities in extracts of human osteoarthritic cartilage. *J Rheumatol* 25: 532-5., 1998.
36. **Sorsa, T., Y. Ding, T. Salo, A. Lauhio, O. Teronen, T. Ingman, H. Ohtani, N. Andoh, S. Takeha, and Y. T. Kontinen.** Effects of tetracyclines on neutrophil, gingival, and salivary collagenases. A functional and western-blot assessment with special reference to their cellular sources in periodontal diseases. *Ann N Y Acad Sci* 732: 112-31., 1994.
37. **Sweet, D. G., and H. L. Halliday.** Current perspectives on the drug treatment of neonatal respiratory distress syndrome. *Paediatr Drugs* 1: 19-30., 1999.
38. **Thibeault, D. W., S. Mabry, and M. Rezaiekhaliq.** Neonatal pulmonary oxygen toxicity in the rat and lung changes with aging. *Pediatr Pulmonol* 9: 96-108, 1990.
39. **Vu, T. H., J. M. Shipley, G. Bergers, J. E. Berger, J. A. Helms, D. Hanahan, S. D. Shapiro, R. M. Senior, and Z. Werb.** MMP-9/gelatinase B is a key regulator of growth plate angiogenesis and apoptosis of hypertrophic chondrocytes. *Cell* 93: 411-22., 1998.
40. **Vu, T. H., and Z. Werb.** Matrix metalloproteinases: effectors of development and normal physiology. *Genes Dev* 14: 2123-33., 2000.
41. **Warner, B. B., L. A. Stuart, R. A. Papes, and J. R. Wispe.** Functional and pathological effects of prolonged hyperoxia in neonatal mice. *Am J Physiol* 275: L110-7., 1998.
42. **Weibel, E. R.** *Morphometry of the Human Lung*. New York: Academic Press Inc., 1963. p. p 38.

## **CHAPTER 6.                  HYPEROXIA AFFECTS PROTEIN MASS OF 5-LIPOXYGENASE AND ITS ACTIVATING PROTEIN, FLAP, AND LTB<sub>4</sub> OUTPUT IN NEWBORN RAT LUNGS**

---

A version of this manuscript is In Press in *Experimental Lung Research*, to be published November/December 2002.

This paper was co-first authored with Kim Koyanagi.

### **6.1 INTRODUCTION**

Hyperoxia exposure during the neonatal period inhibits development of the alveoli. Exposure of neonatal rats to increased levels of O<sub>2</sub> results in altered alveolarization, interstitial and intraalveolar edema and proteinosis (2), which may all be mediated by an inflammatory process. Many of these changes mimic those observed with the human newborn lung disease, bronchopulmonary dysplasia, and for that reason, the newborn rat model is used as a model by many laboratories to elucidate mechanisms related to altered lung development.

The inflammatory mediators, leukotrienes (LTs), have been shown to act as mediators of the oxygen-dependent inhibition of alveolar development in the newborn rat model (2). Exposure of rat pups to > 95 % O<sub>2</sub> *in vivo*, from d 4 to d 14 results in increased release of cysteinyl-LTs from *in vitro* explants on d 14 (2). To further test the possibility that LTs mediate the hyperoxia inhibition of septation, cysteinyl--LT synthesis was inhibited by administration of the 5-lipoxygenase activating protein (FLAP) inhibitor,

MK-0591, from d 4 to d 14 in the hyperoxic environment, and morphometric analysis confirmed normal development of the alveoli (2). More recently we demonstrated a critical-period of hyperoxic exposure mediated by LTs, where exposure from d 4-9 resulted in inhibition of alveolarization whereas exposure from d 1-4 or d 9-14 did not arrest development (15).

Leukotrienes are not stored in the cell, but are synthesized upon appropriate stimulation (18). *De novo* synthesis of LTs from leukocytes requires a complex series of reactions. The initial step involves the release of the substrate arachidonic acid (AA), from membrane lipids within the nuclear envelope, by cytosolic (c) phospholipase A<sub>2</sub> (PLA<sub>2</sub>). Translocation of the enzyme 5-lipoxygenase (5-LO) from the cytosol (peripheral blood leukocytes) or nucleus (alveolar macrophages) (4) is stimulated when levels of intracellular Ca<sup>2+</sup> increase as a result of cellular activation (21). 5-lipoxygenase-activating protein (FLAP) is thought to function as a substrate transfer protein, through binding of arachidonic acid (14). 5-LO causes the lipoxygenation of AA at carbon atom 5 to produce 5(*S*)-hydroperoxy-6-*trans*-8,11,14-*cis*-eicosatetraenoic acid (5-HPETE) and the subsequent dehydration of 5-HPETE to the unstable epoxide LTA<sub>4</sub> (18). LTA<sub>4</sub> can be hydrolyzed to LTB<sub>4</sub> by the enzyme LTA<sub>4</sub> hydrolase or converted to the cysteinyl-LT, LTC<sub>4</sub>, by the catalyst LTC<sub>4</sub> synthase. LTC<sub>4</sub> is normally rapidly metabolized by enzymatic cleavage of successive amino acids from the glutathione side chain, forming LTD<sub>4</sub> and LTE<sub>4</sub>.

Although cysteinyl-LTs (LTC<sub>4</sub>, LTD<sub>4</sub> and LTE<sub>4</sub>) are elevated during hyperoxic inhibition of alveolar development in the rat pup (2, 3, 15), it is currently unknown

whether LTB<sub>4</sub> levels are also increased. The enzyme 5-LO is found primarily in cells of myeloid origin such as polymorphonuclear leukocytes and eosinophils. It has been demonstrated in the rat (and other animal species) that exposure to hyperoxia causes an infiltration of inflammatory cells into the lung (5), which could be potential sites of LT synthesis. LTB<sub>4</sub> may therefore be acting as a chemotaxant to aid the recruitment of inflammatory cells into the lung.

Previous LT inhibition studies did not discriminate between the formation of cysteinyl-LTs and LTB<sub>4</sub>, due to the fact that the inhibitors acted at a common point in the arachidonic acid cascade and that only cysteinyl-LTs were measured in these experiments. Therefore, in these experiments we examined the synthesis of LTB<sub>4</sub> by the newborn rat lung. Further, we assessed the LTB<sub>4</sub> output from lung explants in response to oxygen exposure, *in vivo*, and to elevated Ca<sup>2+</sup> levels, *in vitro*. Finally we examined the protein expression levels of the enzyme, 5-LO, and its associated protein, FLAP, during the period of alveolarization and in response to hyperoxia treatment.

## **6.2 METHODS**

### **6.2.1 *Animals***

Rat pups were exposed to O<sub>2</sub> as described in Methods for the analysis of 5-LO and FLAP. However, for the explant experiments, dams were placed in appropriate chambers in the early morning of the expected delivery date (term = 22 days), pups were therefore born into either hyperoxia or normoxia. The alternate hyperoxic regime consisted of > 95 % O<sub>2</sub> from d 0 to d 7 and 60 % O<sub>2</sub> (in order to decrease mortality in older pups) from d 7 to d 28. Pups were weaned at d 21 and males and females were separated.

### 6.2.2 *Explant technique*

Pups exposed to either normoxia or hyperoxia (5 litters per experimental group for each day were used, with 6 pups from each litter pooled to contribute to the experiment) were euthanized on d 1, d 7, d 17 and d 28 by an i.p. injection of 10 mg Ketamine : 0.6 mg Rompun / g body weight (for preliminary experiment characterizing the explant technique, experiments were performed on d 28 only). The lungs were removed and the left lobe was dissected free of visible blood vessels and airways. The tissue was placed in ice-cold Hank's balanced salt solution (HBSS) and placed on ice. The left lobes were sliced longitudinally to a thickness of 500  $\mu$ m and 40 to 50 mg of tissue (8 to 10 slices per well, depending on age) were placed on nylon mesh grids and placed in 12-well culture plates (18 replicate wells were analyzed per litter). The tissue was washed with cold HBSS. Then pre-warmed HBSS was added to the wells so that the media just reached the surface of the explant (700  $\mu$ l) and plate was incubated in a shaking water bath at 37°C.

#### 6.2.2.1 *Basal LTB<sub>4</sub> release-time course*

To determine the effect of handling and chopping on basal LTB<sub>4</sub> release, explants were prepared as stated above and incubated for 210 min, with the media changed at 30 min intervals. LTB<sub>4</sub> production was determined by RIA from media removed at each 30 min interval.

LTB<sub>4</sub> output was found to be greatest during the first 30 min interval, probably as a result of slicing; levels then declined 5-fold in a linear fashion from a maximum value of 33 pg/mg wet wt/30 min during the first interval, to 5 pg/mg wet wt/30 min at 120 min

where the basal plateau was reached. As it was desirable to choose the shortest possible incubation time in order to minimize tissue alterations from the *in vivo* state, an incubation interval from 120 min to 150 min was used in order to achieve basal release.

#### 6.2.2.2 *A23187 dose response curve*

To determine the maximal levels of  $\text{Ca}^{2+}$  allowing for the optimal activation of the calcium dependant enzymes,  $\text{PLA}_2$  and 5-LO, a dose response to the calcium ionophore A23187 was performed. Explants were incubated to basal  $\text{LTB}_4$  release (120 min with 30 min interval media changes, as determined above). A23187 was added in concentrations from 0 to 75  $\mu\text{M}$  (in 700  $\mu\text{l}$  pre-warmed HBSS) and incubated for 30 min. Basal  $\text{LTB}_4$  release (120 to 150 min) and A23187 media backgrounds were subtracted from the total stimulated release (150 to 180 min) to represent the  $\text{LTB}_4$  synthesized from A23187 stimulation only.

The release of  $\text{LTB}_4$  from explants increased linearly in the concentration range of 1.25 to 50  $\mu\text{M}$  A23187. Output of  $\text{LTB}_4$  reached a maximum at 50  $\mu\text{M}$  and then reached a plateau, as no further increase was seen at 75  $\mu\text{M}$ . From these results it was determined that a concentration of 50  $\mu\text{M}$  A23187 would be used in subsequent experiments.

#### 6.2.2.3 *A23187 time course*

We determined the time required for calcium ionophore to achieve its maximal effect. Explants were incubated for 120 min to reach basal  $\text{LTB}_4$  release and then A23187 (50  $\mu\text{M}$ ) in 700  $\mu\text{l}$  HBSS was added to the wells.  $\text{LTB}_4$  release increased linearly from a basal value of 0.5 ng/mg wet wt/min to 3.7 ng/mg wet wt/min after the first 15 min.

Levels then plateaued and were constant up until 75 min of incubation. In subsequent experiments 30 min incubations were used so that LTB<sub>4</sub> was produced at maximal levels.

#### 6.2.2.4 *Viability of explants*

An increased release of lactate dehydrogenase (LDH) from cells is a conventional index of cytotoxicity (1). Tissue explants were incubated in HBSS for a total of 210 min, with media changes every 30 min. Samples of media were taken at intervals from 0 to 210 min. As well as collecting media, tissue was homogenized in 1.0 ml of ice-cold HBSS containing 0.1 % Triton X-100 and then frozen. LDH was measured in the media and in the tissue sample. The LDH assay was performed using a kit from Sigma (Sigma-Aldrich, Oakville, Ontario, Canada). Briefly 1.0 ml pyruvate substrate was added to a vial containing 1.0 mg/ml NADH and incubated in a water bath at 37 °C for 5 min. Standard or sample (0.1ml) was added and incubated for 30 min. Sigma color reagent (1.0 ml) was added and mixed for 20 min. Sodium hydroxide (10 ml of 0.4 N) was added and standards (varying concentrations of pyruvate) and samples were read at 450 nm on a spectrophotometer. Percent LDH release from the tissue was calculated by:  $\text{LDH in media} / (\text{LDH in media} + \text{LDH in tissue}) \times 100$ .

The greatest LDH release was 9 %, which occurred between 1 and 30 min of incubation and likely reflected tissue damage from the slicing procedure. The percent LDH release then declined between 30 and 120 min, leveling to negligible values by 120 min, the incubation period when experimental results were assessed.



### **6.2.3 Radioimmunoassay**

The LTB<sub>4</sub> antibody (Merck-Frosst Canada, Mississauga, ON, Canada) was diluted in PBSG (PBS with 0.1 % gelatin) to 1:15,000. Tritiated (<sup>3</sup>H) LTB<sub>4</sub> was diluted in PBSG to give approximately 10,000 disintegrations per min (dpm) / 0.1 ml. A standard curve was constructed with standard LTB<sub>4</sub> (Cayman Chemical Company, Ann Arbor, Michigan, USA). <sup>3</sup>H LTB<sub>4</sub> (0.1 ml) and antibody solution (0.1 ml) were added to 0.1 ml aliquots of standards and samples; tubes were incubated at 4 °C for 16 to 20 h. Charcoal solution (0.5 ml) was added and the mixture was incubated for 10 min at 4 °C. The mixture was then centrifuged and the supernatant was added to 4 ml scintillation fluid (Cyto Scint, INC Biomedicals Inc., Irvine, CA, USA). The level of radioactivity was determined in counts per min (cpm) and dpm by a liquid scintillation system (LS 500TD, Beckman Instruments, Fullerton, CA, USA). Total (T), non-specific binding (NSB) and B<sub>0</sub> (maximum binding) were also determined. The standard curve was constructed by plotting the percentage bound (B) of maximum bound (B<sub>0</sub>) on a linear scale versus the LTB<sub>4</sub> concentration on a log scale. Percent B/B<sub>0</sub> was calculated from the dpm values by  $(B - NSB) / (B_0 - NSB) \times 100 = \% B / B_0$ . The levels of LTB<sub>4</sub> were normalized to DNA (assay modified from Downs and Wilfinger (7)).

### **6.2.4 Immunohistochemistry**

The rat pups were killed on d 14 with an overdose of pentobarbitol sodium (as in Preparation of Lung Samples). Incisions were made below the chest area and the diaphragm was pierced from below, with care being taken not to puncture the lungs. A shallow incision was made in the neck of the rat and the surrounding tissue removed so

that the trachea was exposed, and a small hole was cut in the middle of the exposed trachea. A polyethylene tracheal cannula connected to a 10 ml syringe casing was inserted into the trachea and tied in place tightly with thread. A solution of 4 % paraformaldehyde was allowed to flow into the lungs through the cannula at a constant pressure of 20 cm water for 2 h. The trachea was then ligated with thread and the lungs were excised from the chest cavity and immersed in 4% paraformaldehyde overnight at 4 °C. After fixation the lungs were washed in cold PBS for 4 x 2 h and then immersed in 0.1 M glycine in PBS overnight at 4 °C (to remove excess aldehyde agents). The tissues were processed according to the following protocol; 70 % ethanol x 1 h, 80 % ethanol x 1 h, 90 % ethanol x 1 h, 95 % ethanol x 1 h, 100 % ethanol x 1 h, 100 % ethanol x 1 h, 100 % ethanol x 1 h and then clearing in Xylene for 1 h. Samples were immersed in paraffin wax overnight at 55 °C and then blocked in paraffin using stainless steel molds. Transverse slices of the lung (5 µm) were cut and placed on silanized slides.

Tissue slices were deparaffinized in xylene, rehydrated in decreasing concentrations of ethanol from 100 % to 50 % and finally immersed in H<sub>2</sub>O. The slides were placed in 3 % Triton-X 100 for 5 min, followed by a 3 min wash in PBS. Antigen retrieval was achieved by placing the slides in a humid chamber (Tupperware lined with moist towels) and covering the tissue sections with proteinase-K (100 µg/ml in a buffer containing 1 M Tris-Cl and 0.5 M EDTA) for 30 min at 37 °C. The reaction was stopped by immersing slides in 0.2 % glycine at room temperature for 5 min. The slides were washed in PBS for 3 x 2 min then treated with 5 % H<sub>2</sub>O<sub>2</sub> in methanol for 10 min to block any endogenous peroxidase activity. The slides were again washed in PBS for 3 x 2 min. After blotting the

side of the slides on paper towel to remove as much PBS as possible, 10 % goat serum (to block non-specific binding, as all the secondary antibodies were raised in goat) was dropped onto the sections and left for 15 min at room temperature, after which slides were placed in PBS for 3 min. The primary antibodies for 5-LO and FLAP were rabbit polyclonal antisera raised against native purified human leukocyte 5-LO/FLAP (generous gift from Merck-Frosst, Dorval, PQ, Quebec, Canada). The macrophage specific antibody was a mouse anti-rat monocyte/macrophage specific monoclonal antibody (clone ED 1) which recognizes a single chain glycoprotein of 90-100 kD that is expressed on the lysosomal membrane of myeloid cells (6) (Chemicon International, Temecula, CA, USA). The antibodies were diluted 1:400 in 1 % BSA in PBS and enough solution was dropped onto slides to cover the tissue sections. The slides were placed in a humid chamber and incubated at 4 °C overnight. Isotype IgG was used as a negative control in place of primary antibody. Slides were washed for 3 x 5 min in PBS and then incubated with peroxidase-conjugated goat-anti-rabbit IgG (5-LO and FLAP) or peroxidase-conjugated goat-anti-mouse IgG (macrophages) at a 1:500 dilution in PBS for 30 min at room temperature, followed by another PBS wash.

The slides were developed in diaminobenzidine tetrahydrochloride solution until a light brown colour was observed (usually 1- 2 min), then washed in distilled H<sub>2</sub>O for 5 min. The slices were counterstained with hematoxylin for 10 s and placed in running tap water to develop the reaction. Finally, the tissue was dehydrated in increasing concentrations of ethanol (50 % to 100 %) followed by xylene for 2 min. The tissue sections were coated with Permount (Sigma), roofed with a cover slip and allowed to dry before examination.

## 6.3 RESULTS

### 6.3.1 *LTB<sub>4</sub> release*

#### 6.3.1.1 *Basal release from normoxic- and hyperoxic-exposed rat pups.*

To determine whether LTB<sub>4</sub> is released throughout this entire protocol we tested LTB<sub>4</sub> output on d 1, d 7, d 17 and d 28. A postnatal developmental increase in the basal release of LTB<sub>4</sub> was observed in the air-exposed animals; levels of LTB<sub>4</sub> increased 3.4-fold, from 0.98 ng/mg DNA/30 min to 2.7 ng/mg DNA/30 min, (p<0.05) between d 7 and d 17 (Fig. 6.1). Basal LTB<sub>4</sub> release from explants after 1 day of hyperoxic exposure was elevated 1.6-fold (to 1.6 ng/mg DNA/30 min) over control levels (p<0.05). At d 7 this increase was more prominent; the hyperoxic explants released 2.4-times (p<0.05) more LTB<sub>4</sub> than normoxic explants. At d 7 hyperoxic-levels were decreased as older pups do not tolerate extreme hyperoxia as well as the younger pups. By d 17, and continuing to d 28, hyperoxia had no further effect over normoxia on stimulating LTB<sub>4</sub> output (Fig. 6.1).

#### 6.3.1.2 *A23187 stimulated release from normoxic- and hyperoxic-exposed rat pups.*

Calcium ionophore was added to explant media to elevate intracellular calcium concentrations and stimulate enzymatic activity responsible for LT synthesis (e.g. the enzymes PLA<sub>2</sub> and 5-LO). A23187-stimulated LTB<sub>4</sub> production from normoxic explants increased progressively with advancing postnatal age, with a 3.6-fold (p<0.05) increase comparing d 1 to d 28 (Fig. 6.2). After 1 d of hyperoxic exposure, A23187 stimulation of the explants caused release of LTB<sub>4</sub> that was 2.5-times (p<0.05) greater than levels released from normoxic explants (Fig. 6.2). The levels of A23187-stimulated LTB<sub>4</sub>

release from hyperoxic explants remained continuously elevated, 1.75- to 2-times ( $p < 0.05$  for all points measured) above normoxic-stimulated explants, from d 1 to d 28.

### **6.3.2 5-LO and FLAP protein levels**

#### **6.3.2.1 Western Immunoblotting**

As the observed increase in  $LTB_4$  in response to hyperoxia was seen on d 1 and d 7 but had disappeared by d 17, we examined effects of hyperoxia upon the LT synthetic proteins, 5-LO and FLAP in the early postnatal phase and focused specifically on the period of alveolarization, d 4 to d 14. The relative amount of 5-LO protein in normoxia exposed animals increased twofold between days 4 and 14 ( $p < 0.05$ ) (Fig. 6.3). The levels of 5-LO in hyperoxia exposed animals showed a greater rate of increase, reaching 3.5 times d 4 values by d 14 ( $p < 0.05$ ). Further, there was a statistically significant increase of 5-LO protein levels in hyperoxic animals compared to the normoxic controls, resulting in the hyperoxic d 14 groups expressing 1.75 times the level of 5-LO of the normoxic d 14 groups ( $p < 0.05$ ) (Fig. 6.3).

In the normoxic-exposed rat pups, the relative amount of FLAP protein increased slightly, to 1.3 times d 4 levels, by d 14 (Fig. 6.4). In the hyperoxic groups FLAP protein increased to 3.3 times d 4 levels by d 14 ( $p < 0.05$ ) (Fig. 6.4). There was a statistically significant increase of FLAP in the hyperoxic animals compared to the normoxic controls. By d 14 the hyperoxic groups expressed almost 3 times more FLAP protein than the normoxic groups ( $p < 0.05$ ) (Fig. 6.4).

### 6.3.2.2 Immunohistochemistry

Immunohistochemistry staining of lung slices from lungs of d 14 rat pups which had been exposed to room air or > 95 % O<sub>2</sub> from d 4 to d 14 (Fig. 6.5), revealed increased staining for both 5-LO (c) and FLAP (d), when compared to normoxic lungs (a and b). Staining was seen mainly in cells within alveolar spaces (c and d), which when probed with an anti-macrophage antibody were revealed to be alveolar macrophages (Fig. 6.5 e). In oxygen-exposed animals there was staining for both FLAP and 5-LO in the parenchymal cells of the alveoli (Fig. 6.5 c and d). Staining was also observed in the pulmonary arteries, however not in airway cells, confirming earlier reports (13) (results not shown).

## 6.4 DISCUSSION

The experiments reported here show that LTB<sub>4</sub> increased with developmental age and had an initial increase in response to hyperoxia (d 1 to d 7), which was negligible by 4 weeks. These results confirm previous experiments in our laboratory (3) using a similar protocol, which showed an early increase in cysteinyl-LTs in response to hyperoxia. Here, we also demonstrated that hyperoxia increased protein levels of 5-LO and FLAP in the early postnatal period, strongly suggesting that hyperoxic elevation of LT output acts through this mechanism.

In these experiments we utilized a technique whereby freshly isolated slices from the lungs of rat pups were incubated in media, and the release of LTs into the media was measured. As LTB<sub>4</sub> is synthesized in cells upon stimulation, this protocol allows for physiological measurements of the *ex vivo* state in an *in vitro* system and therefore allows

for experimental manipulation *in vitro*. In this paper we highlighted the experiments performed to characterize the appropriate use of this protocol, and then employed this procedure to measure LTB<sub>4</sub> both in a basal and Ca<sup>2+</sup>-stimulated situation.

Using the calcium ionophore A23187 we showed that lung explant LTB<sub>4</sub> release is enhanced by increased [Ca<sup>2+</sup>]<sub>i</sub> in both normoxic and hyperoxic conditions, compared to basal control levels. This observation suggests that the factor responsible for the increase in LTs is Ca<sup>2+</sup>-dependent, and substantiates the involvement of 5-LO. Further, as the hyperoxic group had a greater LTB<sub>4</sub> output than the normoxic group on all days, this implies the upregulation of a Ca<sup>2+</sup> dependant factor in the hyperoxic exposed pups, which causes the greater LTB<sub>4</sub> release over and above that observed in the normoxic group. These Ca<sup>2+</sup>-stimulation (A23187) experiments are consistent with a role for 5-LO as a key regulating enzyme in LT synthesis in this model.

The O<sub>2</sub>-induced increase in 5-LO and FLAP is a potential pathway whereby LTB<sub>4</sub> synthesis may be stimulated, although it is apparent from the complex process of LT synthesis that there are other points in the cascade where the increased oxygen levels could be acting, indeed Taniguchi *et al.* (20) demonstrated that PLA<sub>2</sub> is activated in adult rats during breathing of oxygen. However, our laboratory has now demonstrated an increased production of both LTB<sub>4</sub> and the cysteinyl-LTs from lung explants of rat pups exposed to O<sub>2</sub> *in vivo*, this suggests that the effects of hyperoxia are acting to increase a precursor molecule common to both these LTs, specifically LTA<sub>4</sub>. The increased protein levels of 5-LO and FLAP correlate with this conclusion and are likely involved in the observed increased in LTB<sub>4</sub> synthesis.

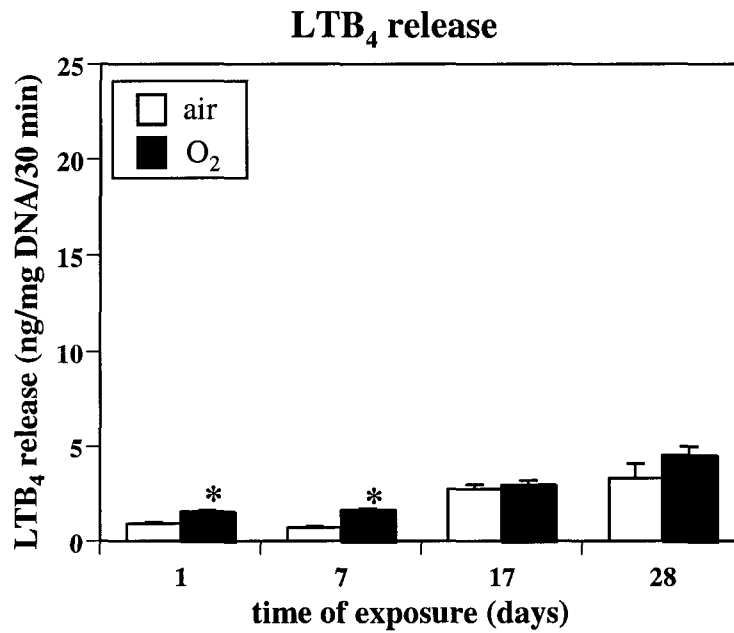
As the increased staining for the enzyme 5-LO and FLAP in the hyperoxic rat pup lungs is mainly localized to the alveolar macrophages, they are likely to be the main source of LT production (Fig. 5 c and d). It has been shown that alveolar macrophages release LTB<sub>4</sub> in response to hyperoxia (11). Further, in adult rats exposed to oxygen for 60 h, LTB<sub>4</sub> levels correlated with the observed increase in inflammatory cells (20). In the same experiments it was demonstrated that an inhibitor of 5-LO, AA861, decreased the infiltration of neutrophils as well as levels of LTB<sub>4</sub>, therefore LTB<sub>4</sub> may exert its actions through the recruitment of neutrophils.

We also observed staining for both 5-LO and FLAP in the parenchyma of the alveoli of 14 hyperoxic-exposed rat pups. From these experiments it was unclear which cell type expressed these proteins. However, it was recently demonstrated that both lung epithelial and fibroblast cell lines can be stimulated to release eosinophil, or neutrophil and monocyte, chemotactic activity; both of which are reduced by a LTB<sub>4</sub> receptor antagonist (16, 19). Also, recent evidence suggests that LTs may also be synthesized in human pulmonary vasculature (13), therefore it is possible that the parenchyma and vasculature of the alveoli may be another important source of LTB<sub>4</sub> production.

Experiments from this laboratory (2) have previously demonstrated that the cysteinyl-LTs are increased in the presence of hyperoxia and that MK-0591, a FLAP inhibitor, restores alveolarization to normal. The results presented in this paper now add to this body of knowledge. This work may be of significant clinical importance for premature infants who develop bronchopulmonary dysplasia (BPD), which was described by Northway *et al.* in 1967 as severe lung injury resulting from oxygen exposure and



mechanical ventilation (17). The disease today occurs commonly in infants born weighing < 1kg, developing in 90 % of very low birth weight infants (9). However since the introduction of effective surfactant therapy, the characteristics of the disease have changed; infants dying of BPD now have fewer and larger alveoli, described as the “New BPD” (10, 12).  $LTB_4$ , produced by neutrophils and alveolar macrophages within the lung, has been shown to be elevated in the bronchoalveolar fluid of infants who developed BPD (8). Therefore it is exciting to contemplate a potential clinical application, using inhibitors of the enzymes causing LT production, in these infants.




---

**Figure 6.1** LTB<sub>4</sub> release from *in vitro* lung explants of rat pups.

Lungs were removed from rat pups after 1, 7, 17 and 28 days of exposure to room air (open bars) or O<sub>2</sub> (closed bars). An increase ( $p < 0.05$ ) was observed in basal LTB<sub>4</sub> release from explants of O<sub>2</sub> exposed animals when compared to air exposed animals on days 1 and 7. \* indicates significant difference from air value on same day. (n=5 litters, 6 pups pooled per litter). Data are expressed as mean  $\pm$  SEM.

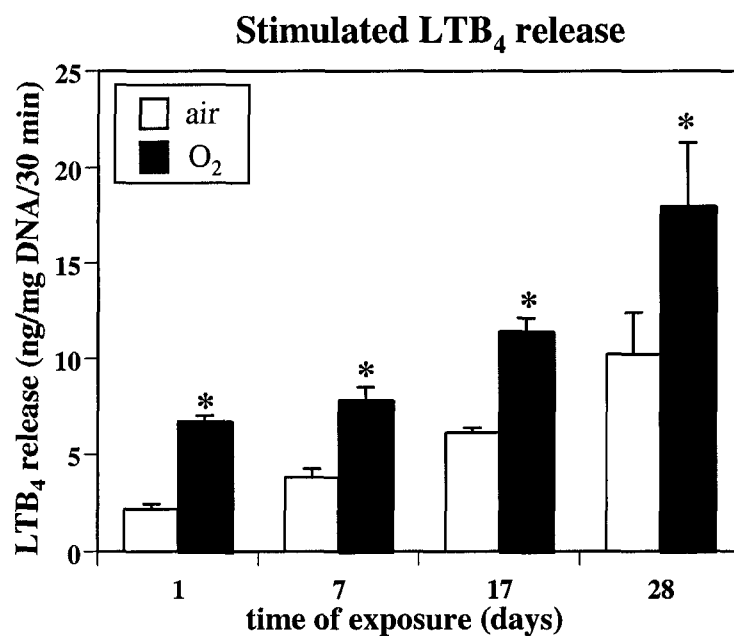


**Figure 6.2** LTB<sub>4</sub> release from *in vitro* lung explants of rat pups stimulated with Ca<sup>2+</sup> ionophore.

Lungs were removed from rat pups after 1, 7, 17 and 28 days of exposure to room air (open bars) or O<sub>2</sub> (closed bars). An increase ( $p < 0.05$ ) was observed in A23189 stimulated LTB<sub>4</sub> release from explants of oxygen exposed animals when compared to air exposed animals on all days measured. \* indicates significant difference from air value on same day. (n=5 litters, 6 pups pooled per litter). Data are expressed as mean  $\pm$  SEM.

### 5-LO protein levels

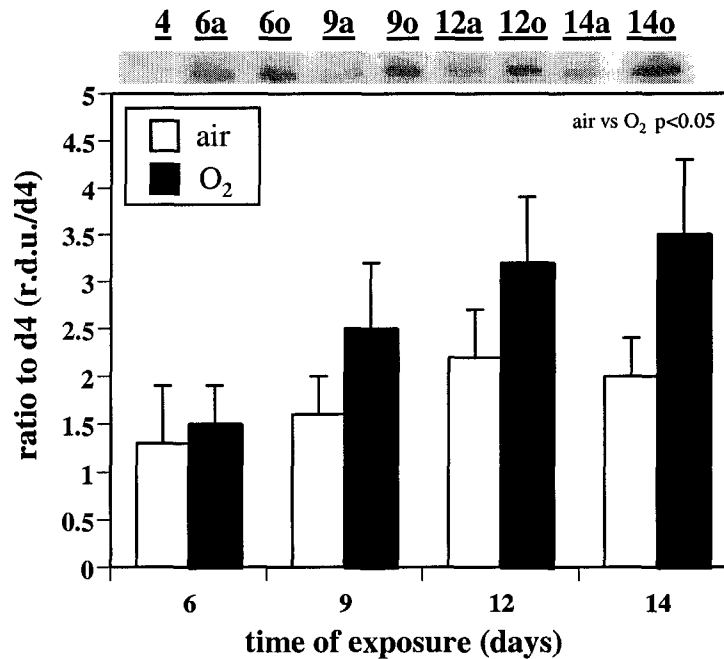


**Figure 6.3** Changes in 5-LO protein levels in newborn rat lung.

Lungs were removed from rat pups after 4, 6, 9, 12 and 14 days of exposure to room air (open bars) or >95% O<sub>2</sub> (closed bars). A representative western blot is shown above the graph indicating the day the lungs were removed and the experimental group; a = air/normoxia, o = oxygen/hyperoxia. An increase in 5-LO protein mass ( $p < 0.05$ ) was observed between d4 and d14. A further increase ( $p < 0.05$ ) was seen in O<sub>2</sub>-exposed animals when compared to air exposed animals. ( $n = 6-7$ /experimental group on each day).

Data are expressed as mean  $\pm$  SEM.

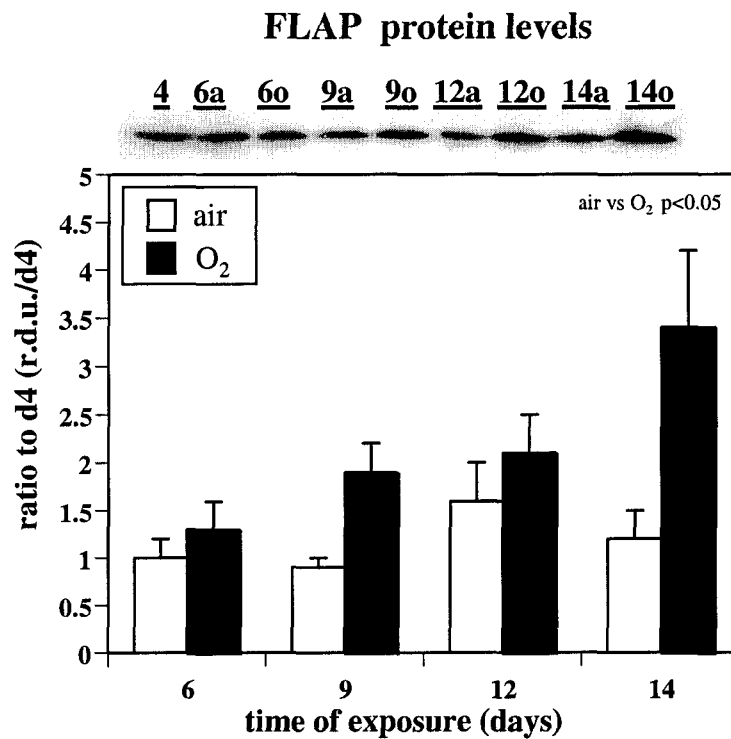


**Figure 6.4** Changes in FLAP protein levels in newborn rat lung.

Lungs were removed from rat pups after 4, 6, 9, 12 and 14 days of exposure to room air (open bars) or >95% O<sub>2</sub> (closed bars). A representative western blot is shown above the graph indicating the day the lungs were removed and the experimental group; a = air/normoxia, o = oxygen/hyperoxia. An increase in FLAP protein mass ( $p < 0.05$ ) was observed between d4 and d14. A further increase in FLAP protein mass ( $p < 0.05$ ) was seen in O<sub>2</sub> exposed animals when compared to air exposed animals. ( $n = 6-7$ /experimental group on each day). Data are expressed as mean  $\pm$  SEM.

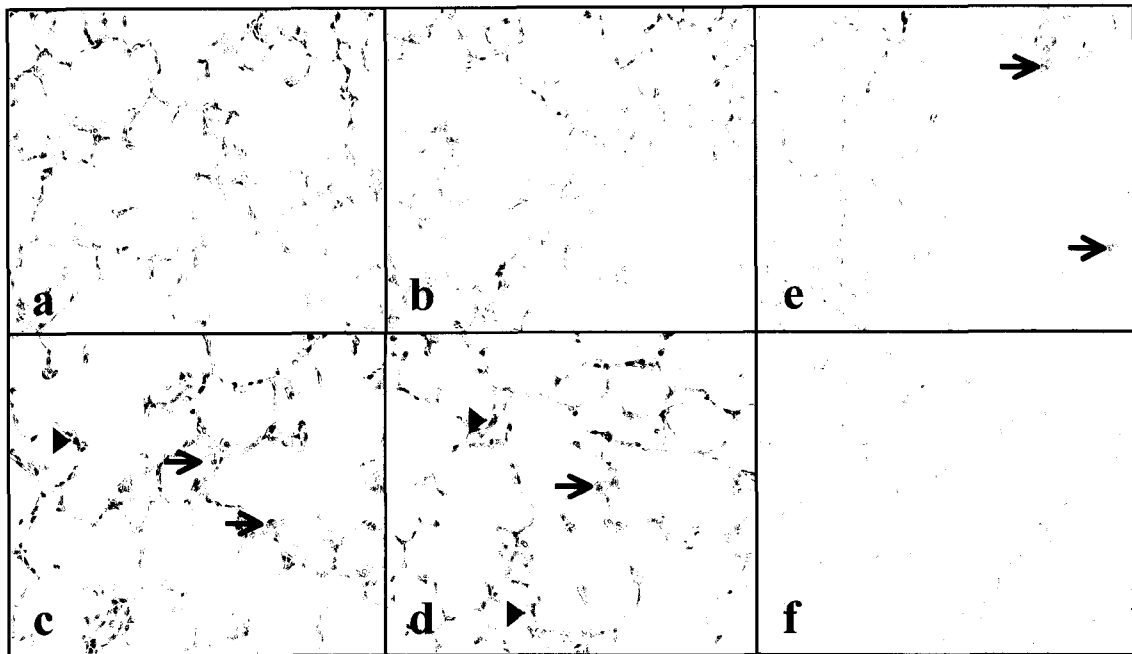


**Figure 6.5** Representative immunohistochemistry demonstrating localization of 5-LO and FLAP in d 14 rat lung.

Rat pups (n=3/experimental group) were exposed to room air (a,b) or >95% O<sub>2</sub> (c,d) from d 4 to d 14. Slices of lung were fixed and stained with antibodies that recognize 5-LO (a,c), FLAP (b,d) or macrophages (e). All micrographs are at a magnification of x 400. O<sub>2</sub> exposure increased staining of both 5-LO and FLAP in the alveoli (c,d) compared to air exposed animals (a,b). The majority of staining was observed to be present in macrophages in the hyperoxic lung (e) shown by → in c,d and e. There was also an increase in staining observed in parenchyma (▶). A negative control, with no primary antibody is shown (f).

## 6.5 REFERENCES

1. **Bergmeyer, H. U., P. Scheibe, and A. W. Wahlefeld.** Optimization of methods for aspartate aminotransferase and alanine aminotransferase. *Clin Chem* 24: 58-73., 1978.
2. **Boros, V., J. S. Burghardt, C. J. Morgan, and D. M. Olson.** Leukotrienes are indicated as mediators of hyperoxia-inhibited alveolarization in newborn rats. *Am J Physiol* 272: L433-41., 1997.
3. **Burghardt, J. S., V. Boros, D. F. Biggs, and D. M. Olson.** Lipid mediators in oxygen-induced airway remodeling and hyperresponsiveness in newborn rats. *Am J Respir Crit Care Med* 154: 837-42., 1996.
4. **Coffey, M., M. Peters-Golden, J. C. Fantone, 3rd, and P. H. Sporn.** Membrane association of active 5-lipoxygenase in resting cells. Evidence for novel regulation of the enzyme in the rat alveolar macrophage. *J Biol Chem* 267: 570-6., 1992.
5. **Crapo, J. D., B. E. Barry, H. A. Foscue, and J. Shelburne.** Structural and biochemical changes in rat lungs occurring during exposures to lethal and adaptive doses of oxygen. *Am Rev Respir Dis* 122: 123-43., 1980.
6. **Damoiseaux, J. G., E. A. Dopp, W. Calame, D. Chao, G. G. MacPherson, and C. D. Dijkstra.** Rat macrophage lysosomal membrane antigen recognized by monoclonal antibody ED1. *Immunology* 83: 140-7., 1994.
7. **Downs, T. R., and W. W. Wilfinger.** Fluorometric quantification of DNA in cells and tissue. *Anal Biochem* 131: 538-47., 1983.
8. **Groneck, P., B. Gotze-Speer, M. Oppermann, H. Eiffert, and C. P. Speer.** Association of pulmonary inflammation and increased microvascular permeability during the development of bronchopulmonary dysplasia: a sequential analysis of inflammatory mediators in respiratory fluids of high-risk preterm neonates. *Pediatrics* 93: 712-8., 1994.
9. **Hudak, B. B., and E. A. Egan.** Impact of lung surfactant therapy on chronic lung diseases in premature infants. *Clin Perinatol* 19: 591-602., 1992.
10. **Husain, A. N., N. H. Siddiqui, and J. T. Stocker.** Pathology of arrested acinar development in postsurfactant bronchopulmonary dysplasia. *Hum Pathol* 29: 710-7., 1998.
11. **Ida, E., A. Sakata, M. Tominaga, H. Yamasaki, and K. Onoue.** Arachidonic acid release is closely related to the Fc gamma receptor- mediated superoxide generation in macrophages. *Microbiol Immunol* 32: 1127-43, 1988.

12. **Jobe, A. J.** The new BPD: an arrest of lung development. *Pediatr Res* 46: 641-3., 1999.
13. **Kiss, L., H. Schutte, K. Mayer, H. Grimm, W. Padberg, W. Seeger, and F. Grimminger.** Synthesis of arachidonic acid-derived lipoxygenase and cytochrome P450 products in the intact human lung vasculature. *Am J Respir Crit Care Med* 161: 1917-23., 2000.
14. **Mancini, J. A., C. Li, and P. J. Vickers.** 5-Lipoxygenase activity in the human pancreas. *J Lipid Mediat* 8: 145-50., 1993.
15. **Manji, J. S., C. J. O'Kelly, W. I. Leung, and D. M. Olson.** Timing of hyperoxic exposure during alveolarization influences damage mediated by leukotrienes. *Am J Physiol Lung Cell Mol Physiol* 281: L799-806, 2001.
16. **Masubuchi, T., S. Koyama, E. Sato, A. Takamizawa, K. Kubo, M. Sekiguchi, S. Nagai, and T. Izumi.** Smoke extract stimulates lung epithelial cells to release neutrophil and monocyte chemotactic activity. *Am J Pathol* 153: 1903-12., 1998.
17. **Northway, W. H., Jr., R. C. Rosan, and D. Y. Porter.** Pulmonary disease following respirator therapy of hyaline-membrane disease. Bronchopulmonary dysplasia. *N Engl J Med* 276: 357-68., 1967.
18. **Reid, G. K., S. Kargman, P. J. Vickers, J. A. Mancini, C. Leveille, D. Ethier, D. K. Miller, J. W. Gillard, R. A. Dixon, and J. F. Evans.** Correlation between expression of 5-lipoxygenase-activating protein, 5- lipoxygenase, and cellular leukotriene synthesis. *J Biol Chem* 265: 19818-23., 1990.
19. **Sato, E., S. Koyama, and R. A. Robbins.** Bleomycin stimulates lung fibroblast and epithelial cell lines to release eosinophil chemotactic activity. *Eur Respir J* 16: 951-8., 2000.
20. **Taniguchi, H., F. Taki, K. Takagi, T. Satake, S. Sugiyama, and T. Ozawa.** The role of leukotriene B4 in the genesis of oxygen toxicity in the lung. *Am Rev Respir Dis* 133: 805-8., 1986.
21. **Ueda, N., S. Yamamoto, J. A. Oates, and A. R. Brash.** Stereoselective hydrogen abstraction in leukotriene A4 synthesis by purified 5-lipoxygenase of porcine leukocytes. *Prostaglandins* 32: 43-8., 1986.



***7.1 DISCUSSION***

Although the three papers presented in this thesis appear to be relatively unrelated, the one common area which may connect the different experiments is that all the factors examined have the potential to affect angiogenesis.

***7.1.1 Angiogenesis and alveolarization***

It has been demonstrated that angiogenesis is likely to be necessary for the development of the alveoli (10), however the mechanism of this action is not clear. As mentioned previously, secondary septa are formed through the uplifting of alternating capillaries from a double capillary network, and no septation is possible without the presence of this network (6); therefore, if angiogenesis is decreased this capillary network may not be as extensive, leading to decreased septation. Another possibility is simply that, due to a decreased capillary network, the primary septa do not receive sufficient nutrients to allow for growth and development of secondary septa. Indeed it has been established that a paucity of nutrients does inhibit lung development (14, 17).

It has also been shown that an increase in VEGF expression can severely disrupt the development of the lung. When VEGF was overexpressed in the developing pulmonary epithelium of the mouse, the lungs on E 15 and E 17 were shown to consist of large, abnormally dilated tubules, and the number of acinar buds and saccules was markedly reduced (25). Vasculogenesis was demonstrated to be markedly advanced in these VEGF

overexpressing embryos, suggesting that abnormally stimulated angiogenesis also (as well as inhibited angiogenesis) has the ability to disrupt the coordinated development of the lung.

### **7.1.2 Angiogenesis: stimulation or inhibition?**

As mentioned in Chapters 4 and 5, decreased VEGF as well as decreased MMP activity in hyperoxic-exposed animals both have the ability to cause a relative inhibition of angiogenesis (8).

However a closer examination of the results suggest a diverse effect of O<sub>2</sub>. When looking at VEGF<sub>165</sub> protein data, it is clear that there is an initial O<sub>2</sub>-induced increase in VEGF<sub>165</sub> up until d 9, before protein levels decrease to below air values on d 12. As VEGF<sub>165</sub> is the major mitogenic variant of VEGF, this indicates that there may be a biphasic effect where O<sub>2</sub> initially drives vessel development before decreasing angiogenesis in the second half of the alveolar stage. Accordingly, in the O<sub>2</sub>-exposed groups, HIF-2 $\alpha$  mRNA, VEGF mRNA and VEGFR2 (the receptor responsible for mitogenesis) mRNA and protein also did not decrease significantly below air values until d 12.

As mentioned previously, MMP-2 and MMP-9 are necessary to degrade the basement membrane and allow for angiogenesis. In relation to the results presented in this thesis, there is no clear-cut timing difference for the MMPs. Although the activity of the cleaved (62 kD form) of MMP-2 is not significantly decreased due to O<sub>2</sub> until d 14, from the mRNA and protein values of MMP-9 it appears that the decrease is seen within 2 days of the start of O<sub>2</sub> exposure. It is interesting to point out here, that it has been proposed that

MMPs have a time-dependent dual function in angiogenesis; although they can promote the formation of microvessels, they may also contribute to the reabsorption and regression of the neovasculature (26). Therefore it is possible that the early decrease in MMP-9 is acting to preserve the vasculature being formed due to the increased VEGF on d 9. Further the mRNA, protein and activity of the pro (72 kD) form of MMP-2 increases slightly (though not significantly) throughout the hyperoxic-exposure protocol and may have some gelatinolytic activity (as described in Chapter 5); as such, it may also promote angiogenesis during the early d 4 – d 9 period. The data for TIMP-2 mRNA also adheres to the pattern where there is only a significant change late in the hyperoxic-exposure protocol (mRNA is increased compared to air-controls on d 14) and again this suggests that angiogenesis may not be significantly inhibited until the second half of alveolarization.

Although not discussed in Chapter 6, LTs also have the ability to promote angiogenesis. Experiments have demonstrated that LTC<sub>4</sub> and LTD<sub>4</sub> can promote angiogenesis via a receptor-mediated interaction in the chick chorioallantoic membrane system (21). In agreement with LTs having angiogenic properties, human umbilical vein endothelial cells have also been found to express the CysLT<sub>1</sub> receptor (20). Early experiments demonstrated that LTC<sub>4</sub> promoted a dose-dependent growth of bovine aortic endothelial cells in culture, which the authors proposed could be receptor-mediated. However LTB<sub>4</sub> did not induce any significant proliferation, consistent with the lack of LTB<sub>4</sub> specific binding sites. These data suggested that LTC<sub>4</sub> could be one of the factors implicated in angiogenesis (18).

In the experiments described in Chapter 6, basal LTB<sub>4</sub> release shows an early increase due to O<sub>2</sub> on d 1, which is continued to d 7, but abolished by d 17. Although the cysteinyl-LTs (the angiogenic LTs) were not measured in these experiments, they have previously been measured in our laboratory, using an identical d 4 to d 14 O<sub>2</sub>-exposure protocol to that described in the Methods chapter, and were found to be elevated at d 14 compared to air-exposed animals (3). As no earlier measurements of cysteinyl-LTs were performed, it is possible that they increased above the levels of the air-exposed animals earlier in the experiment and maintained these levels until d 14. Indeed other experiments have shown that hyperoxia from d 4 – d 9 causes an increase in cysteinyl-LTs measured at d 14 (16). The enzyme needed for the formation of both LTB<sub>4</sub> and LTC<sub>4</sub>, 5-LO, and its activating protein, FLAP, were both found to significantly increase due to O<sub>2</sub>-exposure, and although no individual days were significantly different between the air and O<sub>2</sub> groups, the increase due to oxygen seemed to be present as early as d 6. This may then be a pathway to increase the cysteinyl-LTs during exposure to hyperoxia in the lungs of newborn rat pups.

In short, although, the patterns of VEGF and MMPs and LTs do not exactly follow, it is the overall sum of positive or negative stimuli which may dictate their effect on angiogenesis. There is a growing body of evidence demonstrating that the ‘angiogenic switch’ is regulated by the net balance between positive and negative regulators of new capillary growth (9). In the experiments described in this thesis the ‘angiogenic switch’ would appear to act to stimulate angiogenesis or maintain vessel integrity early in the 10-day O<sub>2</sub> exposure protocol and perhaps inhibit formation of new vessels during the latter

half of the alveolar stage. As previously described, both an inhibition (10) and an abundance (25) of angiogenesis can disrupt lung development. Therefore, it is possible that this interpretation of a biphasic effect of hyperoxia may act to inhibit alveolarization.

### ***7.1.3 Windows of opportunity.***

The idea that there may be different mechanisms employed during the first and last halves of hyperoxic-inhibited alveolarization is consistent with results from our laboratory suggesting that there may be a 'critical period' of oxygen exposure. Exposure of rat pups to > 95 % O<sub>2</sub> from d 4 to d 9 but not from d 1 to d 4 or d 9 to d 14, showed a similar inhibition of alveolarization on d 14 as did the regular exposure protocol of d 4 to d 14 (16). However when rat pups were exposed to hyperoxia from d 4 to d 14, the inhibition of LT synthesis from d 3 to d 9 or from d 9 to d 14 prevented the O<sub>2</sub>-induced inhibition of alveolarization (16). These results highlight the importance of the timing of an insult in relation to its effect on septation.

## ***7.2 SPECULATIONS***

### ***7.2.1 No stimulation of angiogenesis***

Of course it is also possible that angiogenesis is not being stimulated during the early stages of hyperoxic-exposure. There is the prospect that the maintenance of VEGF and MMP levels during the initial exposure to hyperoxia is an adaptive mechanism to try and maintain vessel density in the face of an adverse stimuli which is decreasing overall growth and DNA proliferation in the lung. The decrease in the VEGF and MMP activity seen by d 12 may then inhibit angiogenesis and be causative of the inhibited alveolar

development. Or indeed, as VEGF has shown to be a survival factor for endothelial cells (24), removal of VEGF may even cause regression of already formed alveolar structures at this time, much as is seen in adult rats which develop emphysematous lungs after inhibition of VEGFR2 (11). As for the LTs, there is no evidence in the neonatal rat lung that the cysteinyl-LT receptors are present on the inter-alveolar endothelial cells (which would allow the LTs to stimulate angiogenesis) and even if they are present, hyperoxia may actually decrease the receptor density or shift the location of receptors to other cells. LTs also have many other, non-angiogenic effects which may be more important in this model than the fact that the cysteinyl-LTs can promote vessel development.

### **7.2.2 VEGF effects MMPs**

An interesting possibility that I did not test in these experiments is that the decreased VEGF is responsible for the decreased MMPs and TIMPs. There is a body of literature demonstrating that VEGF can stimulate MMP expression and activity in a variety of tissues. In microvascular endothelial cells VEGF administration significantly increased gelatinase A (MMP-2) levels and decreased TIMP-1 and TIMP-2 levels compared to controls (13). In vascular smooth muscle cells, VEGF treatment significantly enhanced production of MMP-9 at both protein and mRNA levels, and it was shown that this effect was likely mediated by VEGFR1 (22). Therefore it is possible that the decreased VEGF stimulation in hyperoxic-exposed rat pups results in less stimulation of MMP production and activation.

### ***7.2.3 VEGF and epithelial cells***

It is also possible that VEGF and MMPs act to inhibit alveolarization through other mechanisms than decreasing angiogenesis. Indeed there is evidence suggesting that VEGFR2 is present on distal lung epithelial cells and that VEGF induces airway epithelial cell proliferation (4). VEGF has also been shown to cause maturation Type II cells and freshly isolated type II pneumocytes responded to VEGF by increasing their expression of SP-B and SP-C (7). Therefore it is possible that the decreased levels of members of the VEGF signaling family in our hyperoxic experiments may be inhibiting alveolar development through effects on type II epithelial cells.

### ***7.2.4 Basement membrane discontinuities***

Evidence also exists for MMP-2 and MMP-9 activity affecting processes other than angiogenesis. In the rat lung, collagen synthesis increases dramatically at d 6 and is maintained at these higher levels until d 22, however total collagen breakdown, and lysis of type IV collagen both peak on d 11 (2), indicating that rapid turnover of type IV collagen, a major component of the basement membrane, occurs during normal postnatal lung growth. Intriguingly during the first 10 days of postnatal life, Adamson and King have demonstrated a high incidence of basement discontinuities beneath type II epithelial cells (1). These discontinuities are most likely formed by the action of MMP-2 and MMP-9, and seem to allow for foot processes from Type II cells to form connections with the underlying fibroblasts (1). They are likely necessary for the transfer of signals related to differentiation from the mesenchyme to the epithelium. Therefore the observed decrease in MMPs seen in hyperoxic pups may inhibit the formation of these

discontinuities and disrupt alveolar development in this way as well as, or instead of, through angiogenesis.

### **7.2.5 *MMPs and elastin***

Another potential role for MMP-2 in the lung is elastin deposition. As mentioned in the Literature Review, elastin is essential for normal development of the alveoli (23). Recently it was demonstrated that 15 % of MMP-2<sup>-/-</sup> mice had severely impaired alveolarization concomitant with abnormal elastin deposition (12). Exposure of neonatal rats to >95% oxygen from d 2 until d 11 has been shown to significantly diminish the developmental increase in tropoelastin mRNA normally seen on d 9 to d 11, indicating that the postnatal upregulation of tropoelastin gene expression is inhibited by hyperoxic exposure in the postnatal period (5). It is therefore possible that the decreased MMP-2 activity in the experiments reported in this thesis are affecting alveolarization through a decrease in elastin levels.

### **7.3 LIMITATIONS**

The chief limitation of these experiments is that none of the experiments actually establish that VEGF, MMPs or LTs are indubitably involved in hyperoxic inhibited alveolarization in the rat pup; the data mostly associates changes of these factors with the time course of hyperoxic exposure. The first step towards establishing cause and effect of MMPs on alveolarization was the inhibition of MMP activity with doxycycline, however, as discussed in Chapter 5, this experiment was inconclusive in relation to the effects of MMP-2 or MMP-9. Another weak point of the thesis is the fact that many of the changes in protein were observed only in the latter half of the hyperoxic-exposure. As septation is



thought to occur mainly during the first half of alveolarization, and as hyperoxia from d 4 – d 9 has also been shown to inhibit alveolarization, the factors examined here may be affecting other aspects of lung development. A final problem with the data is that, although experimental changes in mRNA were conclusive, protein and activity data did not show such significant changes. This may be due to a lack of sensitivity in densitometric analysis of bands, as opposed to the very precise real time PCR technique.

#### **7.4 CONCLUSIONS**

The results presented in this thesis are consistent with the concept that abnormal angiogenesis may contribute to the inhibition of alveolarization observed when rat pups are exposed to a hyperoxic environment. However no evidence has been presented to prove this hypothesis and much more work needs to be completed before any of the theories discussed in the previous sections can be believed. One of the interesting topics highlighted in this discussion is the idea that there may be different mechanisms at work during the first and last half of the alveolar stage, however this also acts as a confounding factor in deriving a clear answer from these experiments.

#### **7.5 FUTURE DIRECTIONS**

Further experiments are still needed to elucidate the mechanisms responsible for normal and inhibited alveolarization. Some of the experiments which would provide new and essential information in regards to the work presented in this thesis are mentioned below.

1) One of the most important experiments would be the careful examination of the changes in alveolar septal structure during exposure to hyperoxia, using transmission

electron microscopy. It would be particularly interesting to observe any changes in capillary density or position and the timing of these changes, as well as potential changes in epithelial cell maturity, fibroblast density, ECM composition.

2) An important aspect that was investigated is the response of the lung once hyperoxia has been withdrawn. Randell *et al.* showed that after 7 days of neonatal hyperoxia, rats at d 40 had more very small and very large alveoli, suggesting a form of catch-up growth different to normal septation (19). Other studies have shown that VEGF returns to baseline levels in newborn rabbit lungs during a 5 day recovery from hyperoxic exposure (15). I performed a preliminary experiment using our hyperoxic rat model of inhibited alveolarization and looking at gelatinase activity at d 28, after 14 days of recovery. Interestingly the activity of 62 kD MMP-2 appeared to be increased compared to control values, suggesting that MMP-2 may be involved in the recovery process (Figure 7.2). However more experiments need to be performed at various times after hyperoxic-exposure.

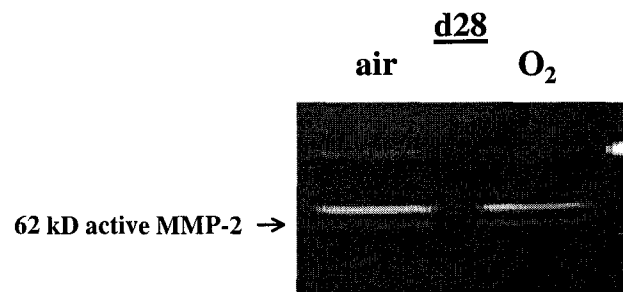


**Figure 7.1** Activity of MMP-2 and MMP-9 at d 28 after exposure of rat pups to air or > 95 % O<sub>2</sub> from d 4 to d 14.

3) An important study in regards to the idea that an increase in angiogenesis during the early days of hyperoxia may be disrupting alveolarization, is to stimulate angiogenesis for discreet time periods during the stage of alveolar development and examine any potential effects on lung morphometry and ultrastructure. This may be through the use of recombinant protein and gene therapeutic approaches to introduce pro-angiogenic agents such as VEGF and FGF.

4) Obvious follow-up experiments would also be to assess the effects of more specific MMP-2 and MMP-9 inhibitors administered during the period of alveolarization, and again to examine the effects on the ultrastructure of the lung. And conversely to administer exogenous VEGF and MMPs for discreet periods during hyperoxic-exposure and see if lung alveolarization can be restored towards normal.

## 7.6 REFERENCES

1. **Adamson, I. Y., and G. M. King.** Epithelial-mesenchymal interactions in postnatal rat lung growth. *Exp Lung Res* 8: 261-74, 1985.
2. **Arden, M. G., and I. Y. Adamson.** Collagen synthesis and degradation during the development of asbestos- induced pulmonary fibrosis. *Exp Lung Res* 18: 9-20., 1992.
3. **Boros, V., J. S. Burghardt, C. J. Morgan, and D. M. Olson.** Leukotrienes are indicated as mediators of hyperoxia-inhibited alveolarization in newborn rats. *Am J Physiol* 272: L433-41., 1997.
4. **Brown, K. R., K. M. England, K. L. Goss, J. M. Snyder, and M. J. Acarregui.** VEGF induces airway epithelial cell proliferation in human fetal lung in vitro. *Am J Physiol Lung Cell Mol Physiol* 281: L1001-10., 2001.
5. **Bruce, M. C., and C. E. Honaker.** Transcriptional regulation of tropoelastin expression in rat lung fibroblasts: changes with age and hyperoxia. *Am J Physiol* 274: L940-50., 1998.
6. **Burri, P. H., J. Dbaly, and E. R. Weibel.** The postnatal growth of the rat lung. I. Morphometry. *Anat Rec* 178: 711-30., 1974.
7. **Compernelle, V., K. Brusselmans, T. Acker, P. Hoet, M. Tjwa, H. Beck, S. Plaisance, Y. Dor, E. Keshet, F. Lupu, B. Nemery, M. Dewerchin, P. Van Veldhoven, K. Plate, L. Moons, D. Collen, and P. Carmeliet.** Loss of HIF-2alpha and inhibition of VEGF impair fetal lung maturation, whereas treatment with VEGF prevents fatal respiratory distress in premature mice. *Nat Med* 10: 10, 2002.
8. **Ferrara, N., and S. Bunting.** Vascular endothelial growth factor, a specific regulator of angiogenesis. *Curr Opin Nephrol Hypertens* 5: 35-44., 1996.
9. **Folkman, J.** Angiogenesis in cancer, vascular, rheumatoid and other disease. *Nat Med* 1: 27-31., 1995.
10. **Jakkula, M., T. D. Le Cras, S. Gebb, K. P. Hirth, R. M. Tuder, N. F. Voelkel, and S. H. Abman.** Inhibition of angiogenesis decreases alveolarization in the developing rat lung. *Am J Physiol Lung Cell Mol Physiol* 279: L600-7., 2000.
11. **Kasahara, Y., R. M. Tuder, L. Taraseviciene-Stewart, T. D. Le Cras, S. Abman, P. K. Hirth, J. Waltenberger, and N. F. Voelkel.** Inhibition of VEGF receptors causes lung cell apoptosis and emphysema. *J Clin Invest* 106: 1311-9., 2000.
12. **Kheradmand, F., K. Rishi, and Z. Werb.** Signaling through the EGF receptor controls lung morphogenesis in part by regulating MT1-MMP-mediated activation of gelatinase A/MMP2. *J Cell Sci* 115: 839-48., 2002.

13. **Lamoreaux, W. J., M. E. Fitzgerald, A. Reiner, K. A. Hasty, and S. T. Charles.** Vascular endothelial growth factor increases release of gelatinase A and decreases release of tissue inhibitor of metalloproteinases by microvascular endothelial cells in vitro. *Microvasc Res* 55: 29-42., 1998.
14. **Lechner, A. J.** Perinatal age determines the severity of retarded lung development induced by starvation. *Am Rev Respir Dis* 131: 638-43., 1985.
15. **Maniscalco, W. M., R. H. Watkins, C. T. D'Angio, and R. M. Ryan.** Hyperoxic injury decreases alveolar epithelial cell expression of vascular endothelial growth factor (VEGF) in neonatal rabbit lung. *Am J Respir Cell Mol Biol* 16: 557-67., 1997.
16. **Manji, J. S., C. J. O'Kelly, W. I. Leung, and D. M. Olson.** Timing of hyperoxic exposure during alveolarization influences damage mediated by leukotrienes. *Am J Physiol Lung Cell Mol Physiol* 281: L799-806, 2001.
17. **Matsui, R., W. M. Thurlbeck, Y. Fujita, S. Y. Yu, and K. Kida.** Connective tissue, mechanical, and morphometric changes in the lungs of weanling rats fed a low protein diet. *Pediatr Pulmonol* 7: 159-66, 1989.
18. **Modat, G., A. Muller, A. Mary, C. Gregoire, and C. Bonne.** Differential effects of leukotrienes B4 and C4 on bovine aortic endothelial cell proliferation in vitro. *Prostaglandins* 33: 531-8., 1987.
19. **Randell, S. H., R. R. Mercer, and S. L. Young.** Neonatal hyperoxia alters the pulmonary alveolar and capillary structure of 40-day-old rats. *Am J Pathol* 136: 1259-66., 1990.
20. **Sjostrom, M., P. J. Jakobsson, M. Heimburger, J. Palmblad, and J. Z. Haeggstrom.** Human umbilical vein endothelial cells generate leukotriene C4 via microsomal glutathione S-transferase type 2 and express the CysLT(1) receptor. *Eur J Biochem* 268: 2578-86., 2001.
21. **Tsopanoglou, N. E., E. Pipili-Synetos, and M. E. Maragoudakis.** Leukotrienes C4 and D4 promote angiogenesis via a receptor-mediated interaction. *Eur J Pharmacol* 258: 151-4., 1994.
22. **Wang, H., and J. A. Keiser.** Vascular endothelial growth factor upregulates the expression of matrix metalloproteinases in vascular smooth muscle cells: role of flt-1. *Circ Res* 83: 832-40., 1998.
23. **Wendel, D. P., D. G. Taylor, K. H. Albertine, M. T. Keating, and D. Y. Li.** Impaired distal airway development in mice lacking elastin. *Am J Respir Cell Mol Biol* 23: 320-6., 2000.

24. **Zachary, I., A. Mathur, S. Yla-Herttuala, and J. Martin.** Vascular protection: A novel nonangiogenic cardiovascular role for vascular endothelial growth factor. *Arterioscler Thromb Vasc Biol* 20: 1512-20., 2000.
25. **Zeng, X., S. E. Wert, R. Federici, K. G. Peters, and J. A. Whitsett.** VEGF enhances pulmonary vasculogenesis and disrupts lung morphogenesis in vivo. *Dev Dyn* 211: 215-27., 1998.
26. **Zhu, W. H., X. Guo, S. Villaschi, and R. Francesco Nicosia.** Regulation of vascular growth and regression by matrix metalloproteinases in the rat aorta model of angiogenesis. *Lab Invest* 80: 545-55., 2000.

## APPENDICES

---

### APPENDIX TO CHAPTER 4

#### **A 1. DIFFERENTIAL CHANGES IN VEGF SPLICE VARIANTS**

As the VEGF gene is spliced into various lengths of RNA to give different isoforms, each with different properties, we wanted to assess changes in the different VEGF splice variants during postnatal development of the rat lung and after exposure to hyperoxia from d 4 to d 14. Ribonuclease protection assays were carried out for each of the 3 splice variants of VEGF; VEGF<sub>120</sub>, VEGF<sub>164</sub> and VEGF<sub>188</sub>. The more recently established 145 and 206 variants were not examined.

##### **A.1.1. *Preparation of cRNA probe***

RNA was isolated from an adult rat lung using Trizol Reagent (see RT-PCR section) and diluted to 500 ng/ $\mu$ l.

A 17  $\mu$ l reaction containing 10 % DMSO, 5 mM MgCl<sub>2</sub>, 1x PCR Buffer (10 mM Tris-HCl, 50 mM KCl), 1 mM each dNTP and 500 ng RNA was heated to 95 °C for 5 min and then cooled on ice. A RT master mix (3  $\mu$ l) containing 50  $\mu$ M Random Hexamers , 20 U RNase Inhibitor and 50 U MuLV Reverse Transcriptase was added to each reaction and run for the thermal cycle: 25 °C for 10 min, 50 °C for 45 min, 85 °C for 5 min.

To the 20  $\mu$ l RT reaction, an 80  $\mu$ l PCR mix containing 1x PCR Buffer (10 mM Tris-HCl, 50 mM KCl), 2 mM MgCl<sub>2</sub>, 0.05 U/ $\mu$ l Taq polymerase, 0.5 pmol/ $\mu$ l forward primer

and 0.5 pmol/ $\mu$ l reverse primer was added. Samples were run for the thermal cycle; [94 °C for 1 min, 52 °C for 2 min, 72 °C for 2 min] x 40, 72 °C for 10 min, hold at 4 °C.

The PCR product was precipitated by addition of an equal volume of phenol, vortexing and centrifuging at 12,000 x *g* for 3 min. The aqueous (top) layer was transferred to a new tube, an equal volume of chloroform was added, and the tube was vortexed and spun again. The aqueous layer was again removed to a clean tube and 1 / 10 volume of 3 M sodium acetate and 2.5 volumes cold 100 % EtOH were added. The mix was precipitated at - 20 °C for 1 h then centrifuged at 12,000 x *g* for 15 min to pellet DNA.

The DNA was resuspended in 50  $\mu$ l TE and 10  $\mu$ l DNA loading dye was added, then the DNA was run on a large 1.5 % agarose gel containing 0.5  $\mu$ g/ml ethidium bromide. The three VEGF splice variants were excised from the DNA gel and purified using the Wizard™ PCR Preps DNA Purification System for Rapid Purification of DNA Fragments Kit (Promega, Madison WI) according to manufacturer's instructions. The DNA was finally eluted with 50  $\mu$ l TE.

To estimate the amount of DNA, 20  $\mu$ l of purified DNA and 5  $\mu$ l of DNA loading dye were run on a 1 % agarose gel containing 0.5  $\mu$ g/ml ethidium bromide with mass as well as base pair markers.

The DNA was then ligated into pGEM®-T vectors (Promega Corporation, Madison, WI) according to manufacturer's instructions. A reaction solution containing 5  $\mu$ l of 2x Rapid Ligation Buffer (T4 DNA ligase), 1  $\mu$ l pGEM®-T vector, 3  $\mu$ l PCR product, 1  $\mu$ l T4 DNA ligase (3 Weiss units/ $\mu$ l) was mixed together. A positive control using 2  $\mu$ l of control



insert DNA and a background control reaction with no DNA were also prepared. Reactions were incubated for 1 h at RT and then overnight at 4 °C.

Products from the ligation reactions were transformed into Subcloning Efficiency DH5 $\alpha$ <sup>TM</sup> Competent Cells (Gibco BRL, Life Technologies). The cells were thawed and 1  $\mu$ l, 2  $\mu$ l and 3  $\mu$ l of the ligation reactions and 2  $\mu$ l of positive control and background were added to separate vials of 50  $\mu$ l of cells. The cells were left on ice for 30 min, heat-shocked for 30 s at 37 °C, and returned to ice for 2 min. LB media (1 % Bacto-tryptone, 0.5 % yeast extract, 0.2 M NaCl, pH 7.5) was added to the cells (950  $\mu$ l) and the contents were transferred to round-bottomed tubes (using sterile technique) and shaken for 1 h at 37 °C. During this time LB plates were spread with 100  $\mu$ g/ml ampicillin (50  $\mu$ l of 50 mg/ml on a 25 ml LB agar plate) and 50  $\mu$ g/ml X-gal. The cells (150  $\mu$ l) were then spread on plates, allowed to dry for 15 min and incubated at 37 °C overnight.

Colonies positive for the ligation reaction were identified as white (where the PCR product DNA has been incorporated into the plasmid, it is inserted in the coding region of the *LacZ* gene so that  $\beta$ -galactosidase is not produced, and therefore does not cleave the X-gal which would cause a blue coloured colony). Tubes of 3 ml of LB<sub>AMP</sub> broth were inoculated with each of 10 positive colonies (for each initial PCR product) and incubated overnight at 37 °C with shaking.

The bacterial cells were pelleted and the plasmid DNA was purified using a QIAprep<sup>®</sup> Spin Miniprep Kit (Qiagen Inc., Mississauga, Ontario) according to manufacturer's instructions. Briefly, pellets were resuspended in buffers (supplied in kit) to lyse and then

precipitate cells. Cells were centrifuged for 10 min and the supernatant was applied to a QIAprep spin column to capture the DNA. The column was spun and the flow-through was discarded, the column was then washed and flow-through was again discarded. The DNA was eluted using 50  $\mu$ l H<sub>2</sub>O.

The products of the miniprep were digested to cut out the DNA from the plasmid. A reaction of 10  $\mu$ l DNA, 2  $\mu$ l 10x enzyme buffer, 1  $\mu$ l Apa 1, 1  $\mu$ l Sac 1 and 6  $\mu$ l H<sub>2</sub>O was placed in a 37 °C water bath for 1 h. The samples were run on a 1 % agarose + EtBr gel. A positive sample was identified for each splice variant (1 band in the appropriate place) and 500 ml of LB<sub>AMP</sub> was inoculated with the remaining broth from the 3 ml culture of the appropriate transformation colony and incubated overnight at 37 °C with shaking. The plasmid DNA was purified using the Quantum Prep® Plasmid Maxiprep Kit (Biorad, Mississauga, Ontario, Canada) according to manufacturer's instructions. The recovered DNA (10  $\mu$ l) was again cut with Apa 1 and Sac 1 and the size of the product was verified on an agarose gel with DNA base pair markers. The concentration of the maxiprep DNA was determined (by spectrophotometry) and 60  $\mu$ g of the DNA was linearized in two separate reactions containing 10  $\mu$ l of Sal 1 or 10  $\mu$ l of Nco 1 overnight at 37 °C. The linearized products were run on a 1 % agarose + EtBr gel and one band was observed to verify linearization (correct product size was the size of the initial PCR product + 3003 bp for the plasmid). The products were sent for sequencing to verify that the correct DNA insert was obtained and to determine the orientation of the DNA in the plasmid.

Finally, a phenol-chloroform back-extraction was performed on linearized probes. To 100  $\mu\text{l}$  of probe, an equal volume of phenol-chloroform was added. The samples were spun at 14,000  $\times g$  for 5 min and aqueous layer was removed to a clean tube, 100  $\mu\text{l}$  of TE was added to bottom layer and process was repeated. The supernatants were added together and an equal volume of chloroform isoamyl alcohol was added and samples were again spun and the supernatant was removed twice. The probe was precipitated with 1/10 volume of 3 M NaAc and 2.5 volumes of cold EtOH for 1 h at - 80 °C. The samples were spun and the pellet was washed twice with 70 % EtOH and then resuspended in 20  $\mu\text{l}$  of TE. The concentration of the probe was determined by spectrophotometry and was then diluted to 1  $\mu\text{g}/\mu\text{l}$  before use.

#### **A.1.2. *RNA Protection Assay***

The plasmid construct containing the appropriate DNA insert was transcribed with bacterial polymerases in the presence of  $^{32}\text{P}$ -CTP (1 mCi / 25  $\mu\text{l}$ ). The transcription reaction contained 5  $\mu\text{Ci} / \mu\text{l}$ , 0.5 mM each nucleotides (A, G, T), 1x buffer (depending on enzyme), 6 mM DTT, 1.2 U/ $\mu\text{l}$  Rnasin, 0.1  $\mu\text{g}/\mu\text{l}$  DNA, 5 U/ $\mu\text{l}$  T7 DNA polymerase or 1.5 U/ $\mu\text{l}$  SP6 DNA polymerase. The correct polymerase to use was decided on depending on whether the reaction was to generate a sense or antisense probe and the orientation of the probe in the plasmid, as determined earlier. The reactions were incubated at 37 °C for 1 h, then 0.6  $\mu\text{l}$  Rnasin (40 U/ $\mu\text{l}$ ) and 6  $\mu\text{l}$  DNase I (10 U/ $\mu\text{l}$ ) were added and reaction was incubated for a further 20 min at 37 °C. Next, 100  $\mu\text{l}$  TE buffer, 150  $\mu\text{l}$  phenol/chloroform and 4  $\mu\text{l}$  yeast tRNA (10  $\mu\text{g}/\mu\text{l}$ ) were added, and the reaction was vortexed and spun at 14,000  $\times g$  for 5 min. The aqueous (top) layer was transferred to a

new 1.5 ml tube and 50  $\mu$ l of 10 M ammonium acetate, 50  $\mu$ l TE buffer and 800  $\mu$ l 100 % EtOH were added to it. The mix was then vortexed and incubated overnight at 20 °C.

A small 6 % acrylamide gel containing 7 M Urea was cast (50 ml 6 % acrylamide/urea mix, 150  $\mu$ l 10 % APS, 35  $\mu$ l TEMED) and pre-run at 300 V. The transcription reaction was centrifuged for 15 min at 14,000 x g and the pellet was then dried and resuspended in 3  $\mu$ l TE and 16  $\mu$ l loading buffer. The radioactively labeled RNA probe was denatured by boiling for 5 - 10 min and then placed on ice immediately. The samples were loaded into the gel and run for 2 h at 350 V. The gel was removed from the glass and exposed to film for 20 - 30 s. The film was developed and windows were cut where the appropriate bands lay; the film was then placed back over the gel and gel slices were cut through the windows. Pre-warmed (37 °C) elution buffer (2 M ammonium acetate, 1 % SDS, 25  $\mu$ g/ml tRNA) (400  $\mu$ l) was added to each gel slice and the slices were incubated at 37 °C for 2 h. The supernatants were removed and transferred to clean 1.5 ml tubes; 1 ml of 100 % EtOH was added to each and the mix was incubated on dry ice for 30 min. The samples were spun at 14,000 x g for 15 min and the supernatants were removed. The pellets were air dried and resuspended in 3  $\mu$ l TE and 50  $\mu$ l hybridization buffer (800  $\mu$ l deionized formamide, 200  $\mu$ l 5x salt (200 mM PIPES, pH 6.4, 2 M NaCl, 5 mM EDTA)). The radioactivity of the RNA probe was determined and the probe was then diluted to 500,000 cpm / 30  $\mu$ l.

The appropriate aliquots of RNA (40  $\mu$ g) were previously stored at - 80 °C in 70 % EtOH and 3 M sodium acetate. A tRNA negative control (10  $\mu$ l tRNA (10  $\mu$ g/ $\mu$ l), 90  $\mu$ l TE, 10  $\mu$ l 3 M sodium acetate pH 5.2, 300  $\mu$ l 100 % EtOH) was prepared. All samples

were spun at 14,000 x g at 4 °C for 10 min, then the supernatants were removed and the pellets were dried in a speed vacuum for 10 min before the samples were placed on ice. The pellets were resuspended in 2 µl TE buffer and 30 µl of the diluted probe was added. Parafilm was placed tightly over the tubes and the samples were boiled for 30 min, vortexed and placed in a 55 °C water bath overnight.

A mix of 10 ml digestion buffer (10 mM Tris-Cl, 5 mM EDTA, 0.3 M NaCl, pH 8.0) and 5 µl RNase A (5 mg/ml) was made up and 300 µl of mix was added to each hybridization reaction, followed by 3 µl RNase T1. The samples were incubated at 30 °C for 30 min, then 3 µl proteinase K (25 µg/ml) and 10 µl of 20 % SDS were added and the samples were vortexed and incubated again at 37 °C for 20 min. The samples were transferred to clean tubes containing 400 µl of phenol/chloroform, vortexed and spun at 14,000 x g for 5 min. The aqueous layer was transferred to clean tubes containing 400 µl isopropanol and 4 µl tRNA (10 mg/ml) was added to each tube; the samples were allowed to precipitate for 1 h at room temperature. The samples were spun at 14,000 x g for 15 min, the supernatant was discarded and the pellet was resuspended in 2 µl TE and 6 µl loading buffer. The probe was diluted in loading buffer so that there were about 700 K / 8 µl. The samples and the probe were boiled for 15 min and then placed on ice before they were loaded onto a pre-run 6 % acrylamide, 7 M Urea sequencing gel. The gel was run at 1500 V for about 2 - 2.5 h. The gel was placed over thick blotting paper and dried for 1 h before exposing it to film overnight at - 80 °C with an intensifying screen.

### *A.1.3.*

### *Results*

No changes were detected in any of the splice variants over different developmental ages or in response to O<sub>2</sub> treatment. After examination of the results obtained it seems likely that this was due to degradation of the RNA probes, as when the radioactively labeled probes were run out on a gel many bands were observed (Figure A.1, A.2 and A.3). This would then explain the many protected fragments observed in the RPA experiments as well as the lack of changes seen in the protected fragment of the appropriate size (Figure A.1, A.2 and A.3), as the amount of radiolabeled probe of the right size would have been insufficient to detect changes.

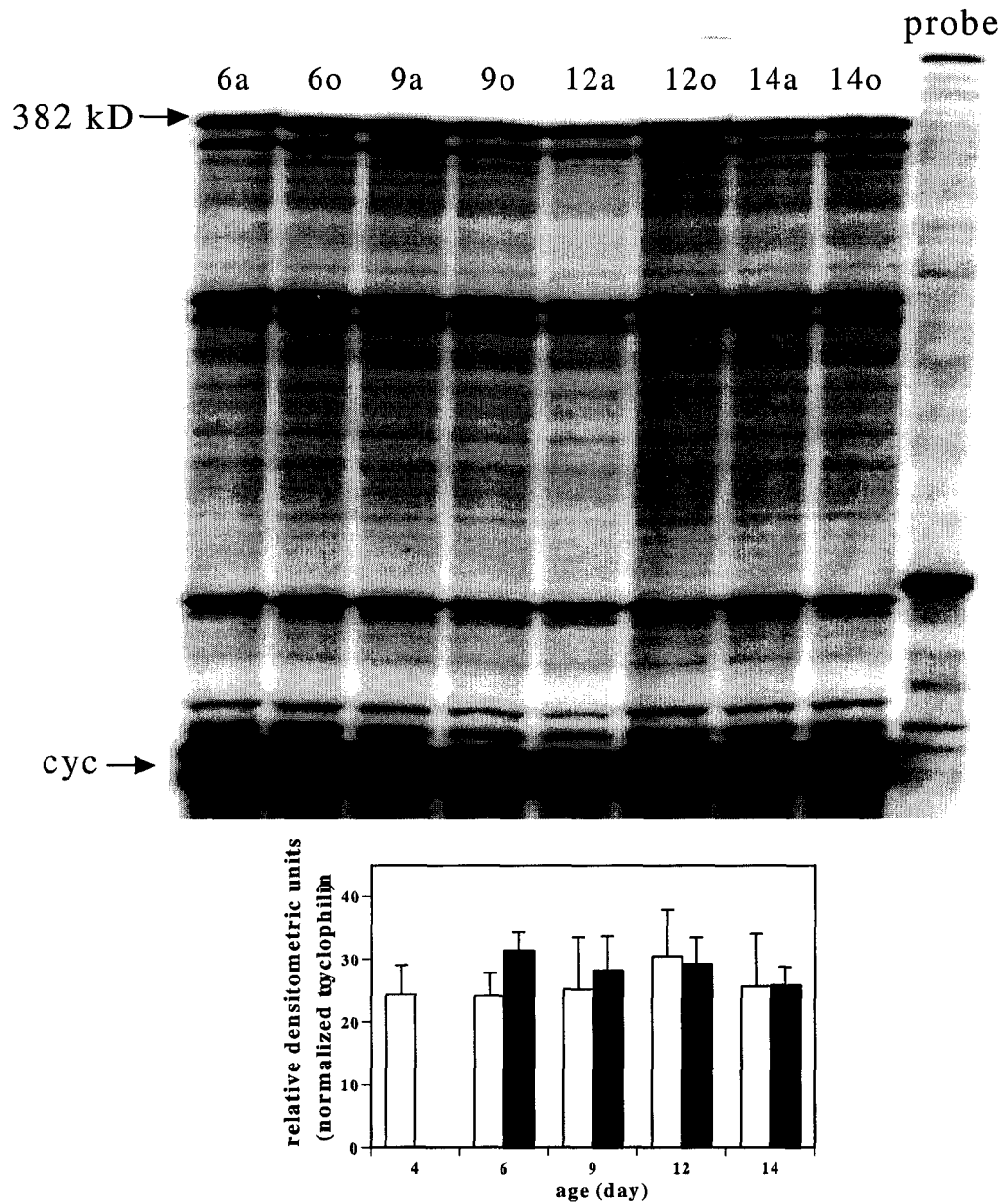


**Figure A.1** Representative Blot of a RPA for VEGF<sub>120</sub>.

Lungs were removed from rat pups after 4, 6, 9, 12 and 14 days of exposure to room air (a) or >95% O<sub>2</sub> (o). A graph of the analysed data normalized to cyclophilin is shown. There were no changes in VEGF<sub>120</sub> with age or after exposure to O<sub>2</sub>.

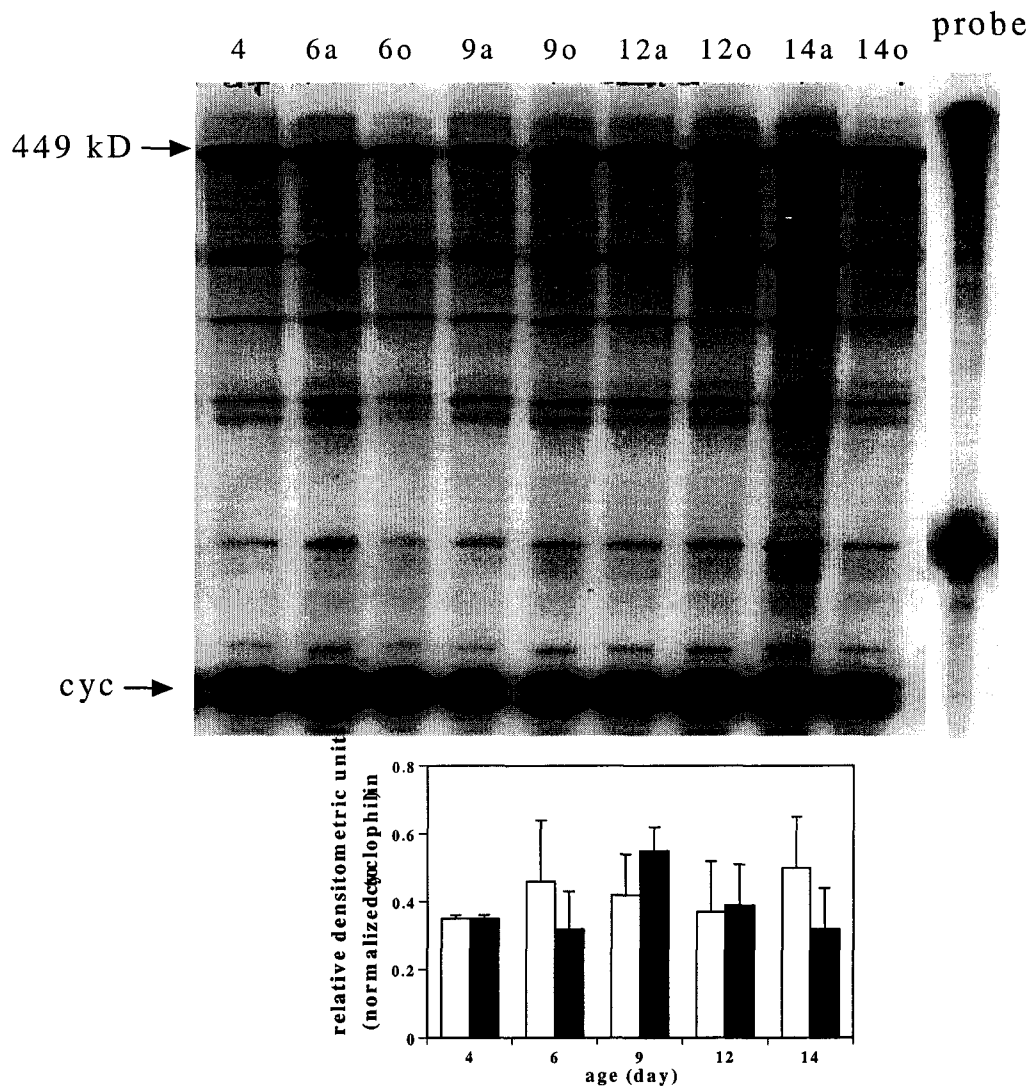


**Figure A.2 Representative Blot of a RPA for VEGF<sub>164</sub>.**

Lungs were removed from rat pups after 4, 6, 9, 12 and 14 days of exposure to room air (a) or >95% O<sub>2</sub> (o). A graph of the analysed data normalized to cyclophilin is shown. There were no changes in VEGF<sub>164</sub> with age or after exposure to O<sub>2</sub>.



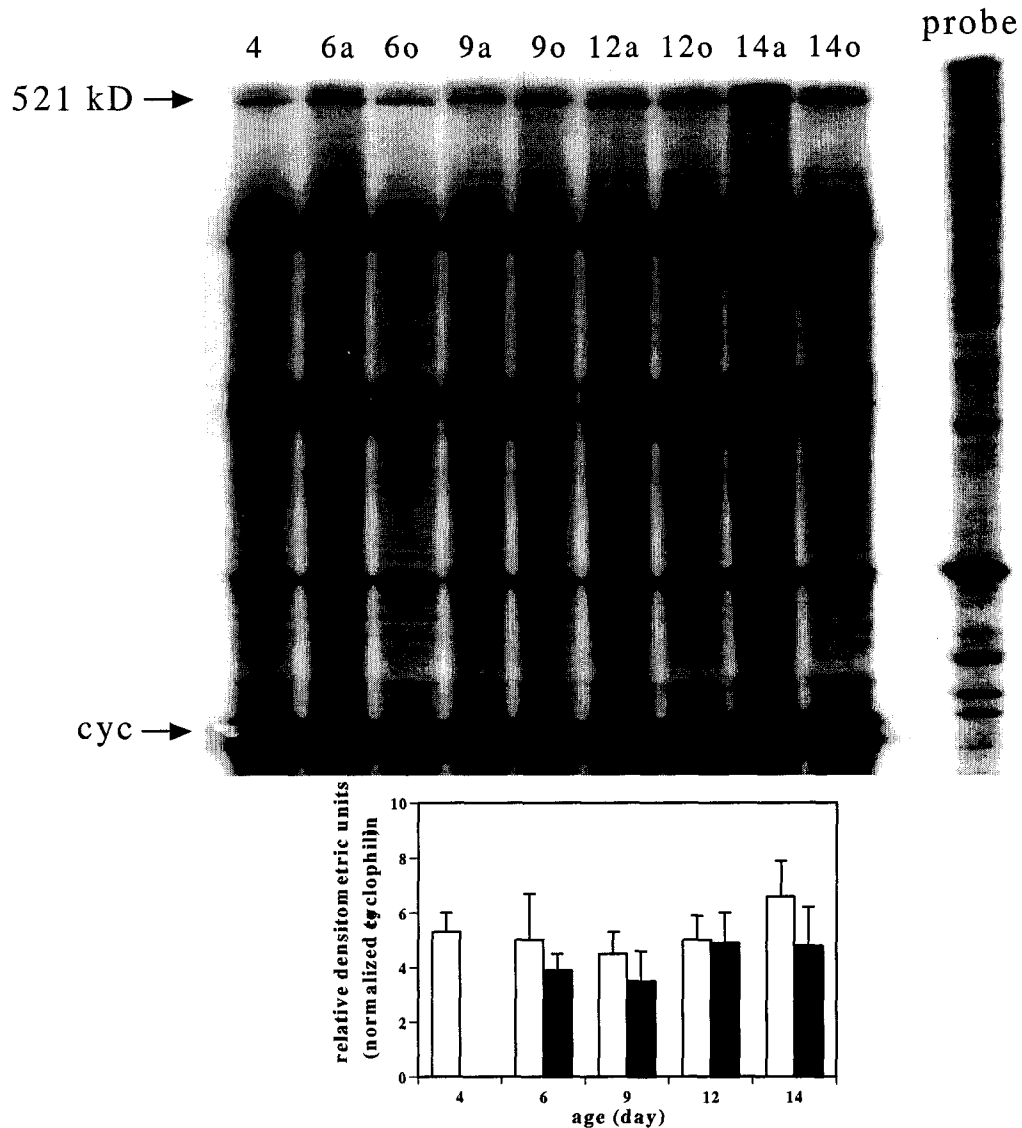


**Figure A 3 Representative Blot of a RPA for VEGF<sub>189</sub>.**

Lungs were removed from rat pups after 4, 6, 9, 12 and 14 days of exposure to room air (a) or >95% O<sub>2</sub> (o). A graph of the analysed data normalized to cyclophilin is shown. There were no changes in VEGF<sub>189</sub> with age or after exposure to O<sub>2</sub>.